The feasibility of standardization of a mono-pile mooring facility for FSRU's

MSc Thesis TU Delft

K.A.A. Watté

Delft University of Technology

Final report

The feasibility of standardization of a mono-pile mooring facility for FSRU's

Author	Kevin Watté
Student number	1376179
E-mail address	k.a.a.watte@gmail.com
University	Delft University of Technology
Faculty	Civil Engineering & Geosciences
Program	Hydraulic Engineering
Company	Royal HaskoningDHV
Location	Rotterdam
Business line	Maritime & Waterways

Graduation Committee

Chairman	Prof. Ir. Tiedo Vellinga
Supervisor TU Delft	Ass. Prof. Dr. Ir. Jarit de Gijt
Supervisor TU Delft	Dr. Ir. Arie Romeijn
Supervisor Royal HaskoningDHV	Ir. Dirk Jan Peters
Supervisor Seaway Heavy Lifting Engineering B.V.	Ir. Vladimir Thumann

Daily supervisor

Supervisor Royal HaskoningDHV	Ir. Priscilla Veldhuizen

Preface

This report presents the results of a study into the feasibility of standardization of a mono-pile mooring facility for FSRU's on exposed locations. The graduation project was carried out at Royal HaskoningDHV in cooperation with Delft University of Technology. This project was performed to obtain the Master's degree in Hydraulic Engineering at Delft University of Technology.

The committee members are listed below.

> Prof. Ir. T. Vellinga
>
> Ass. Prof. Dr. Ir. J.G. de Gijt
>
> Dr. A. Romeijn
>
> Ir. D.J. Peters
>
> Ir. V. Thumann

I want to express my gratitude to Royal HaskoningDHV for providing me with the resources to work on my thesis. I would like to express my appreciation to my colleagues for the enjoyable atmosphere during my graduation time, with a special thanks to Priscilla for the advice and motivation.

I would also like to thank the committee members for the time and energy they dedicated to my work.

On a personal note, I would like to express my gratitude to my parents for their confidence and financial support during all those years.

Kevin Watté,

Rotterdam, January 2015

Abstract

As the LNG market continues to grow internationally, Floating Storage and Regasification Units (FSRU's) have become an increasingly important component as governments and private companies strive for faster, cheaper and more flexible means of re-gasifying.

In order to have a FSRU mooring system which is equally fast deliverable, standardization is considered. In this study standardization of the civil structures is investigated for a jetty-type mooring system on exposed locations, more specifically standardization of the breasting dolphins. The considered dolphins consist of a simple steel mono-pile which transfers the mooring loads to the sub-soil and a pile-head which connects the fender to the mono-pile.

It was concluded that standardization of the mono-piles is only possible to a certain extent, namely in a conceptual design phase. In this report a standardized work approach is presented regarding the design of the mono-piles. Additionally, multiple pile designs are conceived for varying conditions. In an early design stage, when very little information is available, already some insight can be gained regarding the dimensions and the costs of these piles.

In this thesis, also, the pile-head concept is presented which is most suitable for standardization purposes. This is achieved by a Fiber Reinforce Polymers (FRP)-composite, floating structure with a slide-bearing sliding system. The application of composite has some major advantages as it is fatigue resistant, low maintenance, light weighted and corrosion resistant. The form of the pile-head is also optimized for its application so that the fender loads are transferred in the most efficient manner to the mono-pile, while the slide-bearing allows smooth sliding along the pile's shaft.

Next to standardization of the civil structures, the loading conditions are investigated. Since the FSRU is permanently moored at exposed locations, this issue cannot be treated with 'normal' mooring of traveling ship, but must be calculated with the aid of numerical software where the relation between the environmental conditions and the load conditions is critical. The application of such software, however, is considered time-consuming for early design stages. An assessment tool is therefore conceived that calculates the design fender loads in a quick and analytical manner. This report shows that this assessment tool can generate rather accurate results, but that its application is limited.

Keywords

Floating Storage and Regasification Unit, LNG, jetty-type mooring system, dolphins, standardization, permanent mooring

Contents

1 Introduction

Natural gas is used as a major source of energy. However, many cities and industries that need that energy are located far from the gas fields. Since transportation of natural gas may not always be feasible through pipelines, Liquefied Natural Gas (LNG) is created which can then be transported safely and economically by sea. LNG is thus natural gas, predominantly methane, which has been converted to a liquid state for ease of storage and transport. The liquefaction process consists of condensing the natural gas into a liquid by cooling it to approximately -162⁰C, significantly reducing the volume to 1/600 of its original value making it very efficient and thus economically valuable.

$$100 \text{ kg Natural gas} = 140.45 \text{ m}^3$$
$$100 \text{ kg LNG} = 0.22 \text{ m}^3$$

Table 1 *Density of Natural gas and LNG [42]*

The global gas demand has known a significant growth the last couple of years and will be expected to grow even more in the future. The International Energy Agency (IEA) sees natural gas being one of the most important energy sources in the future as it forecasts that the natural gas growth rate will be more than twice the expected growth rate of oil. The growth of the global LNG energy demand, however, is expected to be even stronger. To illustrate this rapid growth the projected growth is given in Table 2 [18].

	Growth last 15 years (per year)	Future growth (per year)
Natural gas	2.7%	1.6%
LNG	7.6%	5%

Table 2 *Global demand of Natural Gas and LNG*

The supply of LNG can be seen as a simplified four step process.
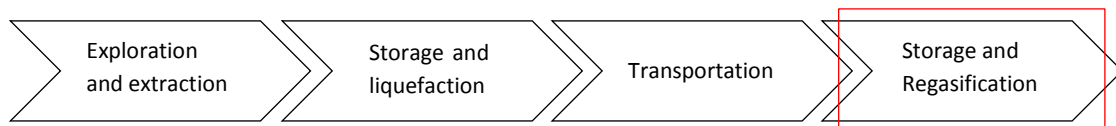
Figure 1 *The LNG supply chain*

Exploration and extraction First deposits of natural gas are detected and pumped to the surface from onshore or offshore wells through pipelines to the liquefaction plant.

Storage and liquefaction process At the liquefaction plant, all impurities are removed from the gas, prior to cooling. Cooling of the natural gas, as mentioned above, will reduce its volume considerable making transport efficient and economically valuable.

LNG transportation The LNG is loaded onto double-hulled ships specially designed to prevent hull leaks and ruptures in the event of accidents. Those ships are knows as LNG carriers (LNGC). Once the ship arrives at the receiving port, the LNG is offloaded and pumped into storage tanks.

Storage and regasification process	LNG is stored in storage tanks at just above atmospheric pressure at a temperature of -162°C. Regasification is used to convert the LNG back into its natural gaseous state by gradually warming the gas back up to a temperature of over 0°C. Finally, the gas enters the domestic pipeline distribution system and is ultimately delivered to the end-user.

The scope of this thesis will focus on the final link of the LNG supply chain, the LNG receiving (import) terminals as highlighted in Figure 1.

Conventional LNG import terminals are land based, situated within ports or as stand-alone facilities. Every terminal would be constructed in combination with a quay or jetty structure to support the mooring of LNG carriers, storage tanks for the LNG and special equipment for the regasification process. Due to the hazardous nature of gas, the construction of such conventional LNG import terminals encountered growing public resistance to terminals located close to populated areas as an unacceptable high risk to public safety was perceived. Consequently, this was in direct conflict with the ambitions of Gas enterprises which are preferably situated close to the market, in proximity of residential areas. New sorts of import terminal were therefore required. This has led to multiple new solutions for importing gas from which offshore terminals, in particular Floating Storage and Regasification Units (FSRU's), would be able to provide a solution capable of meeting the expectations of both the Gas enterprises and the local communities.

A FSRU is an LNG import terminal located offshore. It is a specially designed floating vessel which provides LNG receiving, storage and regasification services. As a hull, a FSRU consist of a LNG carrier (LNGC) converted by attaching a regasification infrastructure. The FSRU is typically 300 meters long and does normally not have a complete propulsion system. There are applications in which rapid disconnection and relocation is required, in these cases propulsion will be part of the FSRU. The main advantages of a FSRU compared to conventional land based terminals are listed below [32], [33]; it must be noted that these are valid for the general case; further information regarding these topics are not treated within this thesis.

Low initial costs	For the construction of the FSRU's less initial CAPEX is needed due to the fact that the storage tanks are already "built in" to the converted LNG carrier, which are the most expensive terminal components. FSRU´s are therefore a more cost-effective way to meet small scale LNG demand or to access new emerging markets
Speed of delivery	A shorter start-up and construction time makes rapid access to high value gas markets possible. Also there is less risk of delays related to land acquisitions.
Flexibility	The FSRU can be relocated, moored offshore or near shore. Due to its flexibility the FSRU is an obvious choice in areas where economic growth is uncertain or where there is an element of political or economic instability.
Lower resistance	Since a FSRU is situated offshore, there is less resistance of local communities.

As the LNG market continues to grow internationally, FSRUs have become an increasingly important component, in particular to smaller and growing economies worldwide. FSRU operations are predicted to double in the next two years as governments and private companies continue to take advantage of a faster, cheaper and more flexible means of re-gasifying LNG [27]. In order to have a FSRU mooring system which is equally fast deliverable, standardization is required. The purpose of this study is thus saving costs and schedule of the civil structures for moorings by investigating the feasibility of standardization. Additionally, the focus shall lie on standardization of a jetty-type system where the mooring of the FSRU is carried out through a combination of both breasting and mooring dolphins.

2 Research description

In this chapter first the scope of the research is described (2.1). Subsequently the problem definition is treated (2.2) from which the research objectives (2.3) will follow. Lastly, an outline of the report will be given (2.4).

2.1 Scope

In order to prevent the FSRU from floating away and allow safe LNG transfer, an appropriate mooring system is indispensable. Vessels station keeping can be divided into two functions:

- Heading control
- Position control

Depending on the operations, one or both functions are required. In this study the focus shall lie on a jetty-type mooring system which is a combination of the abovementioned functions.

The considered jetty-type mooring system consists of four mooring dolphins and four breasting dolphins illustrated in Figure 2. The mooring dolphins are required to withstand lateral forces on the moored vessel, when the vessel is pushed away from the mooring system. From the bow and the stern "breasting lines" are connected to the mooring dolphins restricting these lateral motions. The breasting dolphins are required to withstand the longitudinal forces on the moored vessel; "spring lines" are connecting the vessel to the breasting dolphin in order to achieve this. Additionally, the breasting dolphins are required to withstand the lean-on forces caused by the vessel being pushed towards the "fenders". These fenders have as main function to absorb energy caused by the moving vessels, preventing damage to the structure and vessel. The fenders are located between FSRU and breasting dolphins and between the FSRU and LNGC.
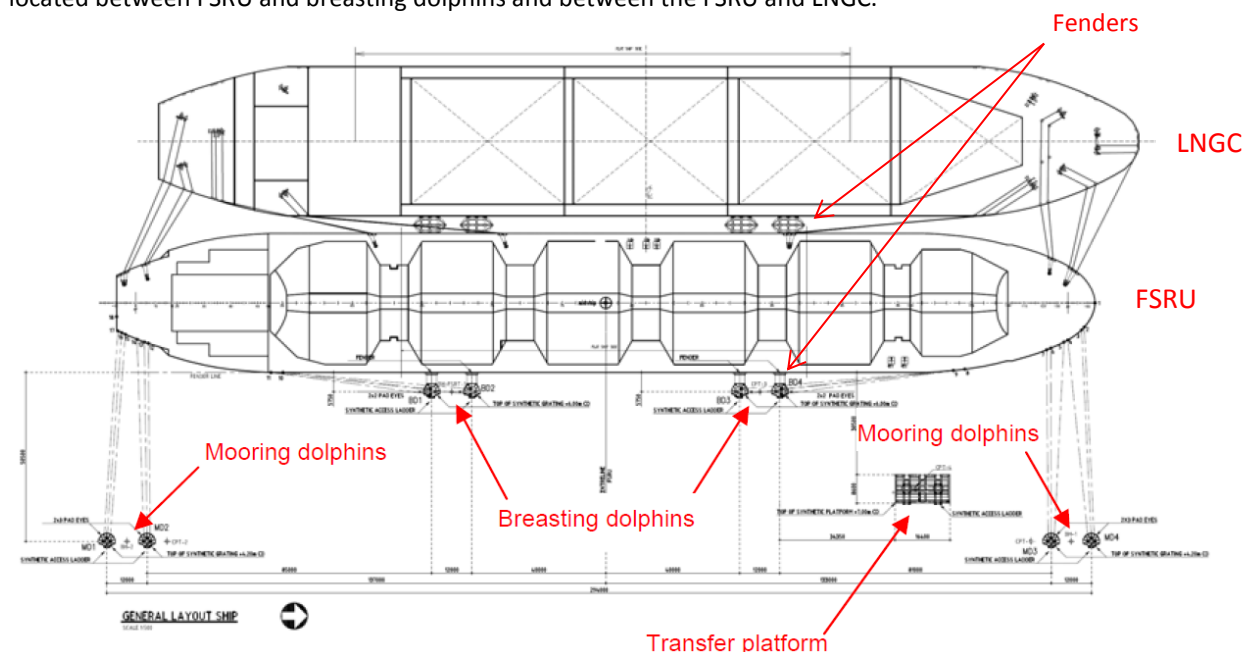
Figure 2 *Jetty-type mooring system; side-by-side mooring configuration between FSRU and LNGC*

This considered mooring system is meant for exposed locations. The FSRU is permanently fastened to the mooring system and shall only be relocated under extreme events. "Quick Release Hooks" are therefore applied which enables quick and easy release of the mooring lines.

For the transfer of LNG, an incoming LNGC will berth along the FSRU in a side-by-side configuration, offloading the cargo by means of "hydraulic arms". Once the LNG is re-gasified, the gas will be transferred to a transfer platform by means of "jumpers" (flexible hoses). Subsequently, from the platform, the gas will be transferred via a "riser" to a fixed seafloor-pipeline to the main land. A more detailed explanation regarding the FSRU-vessel and its operations is included in Appendix I.

This study focusses on dolphins which are constructed from mono-piles. These are large diameter, tubular, steel elements, generally driven into the soil. The load exerted by the moving vessels on the mooring system will be transferred by means of bending deflection to the sub-soil.

Even more specifically, the emphasis of this study will be on the breasting dolphins. Two main elements are to be distinct:

- The mono-pile itself which transfers the mooring forces to the sub-soil,
- The pile-head which connects the fender to the mono-pile

A schematic representation is illustrated in Figure 3.
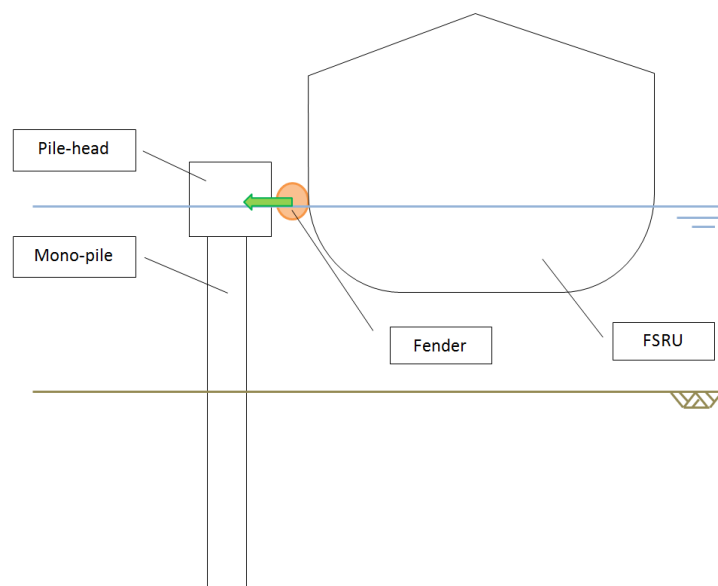
Figure 3 *Schematic representation of a mono-pile breasting dolphin. * Not scaled.*

2.2 Problem definition

2.2.1 Standardization

As LNG makes great strides in the global energy demand, FSRUs become increasingly applied. Their flexibility, low CAPEX and fast deliverance makes them, in many cases, the preferred type in comparison to the conventional land-based terminal. In order to prevent counteracting these advantages, the required FSRU mooring system shall be equally cheap and fast deliverable. In order to achieve these means, standardization is considered.

The purpose of this study is therefore to investigate standardization of the civil structures of a mono-pile mooring facility for permanently moored FSRU's, in particular standardization of the breasting dolphins. The focus shall lie on the design of the mono-pile and the pile-head.

2.2.2 Load conditions

The permanent mooring of FSRU's at exposed locations has implication for extreme loads as well as the number of load repetitions induced by ship motions. With 'normal' mooring of traveling ships these issues can normally be treated differently and simpler. For the considered mooring system the largest loads do not occur during berthing operations, but during the operation phase when the FSRU is fastened to the mooring system.

The relation between the environmental conditions and the load conditions is thus one of the critical issues for the design of the flexible mono-pile dolphins. These design loads are normally determined based on the outcome of a so-called dynamic mooring analysis (DMA). DMA´s are simulated by means of numerical software packages and are used to determine the response of a moored ship to its environment. However, the simulation of DMA's is a complex and time-consuming procedure. In order to prevent using this type of software in early design stages, a standardized method is required that quickly estimates the mooring loads.

2.3 Research objective

The main research objective of this study is to:

'Investigate standardization of a FSRU mooring facility at exposed locations'.

Three main parts are identified:

- Part 1: Defining the design loads
- Part 2: Standardization of the mono-piles
- Part 3: Standardization of the pile-head

The first part concerns the loads acting on the breasting dolphins. As mentioned in the problem definition, currently numerical software is used to calculate mooring loads. The application of such software in an early design stage, however, is considered rather inefficient. A standardized assessment tool has therefore to be designed with which an estimate of the design loads can be obtained in an analytical manner. The relationship between the environmental conditions and the loads due to ship motion are therefore critical. These shall be rationalized covering a large range of wind, current and wave conditions.

Part 2 focusses on standardization of the mono-pile dolphins. A feasibility study shall be performed by analyzing whether standardization is possible without largely over-dimensioning the piles. The effect of the loads and geotechnical parameters on the pile design shall be investigated. Since the mooring facility is to be designed for exposed locations, also fatigue loading needs to be taken into account. The fatigue life of the mono-piles shall therefore be assessed

In the final part, Part 3, special attention is given to the pile-head; a standardized concept shall be designed. For this study multiple materials, forms and properties of the pile-head are to be considered. Different variants shall be conceived and compared by means of an evaluation-study. The variant which will be the best fit for standardization purposes shall subsequently be elaborated; both a structural analysis as a fatigue assessment shall be performed.

2.4 Outline of the thesis

After an introduction and description of the problem the thesis Chapter 3 will discuss the methodology, Chapter 4 through 6 will analyze the different "Parts", Chapter 7 will include a discussion of the results and Chapter 8 will cover the conclusions and recommendations.

Chapter 3: Methodology

In the methodology the general work approach of the three different Parts is described.

Chapter 4: Analysis Part 1, design loads

This chapter concerns the analysis of Part 1. The design conditions on which the assessment tool is based are drafted. Subsequently, a description of the assessment tool including its application is elaborated. Lastly, its accuracy is tested by comparing the obtained results to actual DMA-results from several reference projects.

Chapter 5: Analysis Part 2, mono-piles

Chapter 5 regards the analysis of Part 2; the design of the mono-piles. As standardization is only possible within certain limits, first the design conditions and requirements are defined. Thereafter the modeling procedure and design verifications of the mono-piles are clarified. The influence of the input parameters on the pile design is included in the results. Based upon these results, conclusions regarding standardization will be drawn.

Chapter 6: Analysis Part 3, pile-head

The analysis of Part 3, the pile-head, is included in Chapter 6. Here again, first design conditions are established. Afterwards a brief introduction and specific material properties of FRP-composites will be given. Subsequently, the modelling procedure and performed design verifications are mentioned. The results of the global structural analysis will follow. It must be noted that the structural optimization process is not very much discussed; only the final design is presented.

Chapter 7: Discussion of result

"Discussion of results" consists of a quick recapitulation of the obtained results mentioned in the previous chapters. Additionally, these results will be further enlightened and rationalized.

Chapter 8: Conclusions and recommendations

Based on the obtained results conclusions will be presented. Lastly, some recommendations for further research are given.

3 Methodology

In this chapter the methodology of the different parts is briefly described. These will be further elaborated in Chapters 4, 5 and 6 for respectively Part 1, 2 and 3.

3.1 Part 1: Determination of the design loads

The methodology of Part 1 consists of analyzing large data sets of dynamic mooring analyses and finding the most promising correlations between environmental conditions (input) and fender loads (output). Since such an assessment tool can only be designed for a limited range of environmental conditions, numerous assumptions had to be made restricting the application of this assessment tool to certain locations in the world. The assessment tool including all assumptions is clarified in Chapter 4 "Analysis Part 1".

3.2 Part 2: Standardization of the mono-piles

In Part 2 the mono-pile structures are designed in the Ultimate Limit State (ULS) and checked on their fatigue life in the Fatigue Limit State (FLS).

The laterally loaded pile calculations are performed with "LPile v6.0" software. This software models the pile as an elastic beam on a foundation of uncoupled non-linear springs, representing the soil, the so-called p-y curves. The ULS design verifications for the steel mono-piles include yield stresses and local buckling. The fatigue life is checked based on a cumulative damage factor which is calculated by means of Miner's Law.

In order to see to what extend standardization of the mono-piles is possible; the influence of the load on the pile design is investigated. Also the effect of the subsoil is taken into account by considering two "extreme soil profiles": a stiff sand profile and a soft clay profile. Since standardization will inevitably lead to some over-dimensioning, this is also investigated. The analysis of Part 2 is treated in Chapter 5.

3.3 Part 3: Standardization of the pile-head

Part 3 started off by conceiving multiple variants very different one from another. The properties of those variants were then evaluated and compared by means of a so-called multi criteria analysis (MCA). From this MCA-evaluation the most favorable concept for standardization is worked out.

The structural analysis of this concept is performed with Finite Element-software package "SCIA Engineer" which was used to perform a global elastic analysis. The final design is obtained through an optimization process, constantly adjusting the size and material properties of the different elements. Finally, the design is checked on its fatigue life based on Miner's law and the most critical joint connection is analyzed. The complete analysis including the final design is presented in Chapter 6 "Analysis Part 3".

4 Analysis Part 1: Design loads

4.1 Introduction

The main goal of Part 1 is to design an assessment tool that, in a conceptual design phase, gives a quick estimate of the design loads, thus avoiding having to use DMA software.

With the aid of this assessment tool, for a given set of environmental conditions, the critical loads on the breasting dolphins can be calculated in an analytical manner. Nevertheless, such tool is only designed within defined limits and is therefore only valid for a certain range of wind, wave and current conditions. The range of environmental conditions and additional assumptions are treated in section (4.2) "Design conditions". The assessment tool is described in section (4.3) and its calculated accuracy is included in section (4.4). Discussion of the obtained results is treated in Chapter 7.

4.2 Design conditions

The data used for the conception of the assessment tool was obtained through previous projects of RHDHV: the Golar-project in the Java Sea and the Aqaba-project in the Jordan Sea, both are described in more detail in Appendix II. As the environmental conditions applied in the Dynamic Mooring Analyses (DMA's) are very location bound, the main restrictions are discussed in this section.

4.2.1 Storm conditions

The assessment tool is designed for storm conditions only. These are winds with a rather large spectrum and are defined by a 1-hourly mean wind speed. For locations where other wind conditions may occur such as e.g. cyclones or squalls this method may lead to inaccurate results as different wind-wave correlations will be present.

4.2.2 Short waves

The response of a ship to a certain wave train is described by the hydrodynamic parameters of a ship and the so-called Relative Amplitude Operators (RAO's). From these parameters follows that lower frequency waves lead to larger vessel motions.

For this study only relatively short waves are considered (see Figure 4, each dot is represents one DMA run). For swell environments or near-shore locations where un-bounded long waves may occur, this assessment tool is not applicable.

This method was conceived for waves with a maximum significant wave height of 2 meters. For larger wave heights this method still need validation.
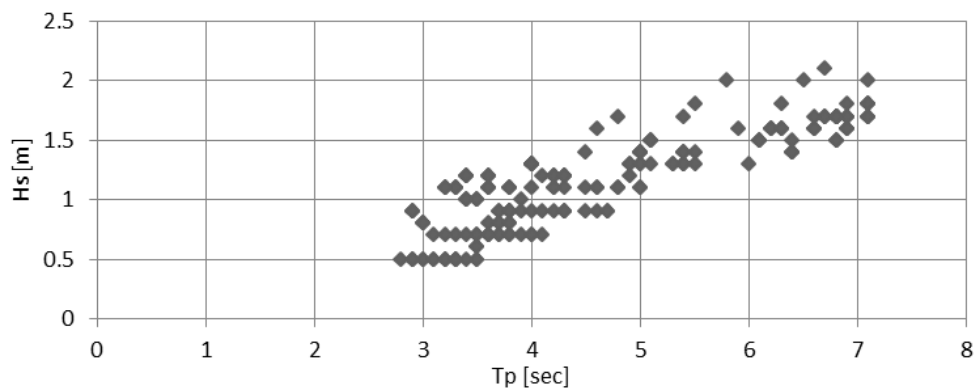
Figure 4 *Wave height/wave period correlation used in the DMA's*

4.2.3 Beam-on and beam-quartering wave/wind directions

The largest fender forces, which eventually lead to the largest forces in the breasting dolphins, are found for waves and winds coming from beam-on to beam-quartering directions, pushing the vessel towards the fenders. The assessment tool is thus conceived for waves and winds coming between 210° and 330° according to the reference system in Figure 5. This is considered an acceptable assumption since it is desired that the largest forces are absorbed by the fenders and not the by the mooring lines.
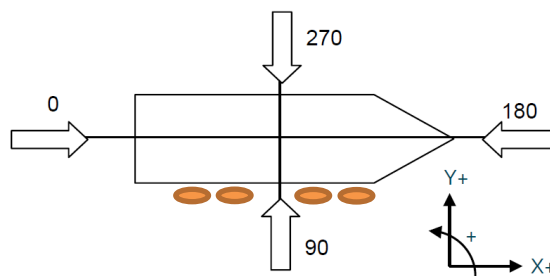
Figure 5 *Direction according to the Cartesian convention [34]*

4.2.4 Fender Loads

As was mentioned previously, the maximum loads on the mooring system are expected to occur during the operational phase and not during berthing of the FSRU. It is assumed that the berthing of the FSRU will occur during good weather conditions, with enough assistance and supervision. The probability of an accidental event is therefore considered small.

Two types of mooring loads are exerted on breasting dolphins: the fender loads and the spring-line loads. When the fender loads are maximal, however, the spring lines are slack, their load zero and are therefore neglected.

4.2.5 Foam filled floating fenders

For mooring facilities on exposed locations large loads can be expected. Only a few fender-types have enough energy absorption capacity to cope with these loads: the Cone/Cell Fenders (Figure 6) and the Foam filled floating fenders (Figure 7).

Due to their wave-shaped force-deflection curve, however, the Cone/Cell fenders are very sensitive to fatigue damage and are therefore not applicable for moorings on exposed locations. The Foam filled floating-types, which have a much flatter force-deflection curve, fatigue is already much less of an issue. These are therefore the only type of fenders which can be applied for the considered mooring facility.
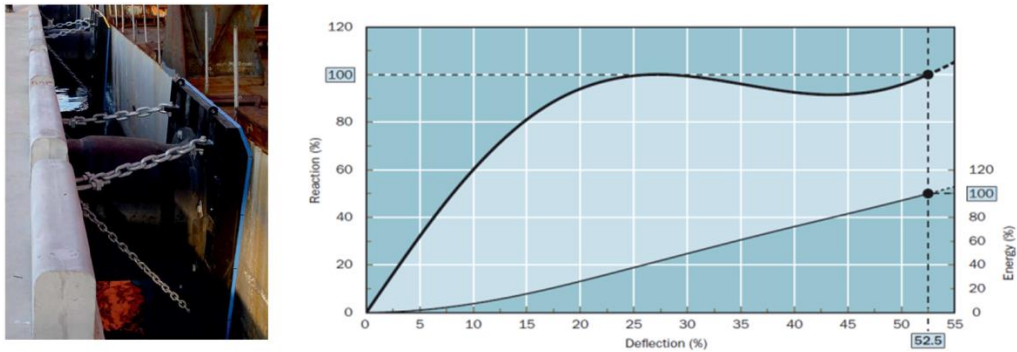
Figure 6 *Picture of a Cell fender and its corresponding force-deflection curve*
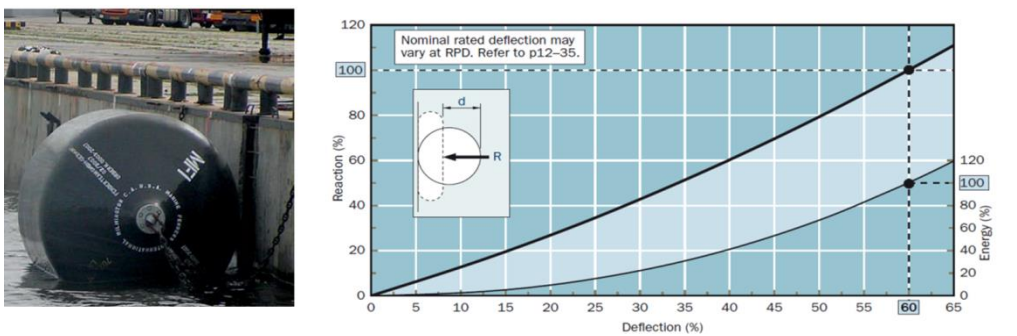
Figure 7 *Picture of a Foam filled floating fender and its corresponding force-deflection curve*

4.2.6 Ballasted condition

The moored FSRU can be found in ballasted- or loaded condition. From the observed DMA-data was concluded that the maximum fender loads are always governing for the ballasted condition.

4.2.7 FSRU-only mooring configuration

The mooring facility is required for the mooring and operating of the FSRU and for side-by-side mooring and LNG transfer between FSRU and LNGC. For this report only the FSRU-only case is considered. It is assumed that moored LNGC's will depart when the environmental conditions become too harsh and the side-by-side configuration will therefore never be governing

4.3   Assessment tool

Two methods are conceived for the estimation of the design fender loads. Both their underlying idea is the separation of the three environmental components: wind, wave and current. This assumption is made possible since foam filled floating fenders are applied with a linear force-deflection curve, as described in the previous section. Additionally, both methods consider winds and currents as quasi-static drag forces as will be explained in (4.3.2). The determination of the fender loads due to wave-action, however, is different for both methods.

In the following section only the method is described which gives the most accurate results. It consists of relating wave heights to fender deflections. The other method consists of normalizing a force-displacement curve. A detailed explanation of the latter is included in Appendix V.

4.3.1   Fender loads due to wave-action

The fender load due to wave action is obtained through the relationship between the significant wave height and the fender deflection. As can be seen from Figure 8, rather accurate results are obtained. The main idea behind this relation is that the FSRU can reach high momentum due to its large mass. This momentum is not easily stopped, regardless of the applied fender type. The fender deflection is thus not significantly influenced by the type of fender which is chosen.
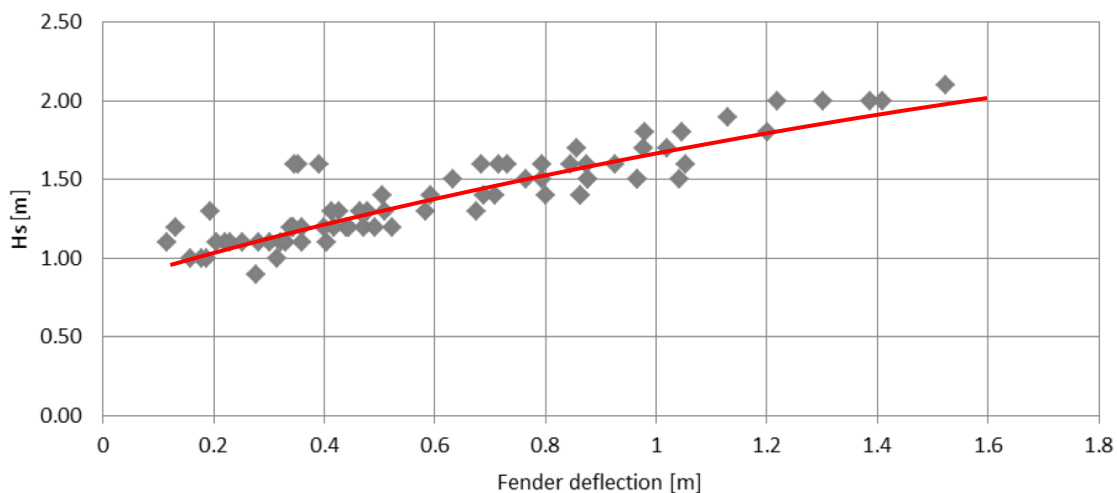
Figure 8 *Wave height / fender deflection*

Thus for a certain wave height, coming from beam-on to beam-quartering direction as was specified, a certain fender deflection can be obtained. Subsequently this fender deflection can be translated to a fender force by means of a chosen force-deflection curve. This results in fender load due to wave-action only (F_{wave}).

4.3.2   Fender loads due winds and currents

The loads due to winds and currents are described as quasi-static drag forces and can be divided into three components:

- A longitudinal force component (F_X) corresponding to the surge motion of the ship.
- A lateral force component (F_Y) corresponding to the sway motion of the ship.
- A yaw moment component (M_{XY}) corresponding to the yaw motion of the ship.
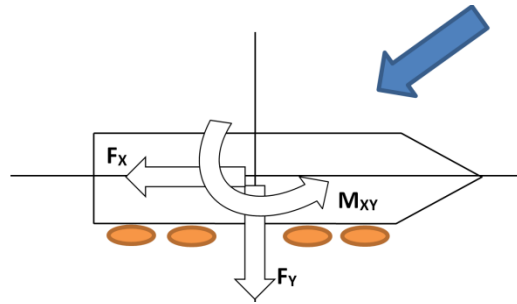
Figure 9 *Drag force components. Blue arrow represents incoming metocean conditions*

For the calculation of the fender load, however, only the lateral force and yaw moment are of interest. The total fender force due to respectively winds and currents can be calculated by means of the following equation:

$$Fwind = \alpha\, \frac{1}{2}\, C_w\, \rho_w\, v_w^2\, L_{BP}\, f\, /\, 1000\ [kN] \qquad\qquad Fcurrent = \alpha\, \frac{1}{2}\, C_c\, \rho_c\, v_c^2\, L_{BP}\, d\, /\, 1000\ [kN]$$

Where:

C_w = Wind coefficient [-] $\qquad\qquad$ C_c = Current coefficient [-]

ρ_w = density in air [kg/m³] $\qquad\qquad$ ρ_c = density in water [kg/m³]

v_w = wind velocity [m/s] $\qquad\qquad$ v_c = current velocity [m/s]

f = freeboard [m] $\qquad\qquad$ d = draught [m]

L_{BP} = Length between perpendiculars [m] $\qquad\qquad$ α = Force distribution coefficient [-]

C_{yw} and C_{yc} dependent on: the angle of attack and the type of vessel. These coefficients have been empirically determined based upon data from physical tests and are illustrated in the OCIMF Guidelines [30].

"Alpha" is a coefficient which takes the distribution of F_y and M_{xy} into account for varying incoming directions. This coefficient is obtained through observed DMA-data and can be extracted from Figure 10. E.g. if the winds and currents would come from beam-on direction (270⁰), the yaw moment would be practically zero and the load will be evenly distributed over the four fenders. Hence a factor of, approximately, 0.25 is found.

For storm conditions, the 1-hourly mean wind velocity is multiplied with a gust factor of 1.37 which is in accordance to the British standard [4].
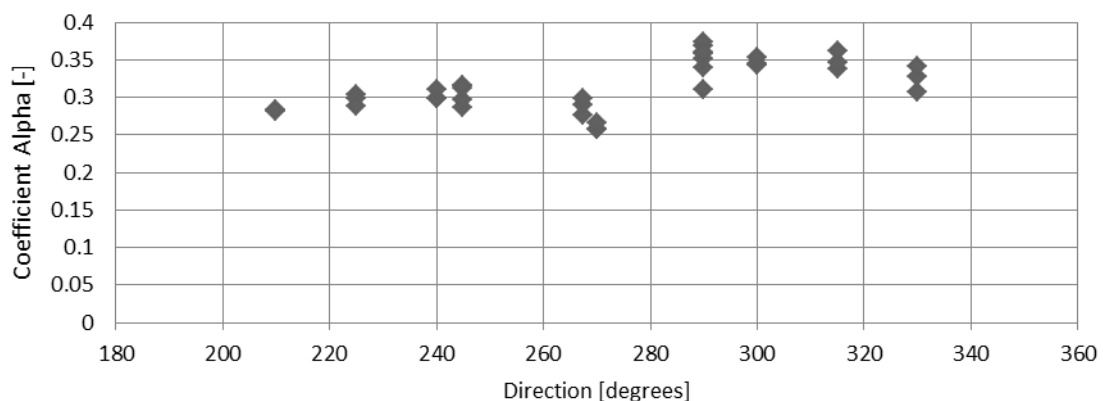
Figure 10 *Coefficient Alpha - incoming direction (according to the Cartesian convention [34])*

4.3.3 Design fender loads

The design fender load is then easily obtained by summing up the contribution of waves, winds and currents:

$$Ffender = Fwave + Fwind + Fcurrent$$

An example of how the application tool should be applied is included in Appendix IV.

4.4 Results

The accuracy of the conceived assessment tool is checked based on the outcome of DMA runs. The DMA runs considered have been taken from the reference projects; Golar and Aqaba.

Fender

The fenders applied within these runs are represented by a maximum fender reaction force ("$F_{reaction}$"). Their force-deflection curves are illustrated in Figure 11. A distinction is made between stiff- and soft fender cases:

- The stiff case includes a +15% manufacturing tolerance on the reaction force.
- The soft case includes a -15% manufacturing tolerance and a -15% multiple cycle reduction on the reaction force.
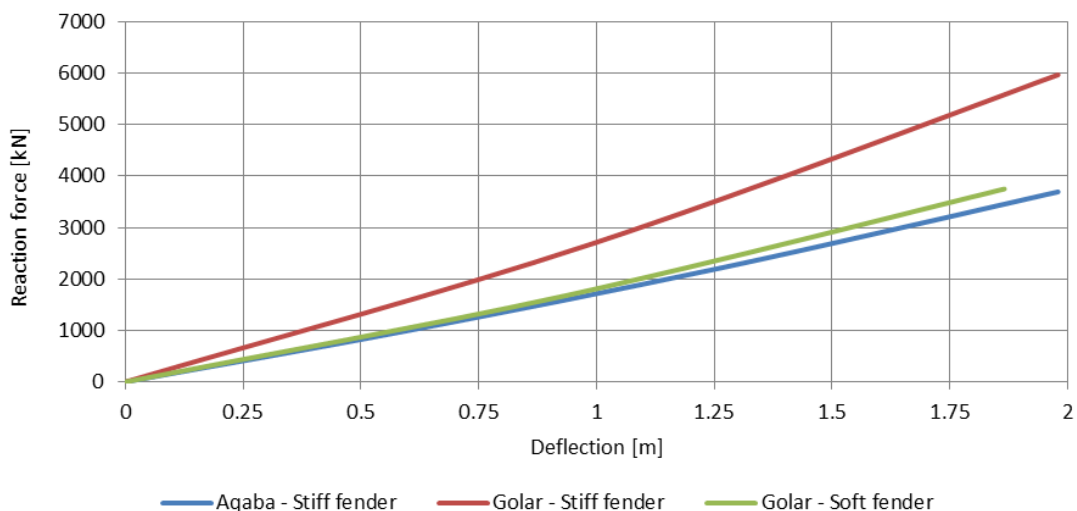
Figure 11 *Fender curves applied in the reference projects*

Environmental conditions

In order to test the accuracy of the assessment tool for somewhat extreme conditions, different types of combinations are considered. The "storm" conditions represent mild storms. The "wave" conditions represent runs which have been made with relatively large wave heights and the "wind" conditions with relatively large wind velocities. The "tsunami" conditions represent runs made with large current velocities.

DMA Results

The outcome of DMA runs consist of a varying fender load over time. The maximum occurring peak load in these runs is described by "MAX F_{fender}". However, since DMA runs in time domain, the maxima are influenced by the length of the runs. The longer the runs, the more likely a larger maximum is found. The Most Probable Maximum (MPM)-method is therefore introduced and is a realization obtained through the distribution of

these maxima. This "MPM F$_{fender}$" is applied as a design value and will therefore be used as comparison for the outcomes of the assessment tool.

Calculated Results

The results were calculated following the procedure discussed in the previous section. The accuracy of these calculated values, compared to the MPM-values, is represented by an error margin.

Project	Aqaba STORM	Golar STORM	Golar WAVE	Golar WAVE	Golar WIND	Golar WIND	Golar TSUNAMI	Golar TSUNAMI
Fender characteristics								
Fender type	Ocean Guard	Ocean Guard	Ocean Guard	Ocean Guard	Ocean Guard	Ocean Guard	Ocean Guard	Ocean Guard
Fender case	Stiff case	Stiff case	Stiff case	Soft case	Stiff case	Soft case	Stiff case	Soft case
F$_{reaction}$ [kN]	3693	5967	5967	3749	5967	3749	5967	3749
Environmental conditions								
Wave direction [deg]	290	270	270	270	270	270	270	270
H$_s$ [m]	2	1.4	1.8	1.8	1.5	1.5	0.75	0.75
T$_p$ [sec]	6.5	5	5.4	5.4	5.1	5.1	2.8	2.8
Wind direction [deg]	290	270	270	270	270	270	270	270
Wind velocity [m/s]	18	18	20	20	24	24	7.5	7.5
Current direction [deg]	170	270	270	270	270	270	270	270
Current velocity [m/s]	0.5	1	1.1	1.1	1.1	1.1	2	2
DMA Results								
MAX F$_{fender}$ [kN]	3359.3	3077	4422	3823	3723	3282	2234	2221
MPM F$_{fender}$ [kN]	3281	2706	3794	3139	3307	2972	2218	2206
Calculated Results								
Deflection [m]	1.52	0.68	1.24	1.24	0.88	0.88	0.2	0.2
F$_{wave}$ [kN]	2743	1841	3511	2356	2383	1555	542	359
F$_{wind}$ [kN]	2048	1969	2431	2431	3501	3501	342	342
F$_{current}$ [kN]	-26	906	1096	1096	1096	1096	3624	3624
α [-]	0.3	0.27	0.27	0.27	0.27	0.27	0.27	0.27
F$_{fender}$ [kN]	3350	2618	4463	3308	3624	2796	1612	1429
Error margin [%]	+ 2%	- 3%	+ 18%	+ 5%	+ 10%	- 6%	- 27%	- 35%

Table 3 *Error margins of the calculated results*

5 Analysis Part 2: Mono-pile

5.1 Introduction

Part 2 consists of standardization of the mono-piles. The design of these piles is very much depend on the local conditions; constitution of the soil, environmental weather conditions and the local water depth. The relations between these variables are studied in order to see to what extent standardization is possible. Once again, this can only be achieved within defined limits. These are described in the "Design Conditions" (5.2).

The design procedure of the mono-piles is treated in the section "Design procedure" (5.3). This consists of determining the dimensions of the mono-pile based on an ULS load case and checking the fatigue damage in the FLS. For the fatigue calculations a case study is used to see whether it may be a decisive factor in the pile design. The results of this analysis are mentioned in section (5.4) and will be further discussed in Chapter 7.

5.2 Design conditions

5.2.1 Requirements and assumptions

A number of starting points have been defined for the design of the mono-piles.

- The mono-piles shall be designed for a 20 year service life.
- The mono-piles shall be designed on the 100 year return period.
- For the design of the mono-piles steel grade X65 will be applied with; yield strength of 448 MPa, density of 7850 kg/m3 and unit cost of 3430 USD/ton. It must be noted that the application of this steel grade is not yet common practice. However, due to the fact that high quality steel is increasingly applied in the offshore industry, it is considered, with a view on the future, an acceptable choice for standardization.
- The ratio between pile diameter (D) and - thickness (t) is set between 65 and 85 as those ratios are often used in practice due to constructability issues.
- Regarding corrosion, no sacrificial steel is included in the design. Cathodic protections will be applied in the form of anodes or impressed-current by means of solar panels.
- Scour is included in the design water depth. If very large scour is to be expected, a bed protection shall be applied.
- Settlement is assumed negligible as the piles have a relatively small self-weight.
- The weight of the pile-head is set on 150 tons.
- The natural frequency of system can be estimated by schematizing the mono-pile & pile-head as a cantilever beam with an end mass. The natural frequency is in the order of:

$$\omega = \sqrt{\frac{3\,EI}{m\,L}} = 9.23\ Hz$$

  The typical period of an FSRU at berth is obtained from previous RHDHV projects and is equal to 6 second (0.17Hz). The natural frequency of the structure is thus much higher than the excitation frequency. Extensive calculations regarding the dynamic effects are therefore left out of consideration.
- Environmental loads acting on the pile are ignored as they are small compared to the mooring loads.
- Torsion due to friction between fender and dolphin is included in the design calculations. The friction force is assumed to be 50% of the fender load.

5.2.2 Water level

As to reduce the investment costs of pipe-laying, LNG transshipment companies will always locate the FSRU as close as possible to the shore. The distance between FSRU import terminal and the shore is thus mainly dictated by the local water depth as a minimum depth is to be maintained for safe maneuvering of the LNGC's. For standardization a constant water depth of 16m is assumed. This includes a tidal difference, an allowance for long-term sea level, possible scour and enough keel clearance. The FSRU reaches a maximum draught of 11,8m in loaded condition. Additionally, the sea bottom is assumed to be flat.

5.2.3 Geotechnical aspects

The geotechnical conditions are very much location bound. In order to analyze the influence of the soil on the design of the mono-pile dolphins, two "extreme cases" are dawn up: a stiff sand profile and a soft clay profile. The parameters have been chosen such that they are still realistic. Other extremes, such as rock and coral, are left out of consideration.

Soft case		Stiff case	
CD -16m until CD -36m Soft Clay	$\gamma' = 6.5 \; kN/m^3$ $c_u = 5 - 55 \; kN/m^2$ $\varepsilon_{50} = 0.02$	CD -16m until -87m Sand	$\gamma' = 8 - 10 \; kN/m^3$ $\varphi' = 32,5°$ $c = 0 \; kPa$ $k = 7500 \; kN/m^3$
CD -36m until CD -66m Stiff Clay	$\gamma' = 7 \; kN/m^3$ $c_u = 55 - 135 \; kN/m^2$ $\varepsilon_{50} = 0.007$ $k = 108000 \; kN/m^3$		
CD -66m until CD -87m Very Stiff Clay	$\gamma' = 9 \; kN/m^3$ $c_u = 150 \; kN/m^2$ $\varepsilon_{50} = 0.005$ $k = 108000 \; kN/m^3$		

Table 4 *Geometrical parameters for the soft- and stiff soil case*

5.2.4 Loadings

5.2.4.1 Permanent load

The permanent load consists of the self-weight of the mono-pile and of the pile-head.

5.2.4.2 Variable load

The variable loads are caused by the vessel motions and are described as a fender load. In order to analyze the influence of this load on the pile design, dummy loads are applied ranging from 2000kN to 9000kN. This 9000kN corresponds to the maximum admissible reaction force of a 3000 x 6500 Foam filled floating Fender Ocean Guard-type, which is the largest of its category. It is assumed that for larger forces, other FSRU mooring systems will be more economically attractive. The fender loads are applied at CD +2.25m.

Furthermore, as the structure is loaded cyclically by the fender due to the constantly moving FSRU vessel at the berth; consequently the mono-piles need to be checked with respect to fatigue. The variable loads which are used for the fatigue assessment are obtained through the case study, Golar-project. These loads were calculated with the aid of Dynamic Mooring Analyses and are included in Appendix XI.

5.2.5 Geometrical boundary conditions

The geometry of a certain mono-pile is represented by its diameter (D), wall thickness (t) and length (L). Since constructing a mono-pile in a single operation is not possible, it will consist of sections. These sections are tubular elements with a certain length which will be welded on top of each other. Their length, however, is limited due to constructability issues and is taken as 2.5m.

Since sustained hard driving may be expected for installation of the piles in the abovementioned soil layer, the minimum wall thickness is in accordance to the API RP-2A-LRFD and should not be less than:

$$t = 6.35 + D/100$$

5.2.6 Standards

The main design considerations are according to the DNV standards. However, for some particular calculations other standards were applied as they were considered more appropriate:

- Structural design of steel structures according to DNV-OS-C101 [12].
- Local buckling according to EN 1993-1-6 [17].
- Modeling of the soil (p-y curves) according to API RP-2A-LRFD [1].
- Fatigue of steel according to DNV-RP-C203 [13] checked with NEN-EN 1993-1-9+C2 [28].
- Geometrical boundary conditions according to API RP-2A-LRFD [1].

5.2.7 Limit States, load factors and combinations

The breasting dolphin piles will be checked in two Limit States:

- Ultimate Limit State (ULS)
- Fatigue Limit State (FLS)

Serviceability Limit State (SLS) and Accidental Limit State (ALS) are left out of consideration as no conditions have been defined with respect to pile deformation and undesired events.

The load and material factors applied to the considered limit states are included in Table 5 and are in correspondence to DNV-OS-C101. For ULS two combinations have been considered: one for structural steel checks ("Steel") and the other for the geotechnical stability ("Soil").

Limit State	LOAD FACTOR		MATERIAL FACTOR	
	Fender Load	Dead Load	Steel Properties	Soil Properties
ULS (Steel)	1.30	1.30	1.15	1.00
ULS (Soil)	1.30	1.30	1.00	1.20 / 1.30
FLS	1.00	1.00	1.00	1.00

Table 5 *Applied load- and material factors for the calculations of the mono-piles*

Regarding the geotechnical stability of the piles, a factor 1.20 will be applied for effective stress analysis (drained conditions[1]) and factor 1.30 will be applied for total stress analysis (undrained conditions[2]):

Effective stress analysis:

$$\tan \varphi'_d = \frac{\tan \varphi'_{char}}{1.20}$$

---

[1] *"Drained conditions" occur when there is no change in pore water pressure due to external loading. In drained conditions, the pore water can drain out of the soil easily, causing volumetric strains in the soil. [3]*

[2] *"Undrained conditions" occur when the pore water is unable to drain out of the soil. In an undrained condition, the rate of loading is much quicker than the rate at which the pore water is able to drain out of the soil. [3]*

Total stress analysis:

$$c_{u,d} = \frac{c_{u,char}}{1.30}$$

5.2.8 Applied software

The design calculations of the laterally loaded piles are performed in the computer package LPile v6.0 (by Ensoft). LPile models the pile as an elastic beam on a foundation of uncoupled non-linear springs (representing the soil), the so-called p-y curves. The program computes deflection, bending moment, shear force and soil response over the length of the pile.

5.3 Design procedure

In this section the modelling and design verifications of mono-piles will be explained. First the geotechnical aspects will be clarified. Then, respectively the structural analysis and the fatigue analysis are clarified.

5.3.1 Geotechnical modelling

The soil resistance against lateral displacement of the pile is modelled with p-y curves. These curves illustrate the nonlinear relation between the soil resistance (p) and the deformation (y). The relation between the resistance and deflection depends on:

- Static or cyclic loading
- Type of soil
- Soil above ground water table
- Depth below surface
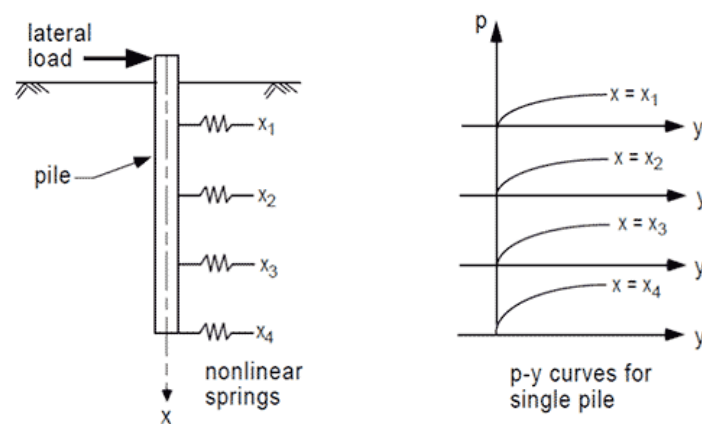
Figure 12 *Schematic representation of the p-y method*

The operational loads on the dolphins have a cyclic character as they are induced by waves. Due to the cyclic loading, degradation of the soil occurs which leads to a loss of strength and stiffness. This effect is taken into account by modified p-y curves. These are described in Appendix VI.

It has to be noted that the determination of the p-y curves are based on results of lateral load tests of piles with a diameter of 0.15m to 0.60m. The application of these curves on larger diameter piles is found to be a conservative approach. However, no other method was found in the literature regarding this matter. The p-y curves are therefore still applied for geotechnical modelling.

5.3.2 Structural analysis

The structural analysis consists of performing laterally loaded pile calculations with LPile and checking the output results on yield strength and local buckling. Such analysis is performed for the Ultimate Limit State and thus for peak loads corresponding to a storm with a 100 year return period as specified in the requirements.

5.3.2.1 Nominal steel stresses

With respect to the steel stresses, linear elastic design is applied; no plastic hinges are allowed to develop under design conditions. When being laterally loaded, four different stresses occur in the piles cross-section: normal stresses, bending stresses, shear stresses and torsional stresses. All are considered for the structural steel check of the structure. However the aforementioned stresses are concentrated in different directions. The equivalent design stress is therefore calculated by means of the Von Mises theory. The steel stresses have been verified in ULS by applying the load- and material factors included in Table 5.

Normal stresses

The normal stresses in the structure are due to the self-weight of the pile-shaft and the pile-head. This stress increases along the pile as the volume of the pile-shaft (and thus the self-weight) becomes larger towards the mud line.

$$\sigma_N = \frac{N_d}{A}$$

σ_N: normal stress [MPa]

N_d: normal force [kN]

A: cross-sectional area [m²]

Bending stress

The bending stresses occur due to two types of bending moments. The first one is due to the operational loads acting in lateral direction. The second is due to the displacement of the top pile, whereby the self-weight exerts a vertical load in an eccentric manner. The general formula for the bending stress reads:

$$\sigma_M = \frac{M_d}{W}$$

σ_M: bending stress [MPa]

M_d: bending moment [kNm]

W: section modulus [m³]

It must be noted that the bending stress due to the lateral acting load is much larger than the bending moment due to self-weight. At the level of the largest occurring bending moments, the self-weight only contributes for 2% of the total moment.

Shear stress

The shear stresses are due to the lateral acting force. The maximum shear stress for a hollow cylinder is calculated as follows:

$$\tau_V = \frac{V\,S_z}{b\,I_{zz}} = \frac{4\,V_d}{3\pi(R-r)}\frac{(R^3-r^3)}{(R^4-r^4)}$$

τ_V: shear stress [MPa]

V_d: shear force [kN]

R: outer radius [m]

r: inner radius [m]

I_{zz}: moment of inertia [m⁴]

S_z: first moment of area [m³]

Torsional stress

Since a friction coefficient of 0.5 is assumed, a torsional moment within the cross-section needs to be taken into account. This torsional moment is equal to the friction forces times the outer radius of the pile. The general formula for torsional stress reads:

$$\tau_T = \frac{T\,R}{I_p} = \frac{T_d\,R}{\frac{\pi}{2}\,(R^4 - r^4)}$$

τ_T: torsional stress [MPa]

T_d: torsional moment [kNm]

I_p: polar moment of inertia [m⁴]

Von Mises equivalent design stress

In case of combined membrane stresses and shear stresses the equivalent Von Mises stress shall be used:

$$\sigma_{vm,d} = \sqrt{\sigma_d^2 + 3\,\tau_d^2}$$

Where σ_d represents the meridional stresses due to bending moments and normal forces and τ_d the shear stresses due to shear forces and torsional moments.

In the cross-sectional check, bending stresses and shear stresses are not combined, as they are concentrated in a different location in the cross-section. The equivalent Von Mises stress is therefore calculated for two locations in the cross-section:

- where bending stresses are maximal and shear stresses are zero:

$$\sigma_d = \sigma_N + \sigma_M$$

$$\tau_d = \tau_T$$

- where shear stresses are maximal and bending stresses are zero:

$$\sigma_d = \sigma_N$$

$$\tau_d = \tau_V + \tau_T$$
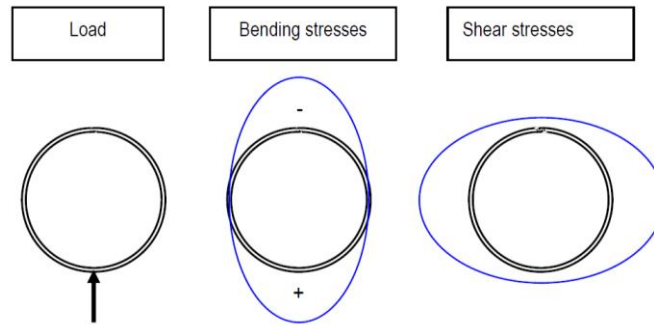
Figure 13 *Illustration of working bending stresses and shear stresses*

The design equivalent Von Mises stress will be the governing value of the abovementioned combinations.

5.3.2.2 Yield strength

The calculated Von Mises stresses are directly compared to the design value of the yield strength of steel. The minimum design yield strength according to DNV-OS-C101 and is calculated as:

$$f_{yd} = \frac{f_{yk}}{\gamma_M}$$

5.3.2.3 Local buckling of piles

The local buckling check is according the Euro code (EN 1993-1-6) and is calculated as follows:

$$\sigma_{Rd} = \frac{f_{yk} * \chi}{\gamma_M}$$

Where χ is a buckling reduction factor, dependent on the relative slenderness of the shell structure. The calculation method for local buckling is included in Appendix VII. The partial factor is based on the DNV-OS-C101.

5.3.3 Fatigue assessment

Cyclic loading of the dolphins may cause fatigue damage. An assessment of the fatigue damage has therefore been made to verify the fatigue life of the dolphins. The assessment is based on S-N-data (Wöhler Curves) and is according to DNV-RP-C203.

Fatigue loading may result during the operational phase due to vessel motions and during the installation phase due to pile-driving. Depending on the soil conditions, pile driving may be of influence on the pile design. In this report, however, only the fatigue loads during the operational phase are taken into account. The effect of the environmental loads on the fatigue life of the dolphin piles had been assessed in a previous study of RHDHV and proven to be negligible compared to the operational loads.

In contrast to ULS calculations, the design stresses for the fatigue assessment ($\sigma_{nominal}$) are not based on maximum occurring loads, but on alternating loads (ΔF) which are the difference between a maximum- and minimum value during a certain time segment (t_{yp}) as is depicted in Figure 14. Critical is the number of times a certain alternating load occurs.
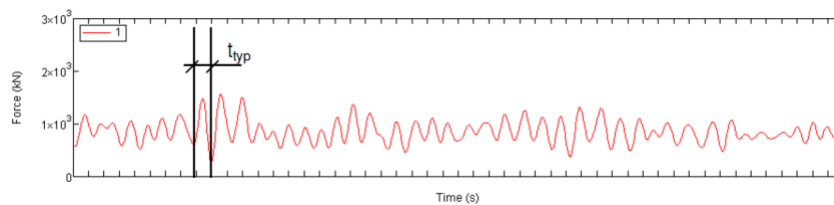
Figure 14 *Example of a time series and time segment needed for fatigue assessment*

The fatigue life will be checked based on data from the Golar- case study, which is an FSRU mooring system located offshore approximately 15km north of Jakarta in the Java Sea. However, since ULS loads and FLS loads are highly correlated it would be unreasonable to check the fatigue life of a pile which has been designed for different ULS loading conditions as the one from the case study. For this reason, only a fatigue assessment is performed on the mono-pile which was designed on the same ULS design load of approximately 5000kN.

5.3.3.1 Processing of DMA-data

The load signals, which are obtained from the DMA runs, have been processed to obtain the required data to perform the fatigue assessment of the dolphins. The load signals, as illustrated above, are translated into sets of alternating fatigue loads (ΔF) and the corresponding number of cycles (n).

For each wave height and incoming direction (16 in total), the number of force fluctuations is described. Below shows an example of the obtained input for the fatigue assessment. The total input is included in Appendix XI.

ΔF	Number of cycles	Conditions
0 – 25 kN	391	Direction: 112.5°
25 – 50 kN	988	H_S = 0.7 m
50 – 75 kN	371	T_P = 3.5 sec
75 – 100 kN	50	U_W = 7.6 m/s

Table 6 *Distribution of number of cycles for alternating loads*

As the DMA models a duration of 6 hours, hence the result is the number of cycles within 6 hours. Based on the probability of occurrence of the considered environmental conditions the total number of cycles during the design life time of the structure (20 years) is calculated:

$$n_{life\ time} = \frac{n_{DMA\ run}}{6\ hr} * 24\ \frac{hr}{days} * 365\ \frac{days}{yr} * 20\ yr * p_{\%}$$

5.3.3.2   Nominal stresses

The alternating fatigue loads (ΔF) which are obtained through Dynamic Mooring Analyses are then translated to fatigue stresses ($\sigma_{nominal}$) by means of the linear relation between load and stress which is expresses as a load transfer function (LTF).

5.3.3.3   Hot spot stresses

Local stress concentrations occur at the welds due to geometric irregularities. The hot spot stresses can be calculated by multiplying the fatigue stresses with the applicable Stress Concentration Factors (SCF):

$$\sigma_{hot\ spot} = SCF * \sigma_{nominal}$$

The SCF is dependent on the type of weld and pile geometry. Since piles are considered without thickness transition, the SCF's are calculated according to the following equation:
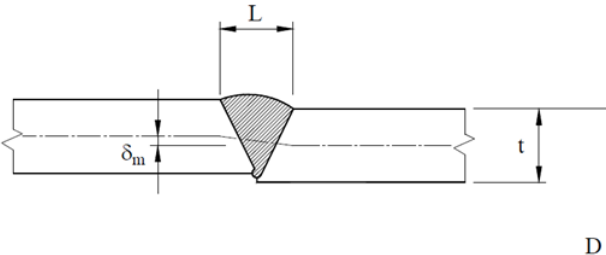
$$SCF = 1 + \frac{3\delta_m}{t}\ e^{-\sqrt{t/D}}$$

Figure 15 *Section through weld*

In above formula "t" is the plate thickness, "D" the diameter and "δ_m" is the maximum allowable misalignment which is equal to 0.1*t and reaches a maximum value of 4mm.

5.3.3.4   Allowable number of cycles

The allowable number of cycles is calculated with the S-N data depending on the required weld properties. For the considered dolphin mono-piles the sections will be connected by good quality butt welds, welded from both sides. These welds correspond to the "C1" S-N-curve [DNV-RP-C203], or to "Class 112" [EN 1993-1-9+C2]. An illustration is showed in the figure below.
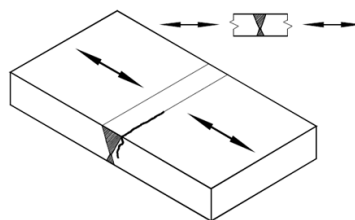
Figure 16 *Transverse butt weld, welded from both sides.*

In general the S-N curves are described by the following formula:

$$\log N = \log \bar{a} - m \log S$$

$$S = \Delta\sigma \left(\frac{t}{t_{ref}}\right)^{k}$$

In which N is the allowable number of cycles and S the stress range. The values of the parameters for the S-N curve C1 in seawater with cathodic protection are included in Table 7:

	N ≤ 10^6 cycles	N > 10^6 cycles
m	3	5
log a	12.449	16.081
k	0.15	0.15
Fatigue limit at 10^7 cycles	65.5	65.5
t_{reff}	25	25

Table 7 *Parameters S-N curve C1 in seawater with cathodic protection*

5.3.3.5 Cumulative damage factor

The fatigue life of the structure is checked based on a cumulative damage factor D_D which is calculated by means of Miner's Law:

$$D_D = DFF * D_C = DFF \sum_{i=1}^{I} \frac{n_c}{N_c} \leq 1$$

The actual number of cycles (n_c) of a certain alternating stress range is divided by the allowable number of cycles (N_c) for that same range. This is done for all occurring stress ranges. The sum of this is referred to as the cumulative damage number and shall not be larger than 1. A design fatigue factor (DFF) of 10 is applied to obtain an overall safety on the calculated fatigue.

A design fatigue factor (DFF) of 10 is normally applied for all the parts of the structure which cannot be inspected during its service life. For the parts that can be expected a lower DFF is allowed. However it is safe to apply a DFF to all sections.

5.4 Results

5.4.1 Structural Analysis

As mentioned previously, the design of the breasting dolphins is very much depended on local conditions; constitution of the soil, fender loads and water depth. In order to determine whether standardization is possible, the influence of these local conditions is investigated. The water depth, however, is taken as a constant for the standardized case and is, as previously stated, set on 16m. The design loads are ranging between 2000kN and 9000kN. Regarding the constitution of the soil, two profiles are considered: the stiff sand profile and the soft clay profile.

For each combination of fender load and soil profile a pile design is made characterized by its dimensions: diameter (D), wall thickness (t) and length (L). For each combination two pile designs are possible; one with an optimized diameter, the other with an optimized wall thickness. For a few combinations, however, the designs were outside the chosen D/t range (65 < D/t < 85), those are marked with a "no".

In the following graphs the influence of the parameters are illustrated. The green dots represent the stiff sand profile; the blue dots the soft clay profile. The lines represent an approximated upper- and lower bound.

In Figure 20 the design loads are plotted against the material costs. Those material costs only comprise the costs of steel. Installation costs due to hoisting and pile driving are not taken into account.

F_D [kN]	Stiff sand profile					Soft clay profile				
	L	D	t	D/t	Check	L	D	t	D/t	Check
	[m]	[m]	[m]	[-]	[-]	[m]	[m]	[m]	[-]	[-]
2000	40	2.5	0.030	83.33	yes	52.5	2.6	0.030	86.67	no
	40	2.3	0.035	65.71	yes	55	2.5	0.035	71.43	yes
3000	40	2.9	0.035	82.86	yes	57.5	3.1	0.035	88.57	no
	40	2.7	0.040	67.50	yes	57.5	2.9	0.040	72.50	yes
4000	42.5	3.1	0.040	77.50	yes	60	3.3	0.040	82.50	yes
	42.5	2.9	0.045	64.44	no	62.5	3.1	0.045	68.89	yes
5000	42.5	3.3	0.045	73.33	yes	62.5	3.6	0.045	80.00	yes
	42.5	3.1	0.050	62.00	no	65	3.4	0.050	68.00	yes
6000	45	3.6	0.045	80.00	yes	67.5	3.7	0.050	74.00	yes
	45	3.4	0.050	68.00	yes	67.5	3.6	0.055	65.45	yes
7000	45	3.8	0.050	76.00	yes	70	3.9	0.055	70.91	yes
	45	3.6	0.055	65.45	yes	72.5	3.8	0.060	63.33	no
8000	45	4.1	0.050	82.00	yes	75	4.2	0.055	76.36	yes
	47.5	3.8	0.055	69.09	yes	77.5	4	0.060	66.67	yes
9000	47.5	4.1	0.055	74.55	yes	75	4.4	0.055	80.00	yes
	47.5	3.9	0.060	65.00	yes	80	4.3	0.060	71.67	yes

Table 8 *Pile designs for varying design loads and soil profiles; "L" is the total length of the pile, "D" is the outer diameter and "t" the wall thickness*
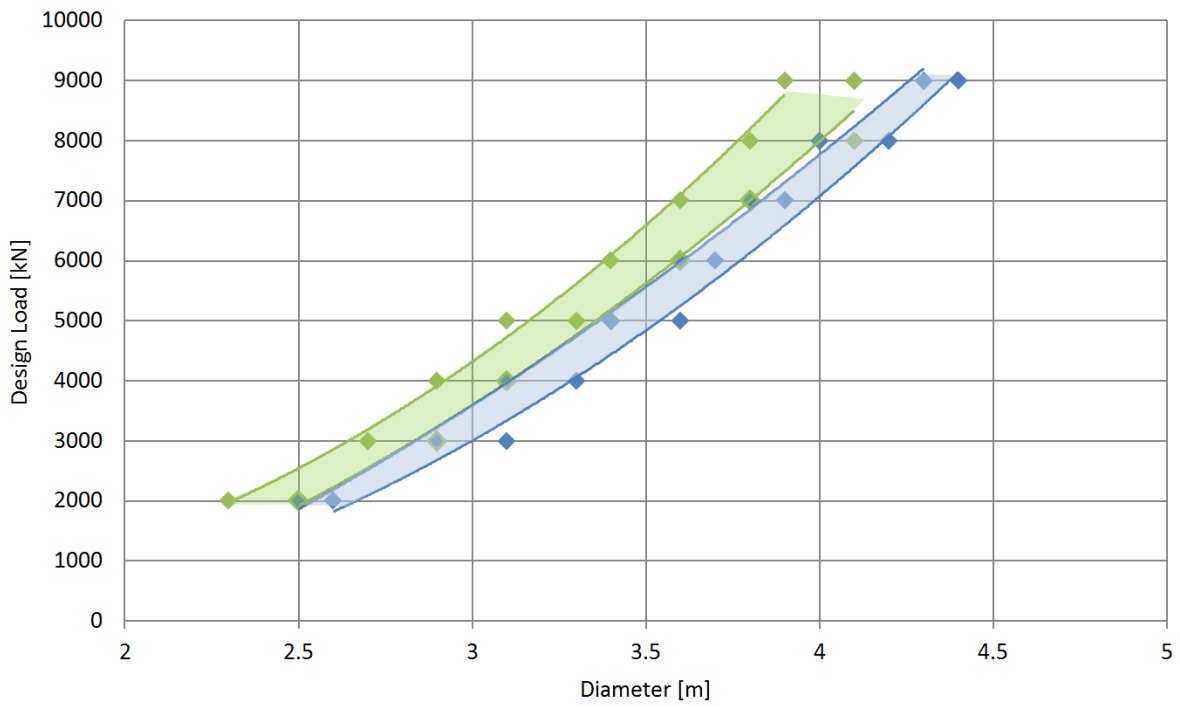
Figure 17 *Design load / Pile diameter; green: stiff soil, blue: soft soil*
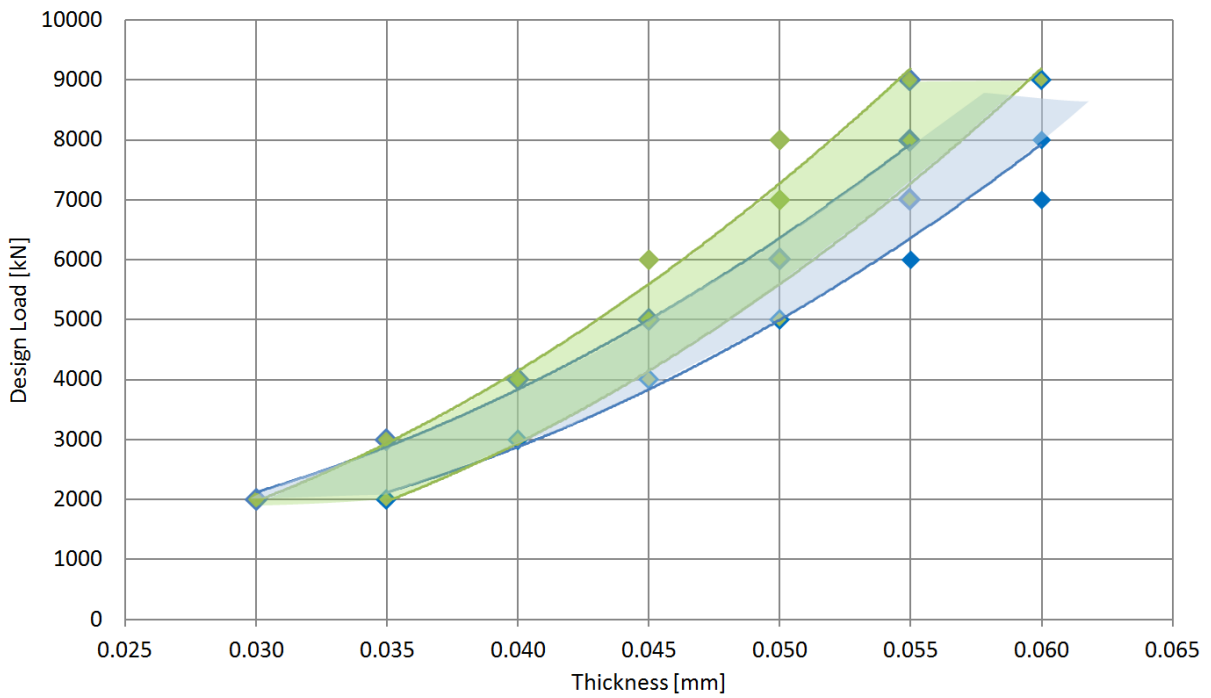
Figure 18 *Design load / Wall thickness; green: stiff soil, blue: soft soil*
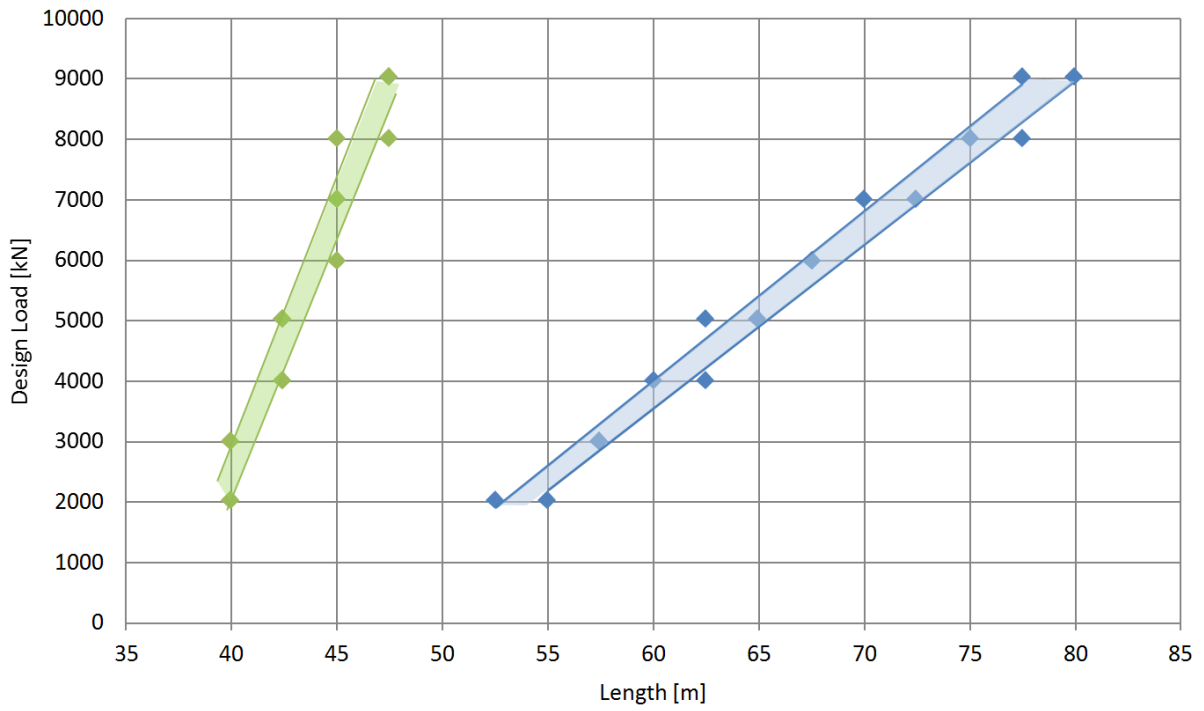
Figure 19 *Design load / Pile length; green: stiff soil, blue: soft soil*
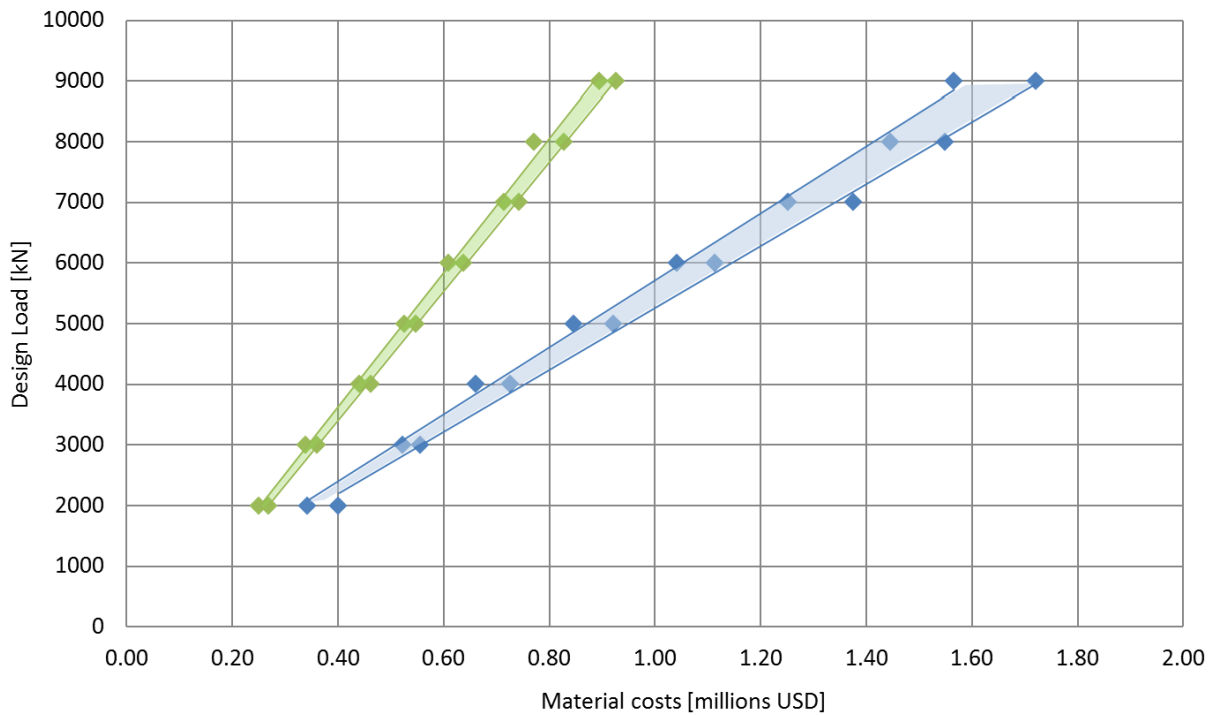
Figure 20 *Design load / Material costs; green: stiff soil, blue: soft soil*

As can be observed from the graphs, for both soil profiles, the pile diameter and wall thickness increases in a rather similar fashion. Those dimensions, moreover, do not differ that much between the two soil cases. The difference in pile length, however, is considerable. For the stiff profile the length increases from 40m to 47.5m, whereas the length for the soft profile increases from 55m to 80m. Due to this large difference, a generalized pile design cannot be achieved without large over-dimensioning.

Additional limits are therefore introduced. As well as distinction in soil profiles, also a distinction in environmental condition is made. Three classes are distinguished; mild, moderate and harsh. The mild environmental conditions result in design fender loads ranging between 3000kN and 5000kN, moderate conditions between 5000kN and 7000kN and harsh conditions between 7000kN and 9000kN.

For each combination of environmental condition and soil profile, a standardized pile design has been defined. These are based on the upper limit.

Soil profile	Dimensions	Environmental condition		
		Mild	Moderate	Harsh
Stiff sand profile	t [mm]	45	50	55
	D [mm]	3300	3800	4100
	L [m]	42.5	45	47.5
Soft clay profile	t [mm]	50	55	60
	D [mm]	3400	3900	4300
	L [m]	65	70	80

Table 9 *Standardized pile dimensions for different combinations of environmental- and geotechnical conditions*

Over-dimensioning

In order to gain an insight in the significance of over-dimensioning of these standardized piles, the excess of steel has been calculated. The over-dimensioning costs increase as the difference between the actual load and the load on which the standardized pile is designed increases. Such is depicted in Figure 21; green for the stiff soil profile, blue for the soft soil profile. It must be noted that the costs of over-dimensioning only cover the material costs of steel.
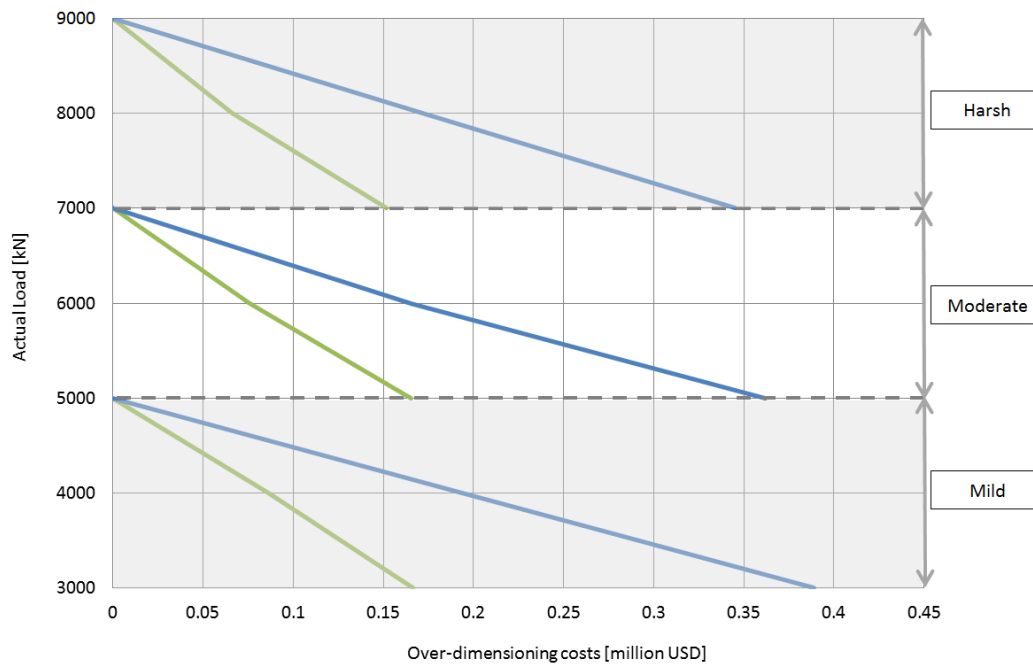
Figure 21 *Over-design in case of standardization [USD]; green: stiff soil profile, blue: soft soil profile*

From Figure 21 can be seen that the over-dimensioning costs of the standardized designs are much larger for the softer soil than for the stiffer soil. These can reach up to 0.38 million USD for the worst case. If compared with the total costs of an FSRU-project, which amounts roughly 25 million USD (based on the Golar-project), these may still be considered small (only 1.5% of the total costs). The averaged range of the over-dimensioning costs per soil profile is listed in Table 10.

Soil profile	Over-dimensioning costs [million USD]	Ratio over-dimensioning costs/ total costs [%]
Stiff sand profile	0 – 0.15	0 – 0.6
Soft clay profile	0 – 0.35	0 – 1.4

Table 10 *Over-dimensioning costs compared to the total costs per mono-pile*

For large scale FSRU-projects, as considered in this thesis, the over-dimensioning costs of the mono-pile breasting dolphins are relatively small. The standardized design discussed in this section can therefore be beneficial for early design stages, where, with little information a good insight can be gained in the dimensions and costs of the dolphins.

Rescaling

Since the FSRU import terminal will always be located as close as possible to the shore, the variation in water depth is considered small. If, however, larger water depths are to be expected, the standardized pile designs presented in Table 9 should be rescaled to an appropriate design. In Appendix IX, the rescaling of the piles has been investigated for a water depth increased by 10 meters (26m total).

In Table 11 rescaling parameters are presented which should be added to the dimensions of the standardized piles in order to increase their size and satisfy their structural stability for a water depth of 26 meters. These rescaling parameters are valid for both soil cases.

Dimensions	Rescaling parameters for 26m water depth
Thickness	+ 5 mm
Diameter	+ 400 mm
Length	+ 12.5 m

Table 11 *Increased pile dimensions for an a water depth of 26m*

5.4.2 Fatigue assessment

The data used within this fatigue assessment was obtained through the case study "Golar-project" which is an FSRU mooring system located in the Java Sea.

Since ULS-loads and FLS-loads are highly correlated, the fatigue assessment is only performed for the mono-pile which had been designed on the same ULS conditions as the one from the case study, namely: soft soil profile and design load of 5000kN. The considered pile dimensions are: 65m x 3.4m x 0.050m (L x D x t).

The results of the assessment are listed below. Respectively: the Stress Concentration Factor, Load Transfer Function and cumulative damage number are:

SCF	LTF	D_D
1.21	0.086	7.83E-02

Table 12 *Results of the fatigue calculations of the mono-pile*

The cumulative damage number is far below one (<< 1). Fatigue damage due to the operational loads can therefore be considered insignificant for the Java Sea. The calculations are included in Appendix XI.

6 Analysis Part 3: Pile-head

6.1 Introduction

This chapter concerns the third and final part of this study, the design of a standardized pile-head. The design procedure started off by conceiving multiple variants very different one from another. The properties of those variants were then evaluated and compared by means of a so-called multi criteria analysis (MCA). From this MCA-evaluation, the pile-head most favorable for standardization purposes is subsequently elaborated.

The variant study is presented in Section (6.2). The requirements and boundary conditions used for the design of the pile-head are mentioned in the "Design Conditions" (6.3). Subsequently more information regarding the applied material and its mechanical properties are described in "Material properties" (6.4), while the design procedure and verifications are treated in the section "Design procedure" (6.5). The structure was modelled in Finite Element-software "SCIA Engineer," where the final design was obtained through an optimization process, constantly adjusting the size and material properties of the different elements. The fatigue life is assessed based on the same case study as the mono-piles. The final design is treated in the section (6.6). Discussion of these results will be included in Chapter 7.

6.2 Variant study

In this Section the MCA is described which led to the designed concept of the pile-head. Primarily the different materials are shortly described (6.2.1). Subsequently different concepts have been conceived from which the forms are adapted to the applied material (6.2.2). Successively, the sliding system for the floating pile-head concepts will be discussed (6.2.3) and the performed Multi Criteria Analysis (MCA) will be clarified (6.2.4).

6.2.1 Material

There are several materials which could be applied for the construction of the pile head. The most common ones are steel and concrete, but also composites becomes more and more practice in hydraulic structures. Regarding sustainability, wood may be an interesting choice.

6.2.1.1 Steel

Steel is the most applied material in offshore and hydraulic engineering due to its high strength to weight ratio and the possibility of welding the connection of different elements for an improved stress distribution. A large disadvantage of the application of steel in wet environments is corrosion which leads to deterioration of the materials properties. The most vulnerable part is located in the splash zone which is intermittently exposed to air and immersed in the sea. Different methods are possible with respect to mitigation and control of corrosion such as coatings, cathodic protections or even design with a corrosion allowance.

6.2.1.2 Concrete

Concrete is very much applied for its high compressive strength. In combination with reinforcement steel (for tensile stresses) it has really good overall properties and is therefore also often applied in hydraulic engineering. However, applying concrete in a wet environment also has its limitation:

- A large concrete cover must be applied for the protection of the reinforcement steel in seawater.
- Poring and hardening of concrete at offshore locations may be problematic. This issue can be partially resolved by applying prefabricated elements.

6.2.1.3 Wood

A wooden pile-head would be a very eco-friendly solution. With respect to durability, only several types of hardwood would be suitable for a construction in a salty environment. Their composition should also be able to

withstand fungus and marine borers. However due to the large expected loads, the strength and mechanical properties are assumed to be insufficient for the design of the pile-head. For this reason wood will not be further discussed in this study. [29]

6.2.1.4   Composite

The application of composites in marine environments is not yet common practice. However, the use of this material may offer significant advantages such as corrosion resistance, fatigue resistance, very high structural damping and low maintenance. Furthermore its low density makes composite an interesting choice for a floating pile-head concept. The main disadvantages include high initial costs and the disability to deform plastically (compared to steel). [20] [31]

6.2.2   Concepts

Multiple concepts have been conceived for the pile-head. A distinction is made between fixed and floating ones. When considering fixed structures, the fender panel may reach very large heights for locations with high tidal variations. The fender itself must then be loose enough to follow the rising and falling of the tide. For a floating pile-head, the height of the fender panel can be reduced significantly. Since the pile-head itself is floating, the fender can be attached in a fixed manner (see Figure 22). The buoyancy can either be achieved by the fender support structure or the fender panel.
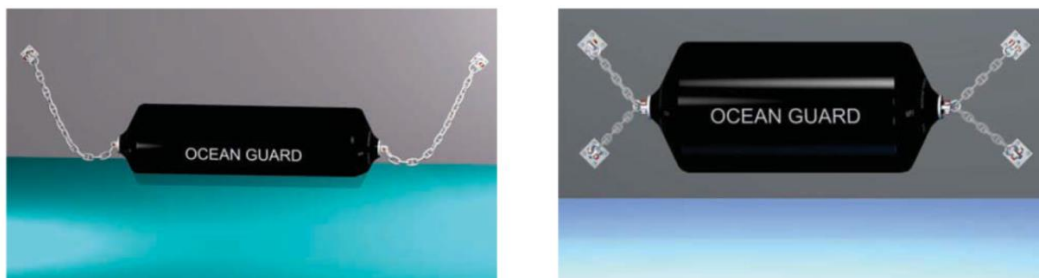
Figure 22 *Foam filled floating fender. Left: floating position, Right: fixed position*

6.2.2.1 Concept 1: Fixed steel pile head

Concept 1 consists of a steel pile-head structure where the fender panel is fully fixated to the mono-pile by means of horizontal plates. The fender loads are transferred in a circumferential manner to the pile.
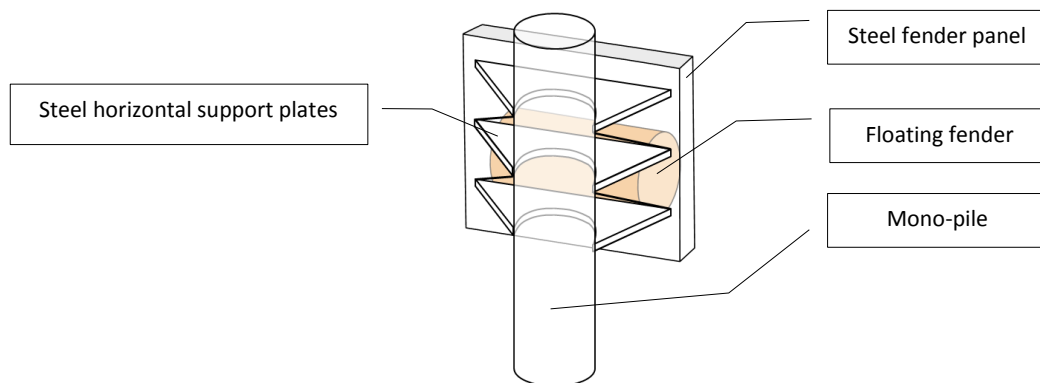
Figure 23 *Steel fender panel connected with steel horizontal support plates to the mono-pile*

- The whole structure can be prefabricated and welded in a single operation onto the mono-pile.
- Ring stiffeners are probably necessary on the locations where the fender support structure is connected to the mono-pile.
- Diagonal trusses required in order to cope with the weight of the fender panel.
- All connections can be welded for an improved stress distribution

6.2.2.2 Concept 2: Fixed concrete cap

The second concept consists of a concrete cap on top of the mono-pile. This type of structure is typically applied for multi-pile dolphins as this method is meant for very stiff structure. The main challenge of this concept lies in the constructability. Since the mooring facility must be designed for open-sea, prefabrication is very much desired preventing having to pour large amounts of concretes on offshore locations.
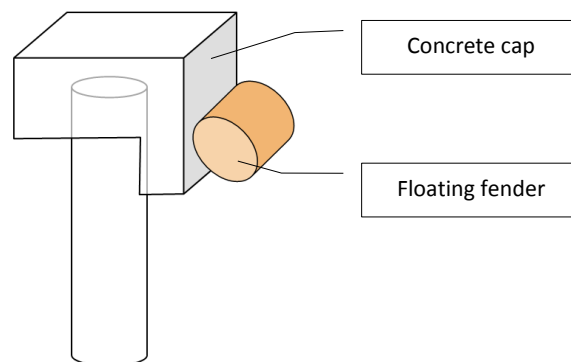
Figure 24 *Fixed concrete cap on top of the mono-pile*

- Easy access for maintenance vessels and simple connection of "secondary structures" such as bollards, ladders, mooring pads, etc.
- Fatigue resistant.
- Good quality concrete is required preventing corrosion of the reinforcement steel.
- For locations where large tidal differences must be overcome, very large amounts of concrete necessary.
- Its large top mass results in a low natural frequency of the whole system which can be within range of environmental loadings.

6.2.2.3   Concept 3: Floating composite cube

Concept 3 consists of a hollow composite cube which floats around the mono-pile. The support structure and fender panel are combined as a single unit resulting in a symmetric shaped pile-head which is favorable for balance issues. The structural stability of the cube is achieved by horizontal plates at various levels inside the cube itself.
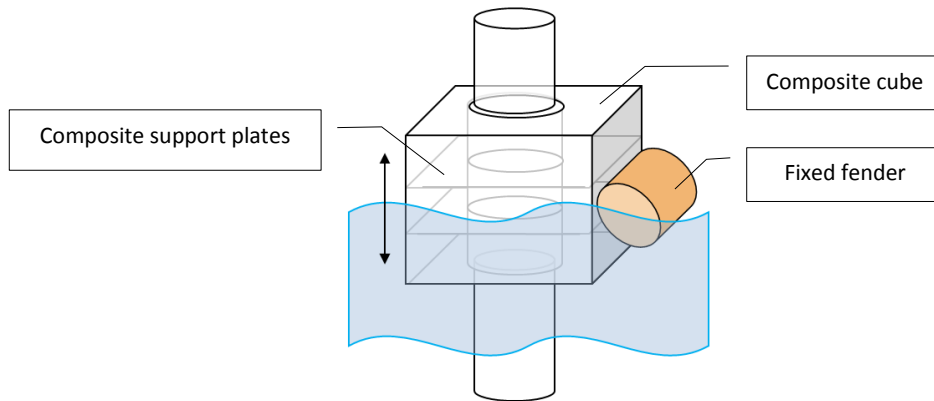
Figure 25 *Floating composite cube*

- The whole structure can be prefabricated and slid in one operation onto the mono-pile.
- Easy access for maintenance vessels and simple connection of "secondary structures"
- The whole structure can be prefabricated and slid onto the mono-pile
- Its rectangular shape can reflect waves which could lead to resonance effects.

6.2.2.4   Concept 4: Floating steel tubular structure

Concept 4 consists of an offshore-like structure constructed with tubular steel elements. The buoyancy is achieved by the bottom-tubes of the support structure. In contrast to concept 3, the fender panel and support structure cannot be combined into a single unit. For balance issues, counterweight is probably necessary in order to cope with the weight of the steel fender panel.
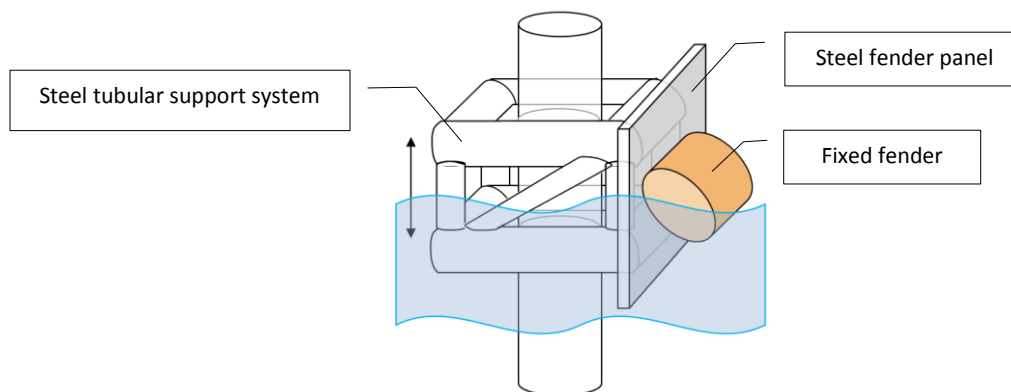
Figure 26 *Floating steel tubular support structure*

- The tubular elements provide improved characteristics against environmental conditions such as drag, inertia and friction.
- The bottom tubes must be relatively large to provide the pile-head with enough buoyancy.
- The whole structure can be prefabricated and slid onto the mono-pile. Since it is made out of steel, relatively large hoisting capacity is required.
- All connections can be welded for an improved stress distribution

6.2.2.5   Concept 5: Floating composite fender panel

Concept 5 consists of a floating composite structure where the buoyancy is performed by the fender panel. The support structure consists of horizontal plates which transfer the loads in a circumferential manner to the pile. For sliding of the pile-head along the pile shaft a sleeve-element is required. Since the center of buoyancy is located eccentrically to the mono-pile a stiff support structure is indispensable.
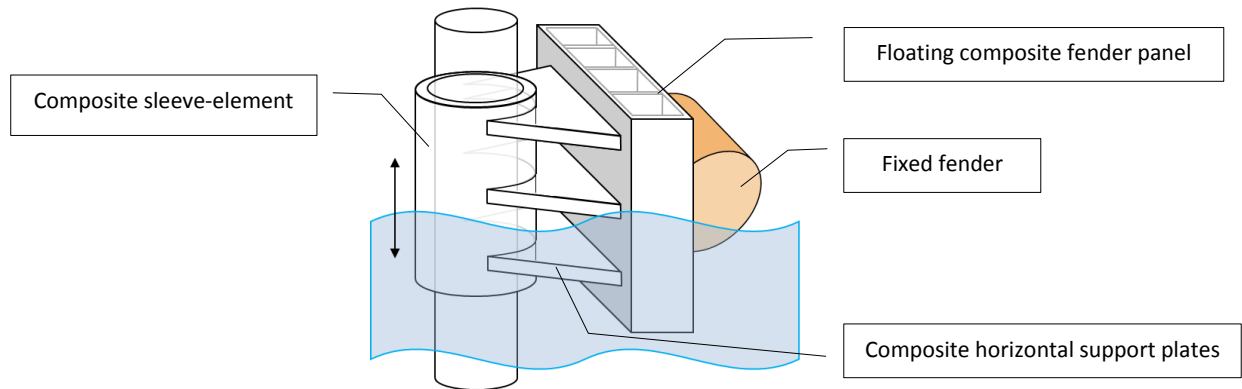
Figure 27 *Floating composite fender panel with horizontal support plates*

- The fender panel must be large enough to provide the pile-head with enough buoyancy.
- Due to the eccentricity of the center of buoyancy, additional loads can be expected in the pile-head.
- The whole structure can be prefabricated and slid onto the mono-pile.
- The floating fender panel must be reinforced by inner compartments which'll acts as vertical stiffeners increasing its flexural rigidity.

6.2.2.6   Concept 6: Floating concrete fender panel

Concept 6 consists of a floating concrete panel. The support structure comprises vertical steel plates which transfer the loads as membrane stresses into the sleeve-element. The support structure must be fixed into the concrete panel during casting operations creating a stiff connection. This can be achieved by e.g. pin dowels.
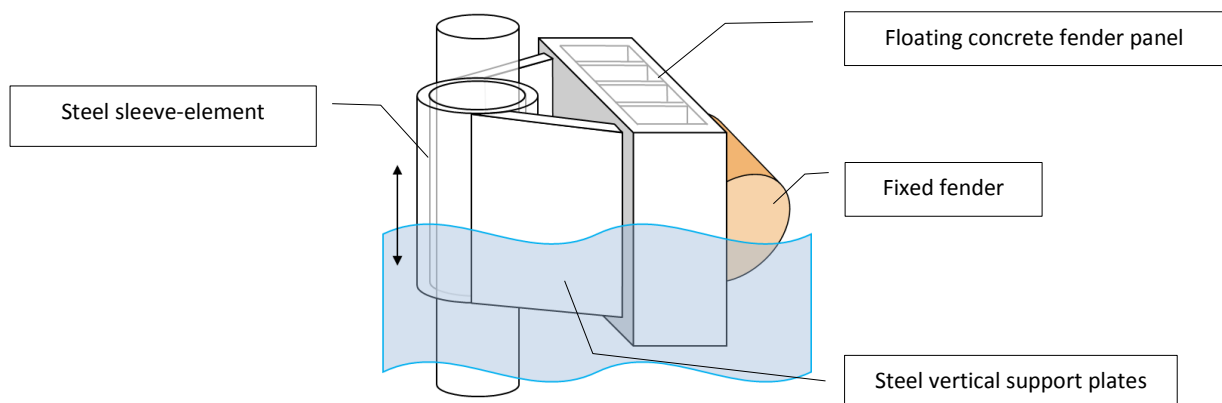
Figure 28 *Floating concrete fender panel with vertical steel support plates*

- The size of the floating concrete fender panel must be considerably larger than the one of concept 5.
- Good quality concrete is required preventing corrosion of the reinforcement steel.
- The support structure will be subjected to lateral flexion due to its non-parallel orientation compared to the exerted load.
- The whole structure can be prefabricated and slid onto the mono-pile. However, due to its very large weight, troublesome hoisting operations are inevitable.

6.2.3 Sliding system

The sliding system is a critical issue for floating pile-head concepts. The only sliding mechanism which allows sliding along- and around the mono-pile (in vertical- and rotation direction) and also provides good load distribution, is a slide bearing system.
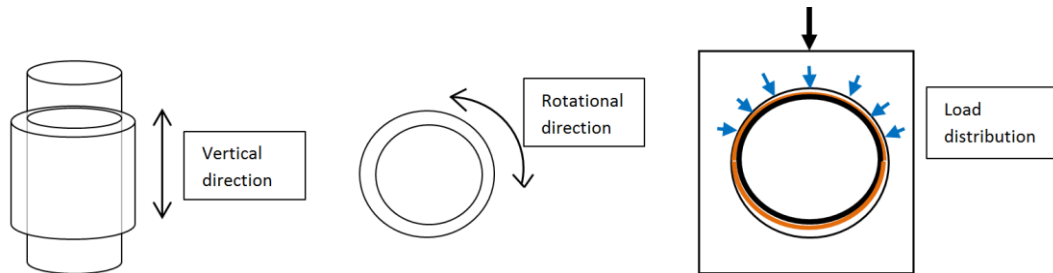
Table 13 *Sliding directions and load distribution of a slide bearing*

Slide bearings consist of a cylindrical bearing with on the inside a fabric of low friction material. This can for instance be; glass fiber bonded with PTFE (polytetrafluoroethylene) or UHMWPE (Ultra high Molecular Weight Polyethylene) [24]. The main features of fiber slide bearings are:

- High load capacity.
- Low friction coefficient.
- Very good corrosion resistance.
- Good resistance to impact.
- No suffer from "stick-slip" effect (rocking motion which can occur when two objects slide over each other).

6.2.4 Multi Criteria Analysis

In this chapter a Multi Criteria Analysis (MCA) is performed in order to compare the different concepts. Those concepts are tested on several criteria listed in Section (6.2.4.1). Since the different criteria have certain degrees of importance; they will first be granted a weighting factor (Section 6.2.4.2). The results of the MCA are included in Section (6.2.4.3).

6.2.4.1 Criteria

Robustness	The robustness of the structure concerns the ability to withstand large impacts and weather it is susceptible for collapse and deformations.
Durability	Durability is the capability of withstanding wear and tear, aging and decay over time. This criterion takes into account whether or not the structure is designed for the full lifespan, or if some elements must be replaced during the service life.
Maintenance	Maintenance regards the ease of replacing certain elements and if the maintenance works can be done in-situ. This criterion also concerns corrosion resistance.
Reparability	Reparability is the ease to repair broken components.
Fatigue resistance	This takes into account the extent to which the structure is resistant to fatigue due to cyclic loading. This criterion mainly concerns the connections since those are the critical elements.
Constructability	Constructability regards the fabrication of the elements, the ease of assembly, and the complexity of the connections. This criterion takes into account whether the structure can be prefabricated or must be constructed in-situ.

Installation	For the installation the weight of the structure is important. Installation mainly regards the installation equipment; whether or not cranes with high hoisting capacity are required.
Transport	This criterion regards the equipment required for transportation.
Costs	The costs in this MCA only mentions the initial material costs depending on the applied material.
Accessibility	This criterion depends on the accessibility of the pile-head for inspection and maintenance works.
Sustainability	Sustainability takes into account the environmental impact; such as CO_2 emissions, use of chemicals, etc.

Table 14 *Criteria applied for the MCA*

6.2.4.2   Weighing factors

The criteria are not equally important. In the following table the mutual relations are determined. If the criteria are equally important they both get a score of 1. If a criterion is more important than the other it will be granted a score of 2 and the other 0.

	Robustness	Durability	Maintenance	Reparability	Fatigue	Constructability	Installation	Transport	Costs	Accessibility	Sustainability	Total	Weighting Factor
Robustness	X	1	2	2	1	2	2	2	2	2	2	18.0	16.4
Durability	1	X	2	2	1	2	2	2	1	2	2	17.0	15.5
Maintenance	0	0	X	1	1	1	1	0	1	1	0	6.0	5.5
Reparability	0	0	1	X	0	1	1	1	1	1	0	6.0	5.5
Fatigue	1	1	1	2	X	2	2	2	2	2	2	17.0	15.5
Constructability	0	0	1	1	0	X	2	2	1	2	1	10.0	9.1
Installation	0	0	1	1	0	0	X	1	1	1	1	6.0	5.5
Transport	0	0	2	1	0	0	1	X	0	1	0	5.0	4.5
Costs	0	1	1	1	0	1	1	2	X	2	1	10.0	9.1
Accessibility	0	0	1	1	0	0	1	1	0	X	0	4.0	3.6
Sustainability	0	0	2	2	0	1	1	2	1	2	X	11.0	10.0
Total												110.0	100.0

Table 15 *Weighing factors applied for the MCA*

6.2.4.3   Comparison of concepts

With the weighting factors from above, the concepts will be compared with each other. Per criteria a score can be granted from 0 to 10. This score is than multiplied with the weighting factor in order to obtain a value. The sum of the values gives the final result.

	Weight. factor	Concept 1		Concept 2		Concept 3		Concept 4		Concept 5		Concept 6	
		Score	Value	Score	Value	Score	Value	Score	Value	Score	Value	Score	Value
Robustness	16.4	8	130.9	9	147.3	6	98.2	5	81.8	7	114.5	7	114.5
Durability	15.5	4	61.8	8	123.6	9	139.1	4	61.8	9	139.1	6	92.7
Maintenance	5.5	7	38.2	8	43.6	7	38.2	4	21.8	6	32.7	6	32.7
Reparability	5.5	5	27.3	2	10.9	8	43.6	8	43.6	7	38.2	4	21.8
Fatigue	15.5	4	61.8	8	123.6	9	139.1	4	61.8	9	139.1	3	46.4
Constructability	9.1	7	63.6	3	27.3	8	72.7	6	54.5	8	72.7	6	54.5
Installation	5.5	7	38.2	2	10.9	7	38.2	6	32.7	9	49.1	2	10.9
Transport	4.5	6	27.3	8	36.4	6	27.3	6	27.3	7	31.8	6	27.3
Costs	9.1	7	63.6	4	36.4	3	27.3	7	63.6	5	45.5	7	63.6
Accessibility	3.6	7	25.5	9	32.7	9	32.7	3	10.9	6	21.8	6	21.8
Sustainability	10.0	4	40.0	6	60.0	2	20.0	4	40.0	2	20.0	5	50.0
Total	100.0		538.2		592.7		656.4		460.0		684.5		486.4

Table 16 *Results of the MCA*

The most favorable pile-head concept is concept 5; floating composite fender panel with horizontal support plates and a slide-bearing sliding system. The design is further elaborated in the following sections.

6.3   Design conditions

6.3.1   Requirements & assumptions

A number of starting points have been defined for the design of the pile-head.

- The pile-head shall be designed for a 20 year service life.
- The pile-head shall be design on the 100 year return period.
- Since a floating pile-head is designed, tidal variations do not have to be taken into account.
- The fender applied for the design is a foam filled floating Ocean Guard-type with a diameter (D) of 3.3m and a length (L) of 6.5m. The corresponding maximum fender reaction force is 7101kN [19].
- It is assumed that the hull of the ship will never be governing. It can be reinforced if necessary.
- The pile-head should be designed for a temperature range of -10C to +30C.
- The fender should be, at all time, located between vessel and fender panel.
- Inspection and maintenance works should be possible.
- Environmental loads acting on the pile are ignored as they are small compared to the mooring loads.

6.3.2   Material

The pile-head will be designed with FRP-composite as was concluded from the MCA. The main pros and cons are listed below [15]. More information regarding the applied composite is further elaborated in Section (6.4).

Pro	Con
Good in-plane mechanical properties	Brittle
High fatigue and environmental resistance	High initial costs
Adjustable mechanical properties	Low to moderate application temperature (-20/+80 °C)
Lightweight	Low fire resistance (sometimes with unhealthy gases)
Low maintenance	Lack of design practice
High material damping	

Table 17 *General pros and cons of FRP composite*

6.3.3   Loadings

6.3.4   Permanent load

The permanent load consists of the self-weight of the structure.

6.3.5   Variable load

The variable loads are caused by the wave induced motions pushing the vessel further into the fenders, transferring a reaction force to the pile. The fender chosen for standardization has a maximum fender reaction force of 7101kN. Further fender characteristics are listed below.

Compression [%]	Deflection [m]	Reaction Force [kN]	Diameter [m]	Flat length [m]	Flat height [m]	Pressure [kN/m²]
0.0%	0.00	0	3.30	4.20	0.00	0
2.0%	0.07	237	3.23	4.23	0.10	560
5.0%	0.17	591	3.14	4.28	0.26	532
10.0%	0.33	1184	2.97	4.35	0.52	523
20.0%	0.66	2367	2.64	4.50	1.04	506
30.0%	0.99	3551	2.31	4.65	1.56	490
36.8%	1.21	4356	2.09	4.75	1.91	480
49.2%	1.62	5823	1.68	4.94	2.55	462
55.0%	1.82	6510	1.49	5.03	2.85	455
60.0%	1.98	7101	1.32	5.10	3.11	448

Table 18 *Fender characteristics, Ocean Guard-type 3.3 x 6.5*

It is deemed good design practice to ensure that the structure can withstand the full reaction of the fender at maximum compression. The structures must therefore be able to resist a maximum reaction force of 7101kN (448kN/m2). In the reaction force a manufacturing tolerance is taken into account of 15% (stiff fender case).

At the interface between the fender and the composite panel a friction coefficient of 0.4 is adopted. A horizontal- and vertical friction force is therefore taken into account working parallel to the fender panel's surface.

Inside the sleeve-element a low friction material is added such as PTFE (polytetrafluoroethylene) or UHMWPE (Ultra High Molecular Weight Polyethylene). For the interface between the mono-pile and the sleeve element a friction coefficient of 0.1 is used which works along the pile-shaft, according the GUR product-catalogue [24].

Furthermore, as the structure is loaded cyclically by the fender due to the constantly moving FSRU vessel at the berth; consequently the structure needs to be checked with respect to fatigue.

6.3.6 Geometrical boundary conditions

6.3.6.1 Mono pile
The mono-pile which is being considered in this study must resist the full fender reaction load of 7101kN, which results in a design load of approximately 9200kN based on the load factors from DNV-OS-C101. This corresponds to a mono-pile with an outer diameter of 4.5m.

6.3.6.2 Fender panel
The fender panel must be large enough in order to cope with the footprint of the fully compressed fender. For a fender with a diameter of 3.3m and a length of 6.5m the maximum footprint is 5.10m by 3.15m (at 60% compression) as can be seen in Table 18.

The dimensions of the fender panel are according to Trelleborg Marine Systems [41] and are depicted in Figure 29:
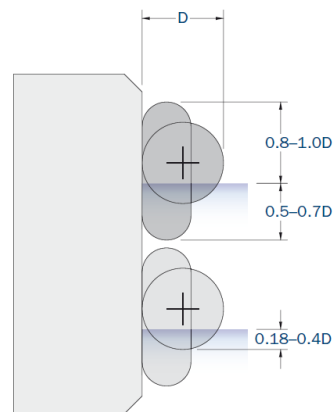
Figure 29 *Mounting area foam filled floating fender [41]*

The required height of the fender panel is:

$$h_{panel} = 0.9\,D + 0.7\,D = 5.3\,m$$

The length of the panel is taken as the length of the fender including a 1m clearance at each side for fastening of the chains:

$$l_{panel} = L + 2 * 1m = 8.5\,m$$

The width of the fender panel must be taken large enough in order provide the whole system with sufficient buoyancy.

6.3.6.3 Support structure

The support structure consists of a sleeve element, which slides around the mono-pile following the rise and fall of the tide, and of horizontal plates which connect the fender panel to this sleeve element.

The sleeve element must fit tightly around the mono-pile, preventing it from moving and deform which would lead to undesired secondary forces. The inner diameter must therefore be a little bit larger than the outer diameter of the mono-pile of 4.5m.

6.3.7 Standards

- Load factors according to DNV-OS-C101 [12].
- Structural design of composite structures according to CUR 096 [7].
- Fatigue of composite according to GL – Wind Energy.

6.3.8 Limit States, factors and combinations

The pile-head will be checked in two limit states:

- Ultimate Limit State (ULS)
- Fatigue Limit State (FLS)

The Serviceability Limit State (SLS) is left out of consideration as no limit is defined regarding deformations of the structure during daily conditions.

The Accidental Limit State (ALS) mostly concerns undesired accidental events. This Limit State is taken into consideration by testing the structure on loads which are exerted in an eccentric manner onto the fender panel. This may occur for example by failing of one of the fender chains. This limit state is included in one of the ULS load cases as will be clarified later on.

The loads will be modified applying a load factor in accordance to the DNV standard. The structural design of the composite and its corresponding material- and conversion factor is in accordance to the CUR 96 [7]. Material and conversion factors will be clarified in section "Material properties".

Limit State	Fender load factor	Dead load factor	Material factor	Conversion factor
ULS	1.3	1.3	1.62	1.57
FLS	1.0	1.0	1.62	1.43

Table 19 *Applied factors for the calculations of the pile-head*

6.3.9   Applied software

6.3.9.1   SCIA Engineer
The structural analysis was performed with software package SCIA Engineer. By means of this software a global elastic analysis of the fender panel and the support structure was made.

6.3.9.2   Kolibri
Kolibri was used to calculate and analyze the mechanical properties of different laminates based on the laminate theory. With this software stiffness matrices were generated which were necessary in order to define certain orthotropic material properties within SCIA Engineer. More information regarding the stiffness matrices will be given in the section (6.4) "Design procedure".

6.4   Material properties

In this section the design material properties will be enlightened. First a brief introduction will be given regarding Fiber Reinforced Polymers and the different types of laminates. Subsequently the choice of the different materials will be clarified based on which the mechanical properties of the laminates will be determined. Finally the design values will be mentioned.

6.4.1   General information

In the most basic form a composite material is composed of two elements working together; a bulk material and a reinforcement to increase the strength and the stiffness of the bulk material. The composite which are considered in this study is the so-called Fiber Reinforced Polymers (FRP). These materials use a polymer-resin as bulk material and reinforcement in fiber form.

Resin systems have limited mechanical properties, but it is when combined with reinforcing fibers that exceptional properties can be obtained. The resin then spreads the load applied to composite between each of the individual fibers and also protects it from damage. Since FRP's combine a resin system with reinforcement fibers, the properties of the resulting composite material will be a combination of both material properties.
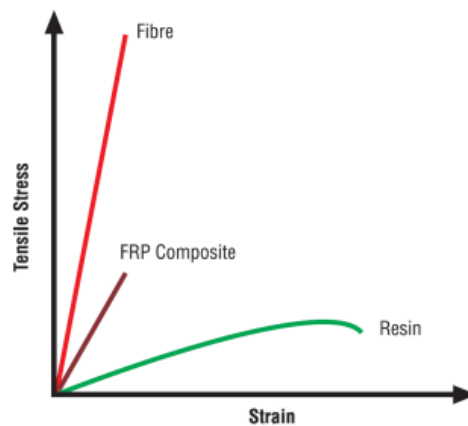
Figure 30 *Material properties FRP Composite [23]*

The properties of a ply are thus very much dependent on the alignment and orientation of the fibers within the ply. In order to have good mechanical properties in all directions, most laminates are built up by stacking plies of fibers of different directions onto each other (see Figure 31).
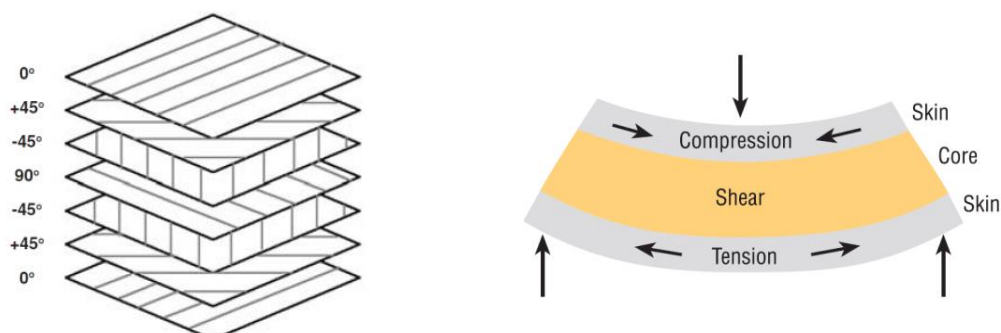
Figure 31 *Left: Stacking sequences, Right: Sandwich panel loading [23]*

For this study quasi-isotropic laminates will be applied as will be explained further on in this report. This implies that that the amount and the type of fibers in each direction of the laminate (0/+45/-45/90) is the same.

For laminates which need extra flexural stiffness, a sandwich structure can be applied. Such a sandwich structure consists of two skins, which are built op by stacks of plies, and a core material in the middle. By inserting a core into the laminate is a way of increasing its thickness without drastically increasing its weight. In effect the core acts like the web in an I-beam.

In this study the two types of laminates will be referred to as:

- Monolithic laminate; a single skin laminate consisting of stacks of reinforced plies only
- Sandwich laminate; two skins separated by a core in the middle.

6.4.2   Material choice

6.4.2.1   Fibers

Three main fiber types are distinct: glass-, aramid and carbon fibers. The carbon fibers have a very low density and a greater stiffness compared to glass fiber. Regarding the impact strength, aramid is the advantageous choice. However, both aramid and carbon are far more expensive than glass fibers (up to a factor 4-8 higher).

Since no "extremely" good mechanical properties are required for the design of the pile head, the costs are the decisive factor in the fiber choice. Glass fiber will therefore be applied.

6.4.2.2   Resin

For resin, three main types are distinct: polyester, vinyl and epoxy. The density, Young's modulus and tensile strength of the different resin do not differ much. Regarding the maximum elongation, epoxy (8.0%) is more advantageous than polyester (2.5%) and vinyl (6.0%).

But also for the resins choice, the costs outweigh the mechanical properties. Because polyester is the most economical resin it is also the preferred choice.

6.4.2.3   Core material

Since quasi-isotropic laminates are applied, also an isotropic core material is required in order to reduce the complexity of the sandwich elements. The core materials choice is therefore the best fulfilled by an isotropic foam.

From preliminary designs could be concluded that certain elements of the support structure are subjected to very large shear forces. In order to increase the shear capacity, very high density foam is therefore applied, type PMI foam 200s. Further design characteristics are listed in Table 20 [5].

6.4.3   Design values

The design values are determined with the following equation:

$$X_d = \frac{X_k}{\gamma_m \gamma_c}$$

Where; X_k is the characteristic value of a certain materials properties; γ_m is the material factor and γ_c the conversion factor.

6.4.3.1   Characteristic values

As mentioned previously two types of laminates are considered; the monolithic laminate constituted of a single skin structure and a sandwich laminate consisting of two skins and a core.

The skin material is quasi-isotropic and consists of 50% resin and 50% fiber from which 25% is orientated in each direction: 0/ +45 / -45 / 90.

The strength of the skin material in each direction (for tension, compression and shear) is based on a single strain criterion. This strain criterion is according the CUR 96 and amounts 1.2%. The characteristic values of both skin material and core material are listed below:

Properties	Unit	Skin Material	Core Material
Density	[kg/m³]	1850	205
E, compression	[MPa]	18600	388
E, tension	[MPa]	18600	352
ν	[MPa]	0.33	-
G	[MPa]	6992	138
σ, compression	[MPa]	223.2	7.66
σ, tension	[MPa]	223.2	8.48
τ	[MPa]	168	5.47

Table 20 *Mechanical properties skin- and core material*

6.4.3.2 Material factor

The material factor consists of the following components

$$\gamma_m = \gamma_{m,1} * \gamma_{m2}$$

With:

γ_{m1}: takes into account uncertainties in the material properties and is equal to 1.35

γ_{m2}: takes into account uncertainties in the manufacturing process. For vacuum- and pressure injection a partial factor of 1.2 applied.

6.4.3.3 Conversion factor

The conversion factor consists of the following components:

$$\gamma_c = \gamma_{ct} * \gamma_{cv} * \gamma_{ck} * \gamma_{cf}$$

With:

γ_{ct}: conversion factor for temperature effects and is equal to 1.1

γ_{cv}: conversion factor for moisture effects. For a FRP structure which is constantly exposed to humid conditions, as is the case in this study, a partial factor of 1.3 is applied.

γ_{ck}: conversion factor for creep. Since the structure is subjected to short impact loads this partial factor is set as 1.0.

γ_{cf}: conversion factor for fatigue and is equal to 1.1.

Table 21 indicates which partial conversion factors need to be applied for the different Limit States and is in accordance to the CUR 96. The conversion factor for fatigue and creep only needs to be applied for stiffness issues which are required for ULS design checks.

Conversion factors	Stability	Fatigue
Temperature	X	X
Moisture	X	X
Creep	X	
Fatigue	X	

Table 21 *Conversion factors for the different Limit States*

6.5 Design procedure

In this section the modelling of different elements within SCIA will be explained. First will be clarified how different materials are modelled within SCIA and how their design verifications are made. Subsequently the modelling of the loads will be enlightened, including the different load cases on which the structure has been tested.

6.5.1 Material

6.5.1.1 Monolithic laminate

The monolithic laminates consist of glass-fiber and polyester-resin only. Those laminates are modelled as an isotropic material, thus with similar mechanical properties in every direction. The design check of elements designed as monolithic laminates is therefore very straight forward. By means of SCIA Engineer the Von Mises equivalent stresses can be modelled, which can directly be compared to the maximum allowable stresses of that laminate.

6.5.1.2 Sandwich laminate

For sandwich laminates the modelling and design check is less obvious. Since sandwich laminates consist of both skin- and core material, it must be considered as an orthotropic material. The mechanical behavior of such a laminate is described by a so-called ABD-matrix, also known as a stiffness matrix. Such ABD matrices are calculated by means of software package Kolibri and manually inserted in SCIA for each element [11].
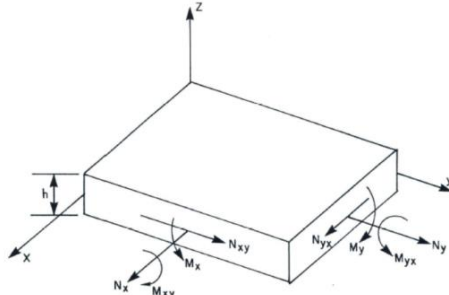
$$
\begin{bmatrix} N_x \\ N_y \\ N_{xy} \\ M_x \\ M_y \\ M_{xy} \end{bmatrix} = \begin{bmatrix} A_{11} & A_{12} & A_{16} & B_{11} & B_{12} & B_{16} \\ A_{12} & A_{22} & A_{26} & B_{12} & B_{22} & B_{26} \\ A_{16} & A_{26} & A_{66} & B_{16} & B_{26} & B_{66} \\ B_{11} & B_{12} & B_{16} & D_{11} & D_{12} & D_{16} \\ B_{12} & B_{22} & B_{26} & D_{12} & D_{22} & D_{26} \\ B_{16} & B_{26} & B_{66} & D_{16} & D_{26} & D_{66} \end{bmatrix} \begin{bmatrix} \epsilon_x^0 \\ \epsilon_y^0 \\ \gamma_{xy}^0 \\ \kappa_x \\ \kappa_y \\ \kappa_{xy} \end{bmatrix}
$$

Figure 32 *ABD-matrix [43]*

This laminate stiffness matrix is used to express resultant forces (N) and resultant moments (M) in terms of mid-plain strains (ϵ^0) and mid-plain curvatures (κ). The matrix consists of thee sub-matrices: an extensional stiffness matrix [A], a bending stiffness matrix [D] and an extension-bending coupling matrix [B].

When a composite is built up in an asymmetric manner, coupling may occur between normal forces and bending moments described by matrix B. However also other coupling effects may arise, all shown in Figure 33.
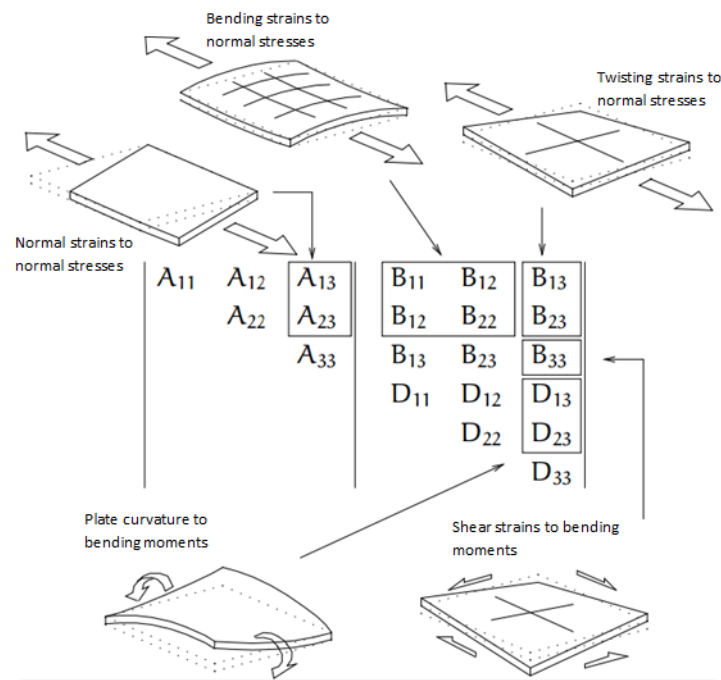
Figure 33 *Coupling effects [16]*

Nevertheless, for this study both the skin material as the core material are chosen isotropic, which means that the laminate is symmetric and the mechanical properties are similar in x- and y-direction. The coupling effects can therefore be neglected and the terms showed in Figure 33 are equal to zero.

Regarding the design check of the sandwich plate, those cannot be achieved by modelling the Von Mises equivalent stresses as is the case for the monolithic laminates. For sandwich panels the unity check must be performed by comparing the local strain to the maximum strain criterion of 1.2%. The local strain variation in the laminate can be calculated with the equation showed below, where 'z' is the level within the laminate and the other parameters are calculated through the ABD matrix.

$$
\begin{bmatrix} \varepsilon_x \\ \varepsilon_y \\ \gamma_{xy} \end{bmatrix} = \begin{bmatrix} \varepsilon_x^0 \\ \varepsilon_y^0 \\ \gamma_{xy}^0 \end{bmatrix} + z \begin{bmatrix} \kappa_x \\ \kappa_y \\ \kappa_{xy} \end{bmatrix}
$$

6.5.2   Load

6.5.2.1   Modelling

The impact load is induced by the FSRU being pushed into the fender which is then transferred as a fender reaction force onto the structure. This reaction force is referred to as the primary load and consists of:

- The load (in x-direction) which is due to the direct impact of the vessel onto the fender.
- Horizontal- (y-direction) and vertical friction loads (z-direction) at the interface between fender and fender panel.

Since the vertical friction load is much larger than the buoyancy force, the structure has the tendency to move up and down during impacts. This leads to a secondary friction forces along the pile's shaft, at the interface between steel and the low friction material (yet to be defined), see left Figure 34.
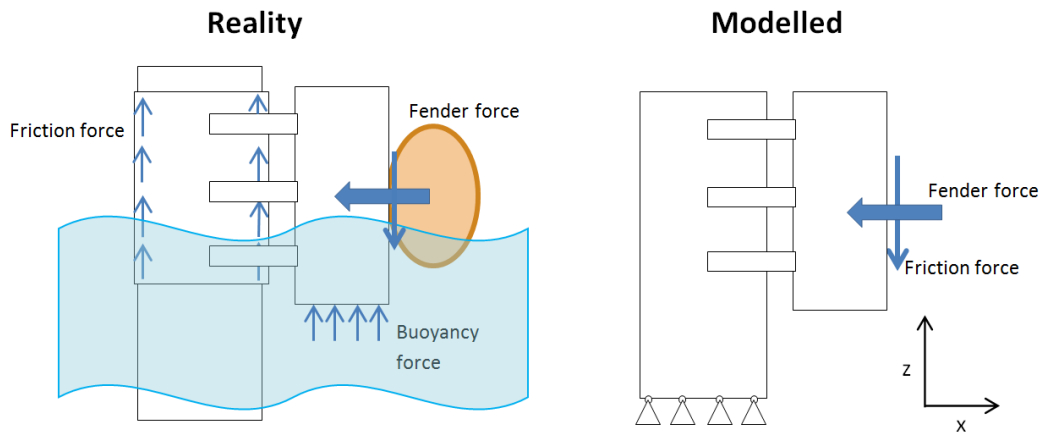
Figure 34 *Schematization of the modelled pile-head within SCIA Engineer*

Since it is not possible to model the contact area between the sleeve element and the pile within SCIA, they are defined as one single element. This is considered a safe assumption since, during very large impacts, the mono-pile and the sleeve element will function together as one stiff element temporarily losing its ability to slide.

The vertical friction component is taken differently for ULS and FLS. For the ULS case, the horizontal impact force is so large that the pile-head will not be able to slide in vertical direction. The maximum friction force is thus taken as $0.4 \cdot F_{fender}$ (friction coefficient between fender and panel). For the FLS case the impact loads are considerably less during which the pile-head will still be able to slide along the mono-pile. For this limit state the maximum friction force is taken as $0.1 \cdot F_{fender}$ (friction coefficient between mono-pile and sleeve element).

The upward buoyancy force is a factor 17 smaller than the vertical friction load and is therefore neglected in the model.

Also the chain loads are left out of consideration as they do not contribute to the general stability of the system. In a more detailed phase however, the connection between the fender chains and fender panel must be looked into.

6.5.2.2 Load cases

For the ULS two load cases are distinct. One where the fender is located central on the fender panel. This is its usual position as it is kept in place by fender chains. In the second ULS load case the fender is located eccentrically on the fender panel. Such a position may be reached during failure of one of the fender chains. The FLS is modelled for daily conditions where the fender is also located central on the panel.

Additionally, for every case, the fenders footprint is positioned at the bottom of the panel as this leads to the most critical loads within the structure.

In the following section, the direct fender reaction force (in x-direction) is referred to as "F_F". The vertical- and horizontal friction components are respectively described by "F_{VER}" (z-direction) and "F_{HOR}" (y-direction).

ULS 1: fender central on panel

For the ULS 1 load case the fender is located centrally on the panel. Additionally, both friction coefficients are taken as 0.4.

$F_F = \gamma_{ULS}*7101 \text{ kN}$
$F_{VER} = 0.4*F_F$
$F_{HOR} = 0.4*F_F$
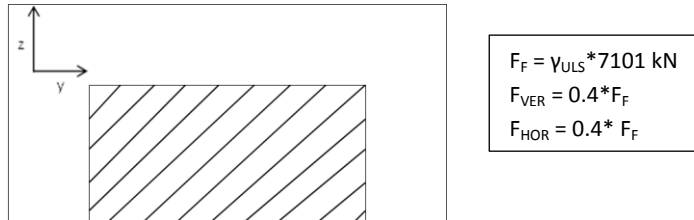
Figure 35 *Position of the modelled load for ULS 1- load case*

ULS 2: fender eccentric on panel

For this load case the horizontal friction load is not taken into account. It was already considered very unfavorable having the load in an eccentric position. Besides, the probability of failure of the fender chains is considered very small.

$F_F = \gamma_{ULS}*7101 \text{ kN}$
$F_{VER} = 0.4*F_F$
$F_{HOR} = 0$
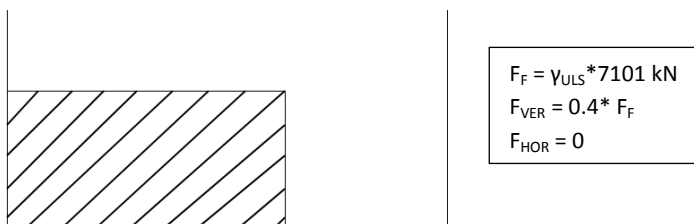
Figure 36 *Position of the modelled load for ULS 2- load case*

FLS: fender central on panel

For the FLS load case the fender is located centrally on the panel. The vertical friction coefficient is taken as 0.1 and the horizontal coefficient as 0.4.

$F_F = \gamma_{FLS}*7101 \text{ kN}$
$F_{VER} = 0.1*F_F$
$F_{HOR} = 0.4*F_F$
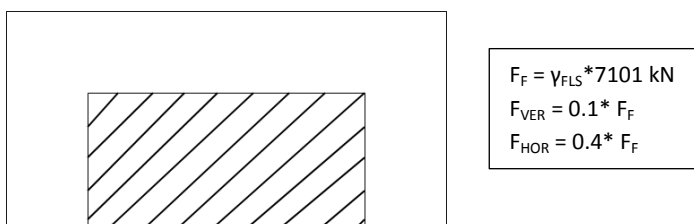
Figure 37 *Position of the modelled load for FLS- load case*

6.5.3 Fatigue analysis

Fatigue failure arises from cyclic loading whereby cracks initiate and grow under fluctuating stresses. The fatigue strength of a particular FRP composite does not only depend on the cyclic loading but also on the mean stress present in the component under consideration. As for metals this mean stress is neglected, for FRP composites this has been found to overestimate fatigue strengths since creep effects are ignored [5].
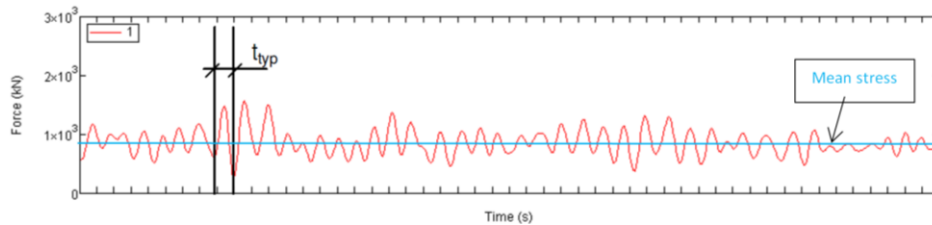
Figure 38 *Time series of varying fender load*

The relation between mean- and alternating stress is illustrated through the Goodman diagram. At zero mean stress, the allowable stress amplitude is the effective fatigue limit for a specified number of cycles. As the mean stress increases, the permissible amplitudes steadily decrease. At a mean stress equal the ultimate (tensile/compression) strength of the material, the permissible amplitude is zero. [24]
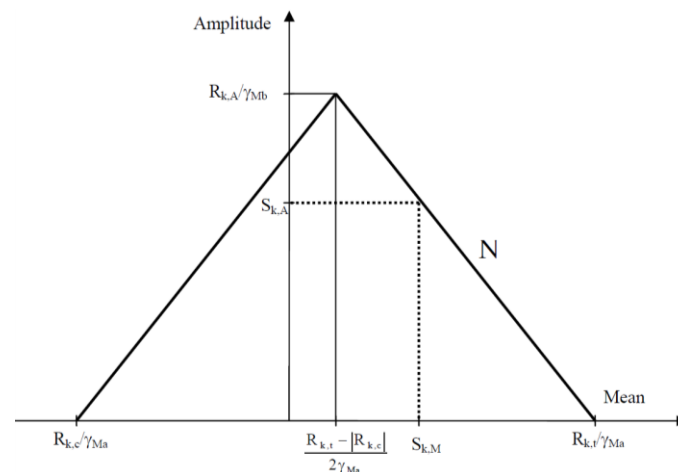
Figure 39 *Goodman diagram [21]*

This Goodman diagram can be used to calculate the permissible load cycle numbers "N" and is in accordance to GL [21];

$$N = \left(\frac{R_{k,t} + |R_{k,c}| - \left| 2\,\gamma_{M,a}\,S_{k,M} - R_{k,t} + |R_{k,c}| \right|}{2\,(\gamma_{Mb}/C_{1b})\,S_{k,A}} \right)^m$$

$S_{k,M}$:   mean value characteristic actions

$S_{k,A}$:   amplitude of the characteristic actions

$R_{k,t}$:   characteristic structural member resistance for tension

$R_{k,c}$:   characteristic structural member resistance for compression

m: slope parameter of the S-N curve (m = 9 for laminates with polyester resin)

γ_M: material factors

The fatigue life of the structure is checked based on a cumulative damage D_D which is calculated by means of Miner's Law:

$$D_D = \sum_{c=1}^{I} \frac{n_c}{N_c} = \frac{n_1}{N_1} + \frac{n_2}{N_2} + \cdots + \frac{n_M}{N_M} \leq 1$$

The actual number of cycles (n_c) of a certain stress range is divided by the allowable number of cycles (N_c) for that same stress range. This is done for all occurring stress ranges. The sum of this is referred to as the cumulative damage number and shall not be larger than 1.

For the fatigue assessment, again, the Golar-project is used as a case study.

6.5.3.1   Mean stress

The mean fender force is due to pre-tensioning of the mooring lines and second-order drift forces. Regarding the latter, it sometimes contributes as an increase of the mean force and sometimes as a decrease, depending on the direction of the incoming waves and currents. For this study, however, this component is neglected due to a lack of data regarding this matter.

Regarding the pre-tensioned mooring lines, 16 are used for fastening of the FSRU; 12 breasting lines and 4 spring lines. In order to calculate the net resulting lateral force pushing the vessel towards the fenders, only the breasting lines are taken into account. As the spring lines are mainly meant for longitudinal stability of the moored ship their contribution to the lateral force is considered negligible.

The breasting lines applied in the Golar project consist of a standard ISO-2408, 8-strand steel rope with a steel wire diameter of 56mm combined with a nylon tail with a diameter of 129.4mm and a Minimum Breaking Load (MBL) of 3335kN. The pre-tensioning force is 3% of the MBL, leading to a force of 100kN in each line. The resulting lateral force is obviously also depending on the fairlead's positions.
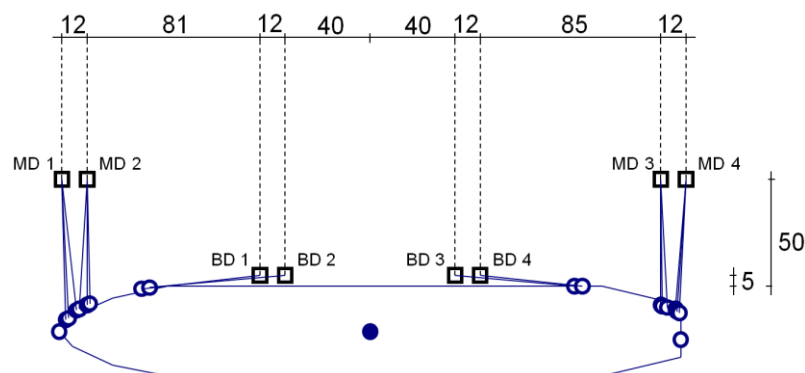
Figure 40 *Mooring lay-out, Golar-project in the Java Sea *Dimensions in meters*

Line number	Type of line	Length [m]	Hor. angle [degrees]	Vert. angle [degrees]	Force [kN]
1	Breast line	65.0	1.9	11.9	97.80
2	Breast line	64.2	2.6	12.1	97.68
3	Breast line	61.6	6.7	12.7	96.89
4	Breast line	60.7	3.7	12.8	97.31
5	Breast line	58.8	0.1	13.2	97.36
6	Breast line	58.4	1.3	13.3	97.29
11	Breast line	60.2	0.4	12.9	97.47
12	Breast line	60.6	0.8	12.8	97.51
13	Breast line	61.5	2.9	12.6	97.47
14	Breast line	63.1	5.1	12.3	97.32
15	Breast line	63.5	4.1	12.2	97.49
16	Breast line	63.9	3.0	12.1	97.64
				Total pre-tensioning force	1169.22
				Pre-tensioning force per fender	292.31

Table 22 *Resulting lateral pre-tensioning force*

The total lateral pre-tensioning force has then to be distributed over four fenders. Subsequently, the mean force per fender (F_F = 292.31kN) is inserted in SCIA Engineer in order to calculate the critical mean stresses for the different elements of the pile-head. Since this pre-tensioning can be seen as a static force, the horizontal- and vertical fender friction components are set equal to zero (F_H = 0, F_V = 0).

6.5.4 Alternating stresses

The alternating fatigue loads (ΔF) are induced by the dynamic behavior of the ship exposed to environmental conditions and had been modelled in Dynamic Mooring Analyses (DMA's). In order to translate those fatigue loads to fatigue stresses within the structure, dummy loads are applied. The fatigue stresses in the pile-head can be found with the linear relation between load and stress which is expresses as a load transfer function (LTF).

It must be noted that this approach is not fully correct for the elements consisting of sandwich laminates. However, it already gives good estimation of the fatigue stresses and therefore the fatigue damage.

The alternating fatigue loads are time-varying impact loads. When modelling those within SCIA, the friction components are taken into account (F_H = 0.4*F_F, F_V = 0.1*F_F).

6.6   Derived solution

6.6.1   Final design

The pile-head is constructed of two main elements; the fender panel and the support structure. The fender panel consists of an empty box-element which provides floatation capacity for the whole structure and a continuous facing for the compressed fender. The support structure consists of horizontal plate element, which transfer the loads to the mono-pile, and a sleeve element which slides along the pile shaft. All components of the pile-head are shortly described below.

The **sleeve-element** is a cylindrical bearing which is constructed of 40mm thick monolithic laminate with on the inside a fabric of low friction material for smooth sliding operations.

The **horizontal plates** transfer the loads from fender panel in a circumferential manner to mono-pile. Those elements contain high axial- and flexural rigidity in order to cope with respectively large normal forces and bending moments. The horizontal plates consist of sandwich laminates with two outer skins of 20mm and a foam core of 300mm.

The **side plates** increases the stiffness of the horizontal plate's extremities. They prevent large deformations and transfer horizontal loads directly into the membrane of the sleeve-element. The side plates are monolithic laminates with a height of 400mm and thickness of 30mm.

The **front plates** increase the stiffness of the horizontal plates at the connection with the fender panel and improve the load distribution within these horizontal plates. The front plates are monolithic laminates of 400mm high and 40mm thick.

The **front panel** is the element on which the fender is compressed. It consists of a sandwich laminate with two outer skins of 10mm and a core of 250mm

The **rear panel** provides the back facing of the whole fender panel. This element distributes the fender loads over the three horizontal plates. It has similar dimensions as the front panel.

The **inner walls** connects front- and rear panel. Also they function as vertical stiffeners for the front panel increasing its flexural stiffness. The inner walls are 2m wide, 5.3m high and are built up as 30mm thick monolithic laminates.

The **top and bottom plates** have as main function to keep the fender panel watertight as they do not really contribute to load transfer. Those plates are 2m wide, 8.5m long and are 30mm thick monolithic laminates.
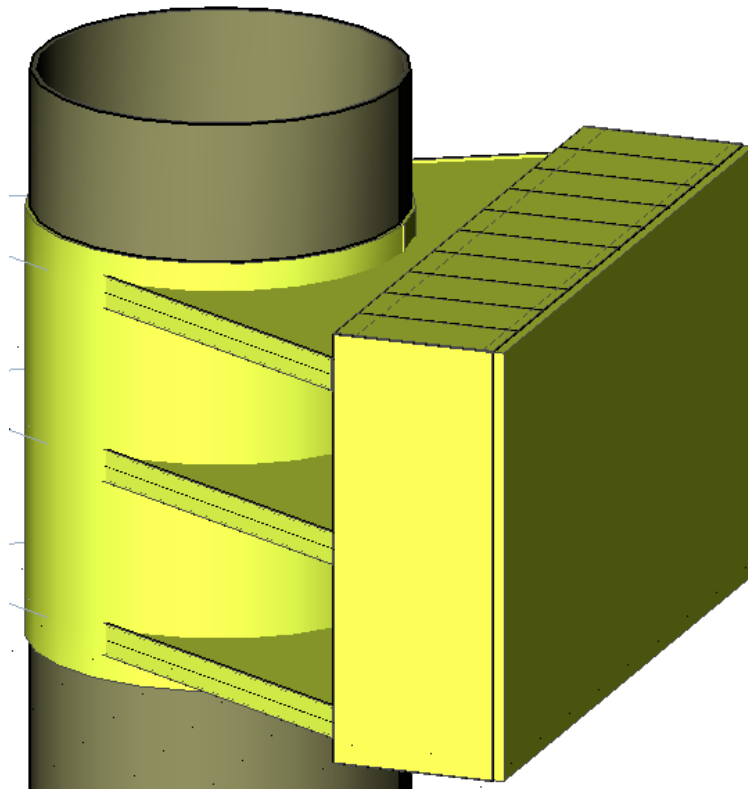
Figure 41 *Front view final design pile-head*
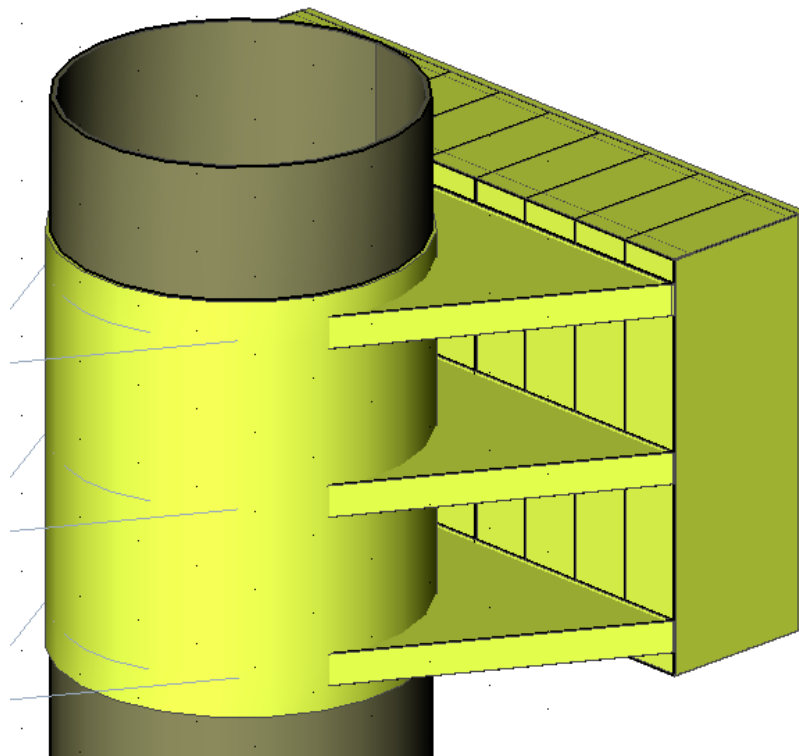
Figure 42 *Rear view final design pile-head*

6.6.2 Dimensions
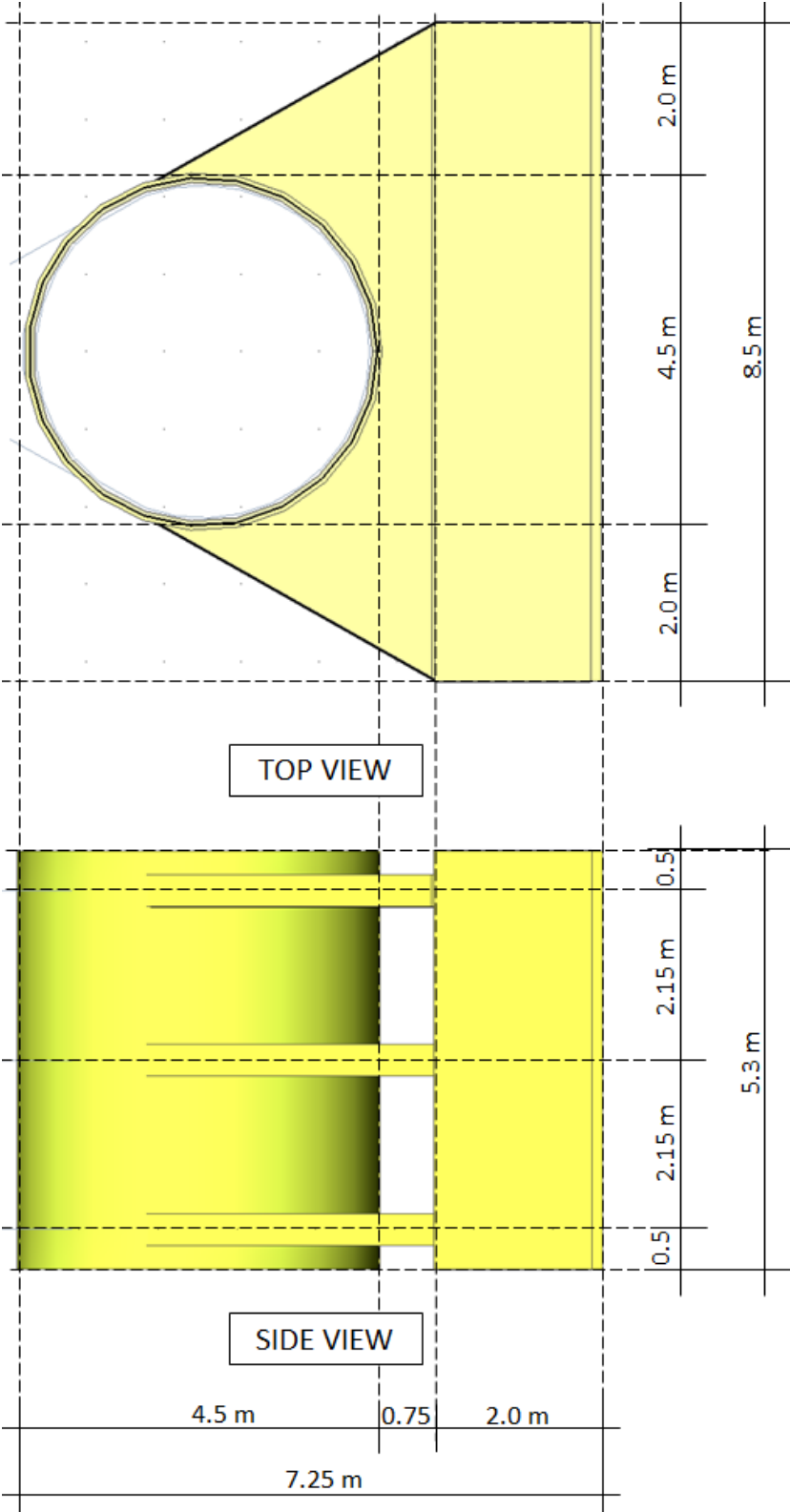
Figure 43 *Top- and Side view of the pile-head including dimensions*

6.6.3 Structural analysis

As was mentioned previously, the structure is designed on two ULS load cases: ULS 1 where the load is placed centrally and ULS 2 where the load acts in an eccentric manner. In the following section only the Finite Element Analysis (FEA)-results of load case 1 are showed as it is the most governing load combination. A summary of the results of both cases are included in Appendix X.

6.6.3.1 Horizontal plates

The horizontal plates are sandwich laminates and are characterized by the following stiffness matrix:

$$[ABD] = \begin{bmatrix} 3.7552 \cdot 10^8 & 1.1845 \cdot 10^8 & 0 & 0 & 0 & 0 \\ 1.1845 \cdot 10^8 & 3.7552 \cdot 10^8 & 0 & 0 & 0 & 0 \\ 0 & 0 & 1.2854 \cdot 10^8 & 0 & 0 & 0 \\ 0 & 0 & 0 & 8.6342 \cdot 10^6 & 2.6337 \cdot 10^6 & 0 \\ 0 & 0 & 0 & 2.6337 \cdot 10^6 & 8.6342 \cdot 10^6 & 0 \\ 0 & 0 & 0 & 0 & 0 & 3.0003 \cdot 10^6 \end{bmatrix} \; N, m$$

Because the loads are acting on the lower side of the fender panel, the lower horizontal plate takes up the largest forces and is thus governing over the other two. Only the results of this plate are therefore illustrated.
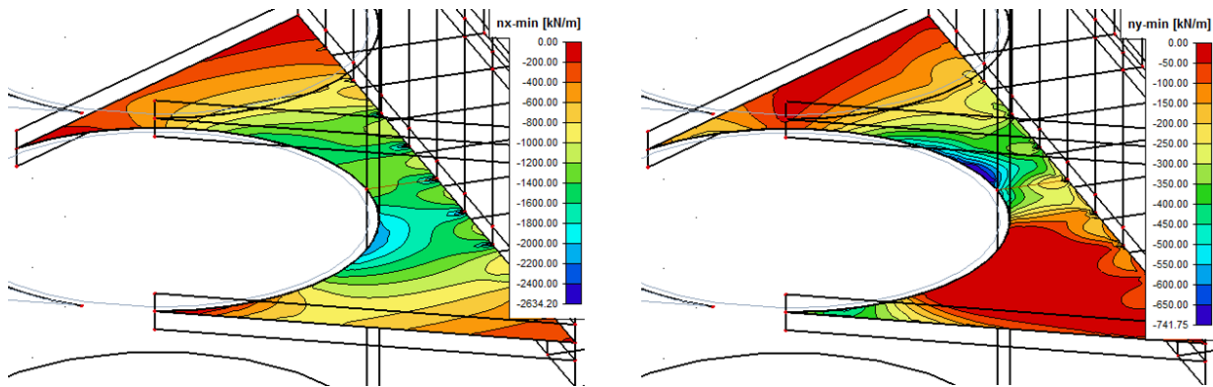
Figure 44 *Left: Nx, Right: Ny, plots of the horizontal plates*
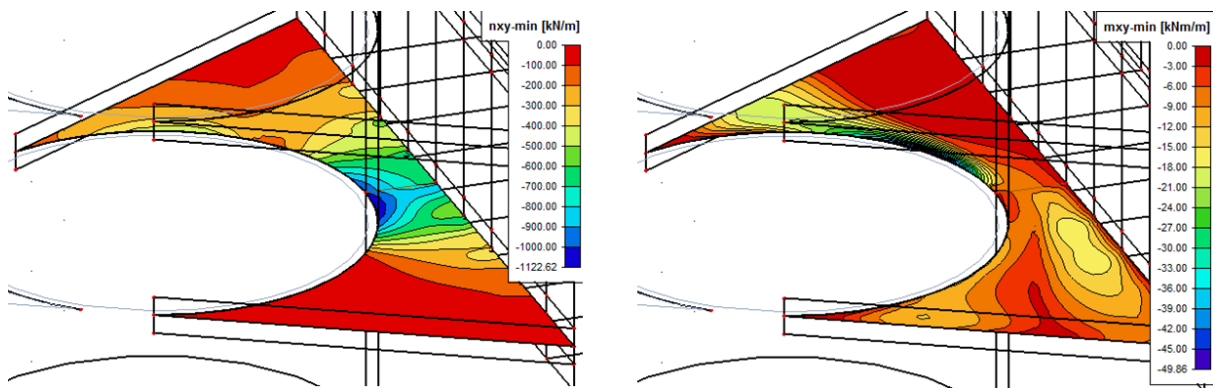
Figure 45 *Left: Nxy, Right: Mxy, plots of the horizontal plates*
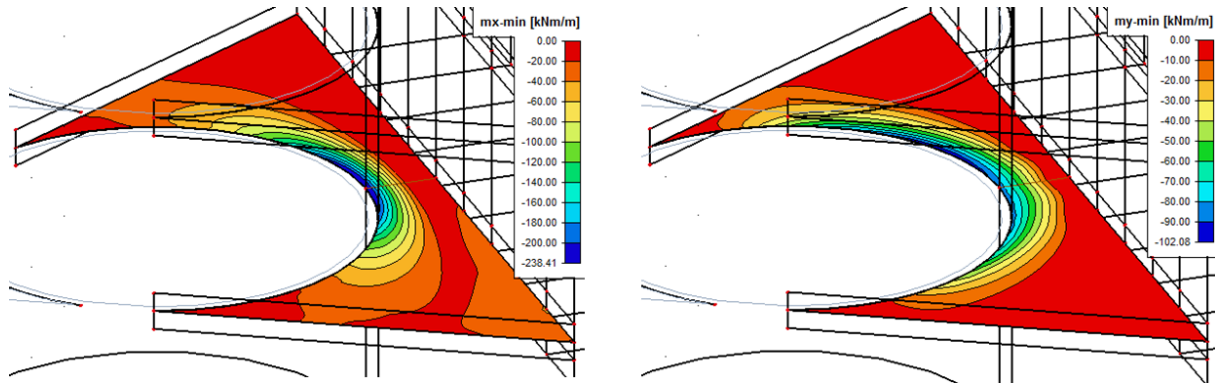
Figure 46 *Left: Mx, Right: My, plots of the horizontal plates*
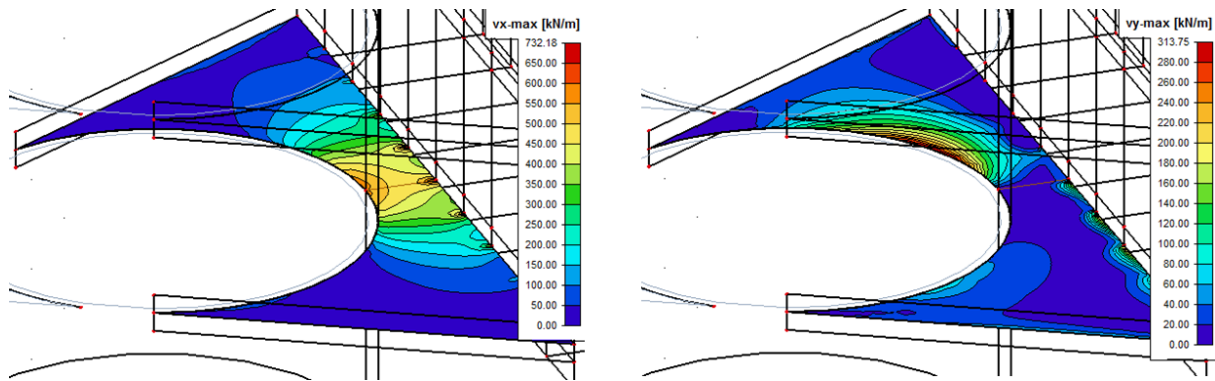
Figure 47 *Left: Vx, Right: Vy, plots of the horizontal plates*

Since the horizontal plates consist of sandwich laminates, these elements must be checked on the strain criterion. The most critical location is at the connection with the sleeve member, in the middle of the plate. At this critical location, the corresponding loads are:

Symbol	Maximum value
N_x	- 2634.20 kN/m
N_y	- 741.75 kN/m
N_{xy}	- 1122.62 kN/m
M_x	- 238.41 kNm/m
M_y	- 102.08 kNm/m
M_{xy}	+ 49.86 kNm/m
V_x	+ 732.18 kN/m
V_y	+ 313.75 kN/m

Table 23 *Critical loads horizontal plates*

These forces are converted to maxima strains by means of the ABD-matrix and checked with the strain criterion.

Symbol	Maximum strain	U.C.
ε_x	- 0.88 %	0.73
ε_y	+ 0.08 %	0.06
γ_{xy}	- 0.99 %	0.83

Table 24 *Maximum strains horizontal plates*

The shear forces within these elements are induced by the vertical friction force. This shear component has to be taken by the core, which has a maximum shear capacity of:

$$V_{max} = \tau_c \, b \, h_c = 2.15 * 1000 * 300 = 645kN$$

The largest shear forces are located in the middle of the horizontal plates, at the shortest distance between fender panel and mono-pile. As is illustrated in Figure 47, the critical shear force (marked in orange and yellow) is approximately 600kN/m (U.C. = 0.93). However at the intersection with the inner walls higher peak values are modelled (until 730kN/m). Nevertheless, those peak values act on such small areas they are considered not normative for the design.

6.6.3.2   Side plates
The side plates are made out of isotropic monolithic laminates and are therefore checked directly with the Von Mises equivalent stresses. Only the lower four (of six) side plates are illustrated as they contain the critical stresses.
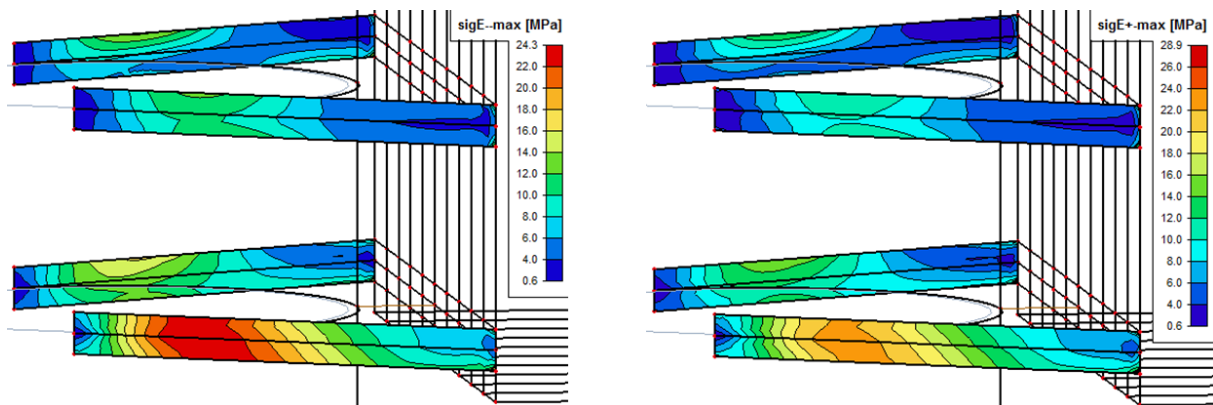
Figure 48 *Left: sigE-, Right: sigE+, plots of the side plates*

The critical stresses are found at two locations: where the horizontal plates have a tendency to deform and at the corners on the fender panel's side. The signs plus and minus indicate respectively the upper and lower side of the plate.

Symbol	Maximum stress	U.C.
σ_{eq} -	24.3 MPa	0.28
σ_{eq} +	28.9 MPa	0.33

Table 25 *Critical stresses, side plates*

6.6.3.3   Front plates
The front plates consist of monolithic laminates. Also, for this element, only the lower two are illustrated.
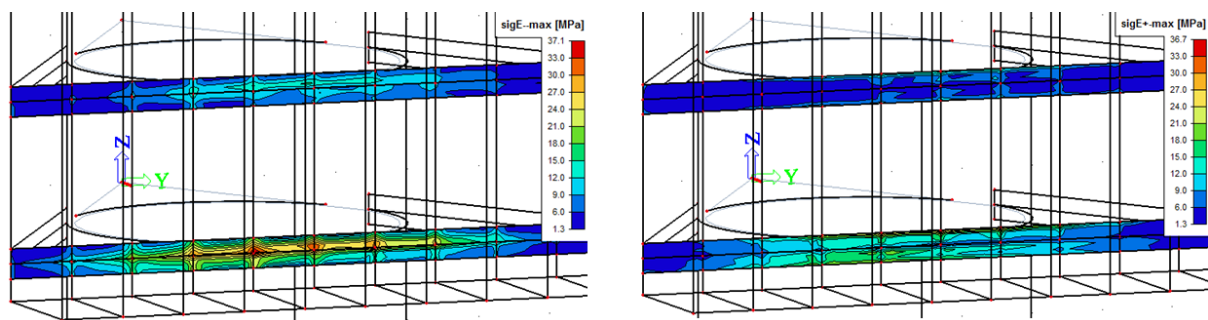
Figure 49 *Left: sigE-, Right: sigE+, plots of the front plates*

The critical stresses occur at the level of the inner walls.

Symbol	Maximum stress	U.C.
σ_{eq} -	37.1 MPa	0.42
σ_{eq} +	36.7 MPa	0.42

Table 26 *Critical stresses, front plates*

6.6.3.4 Rear panel

The rear panel consists of a sandwich laminate and is characterized by the following stiffness matrix:

$$[ABD] = \begin{bmatrix} 2.0939 \cdot 10^8 & 7.2559 \cdot 10^7 & 0 & 0 & 0 & 0 \\ 7.2559 \cdot 10^7 & 2.0939 \cdot 10^8 & 0 & 0 & 0 & 0 \\ 0 & 0 & 6.8417 \cdot 10^7 & 0 & 0 & 0 \\ 0 & 0 & 0 & 3.0073 \cdot 10^6 & 1.0104 \cdot 10^6 & 0 \\ 0 & 0 & 0 & 1.0104 \cdot 10^6 & 3.0073 \cdot 10^6 & 0 \\ 0 & 0 & 0 & 0 & 0 & 9.9843 \cdot 10^5 \end{bmatrix} \text{N, m}$$
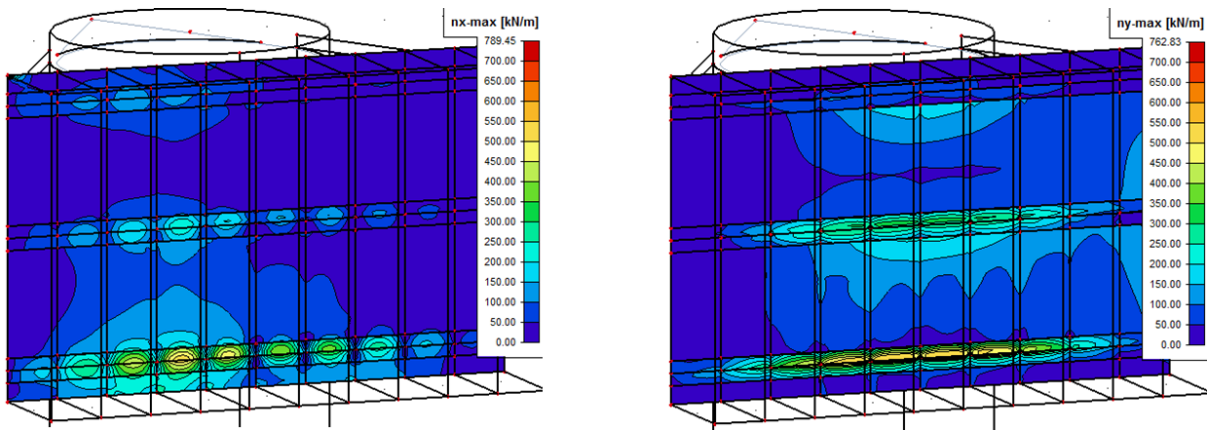
Figure 50 *Left: Nx, Right: Ny, plots of the rear panel*
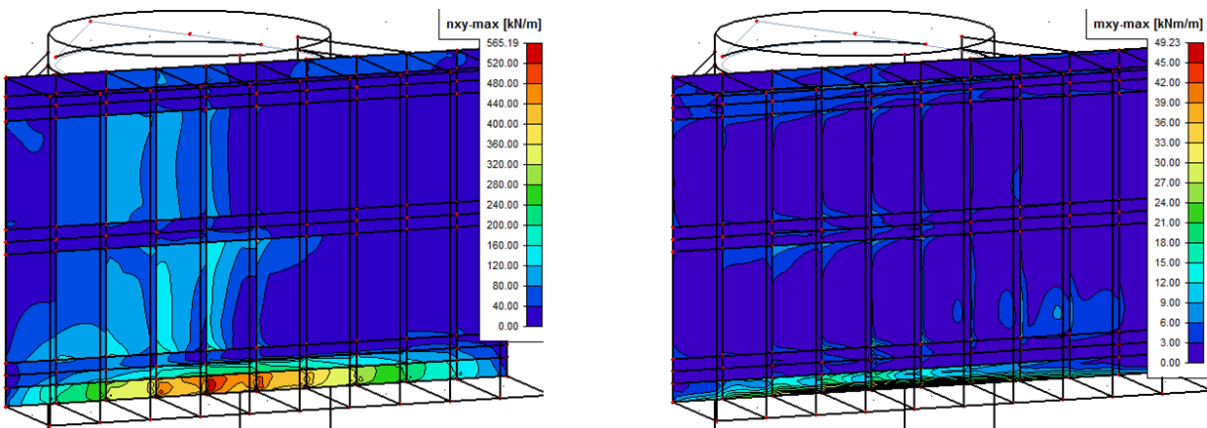
Figure 51 *Left: Nxy, Right: Mxy, plots of the rear panel*
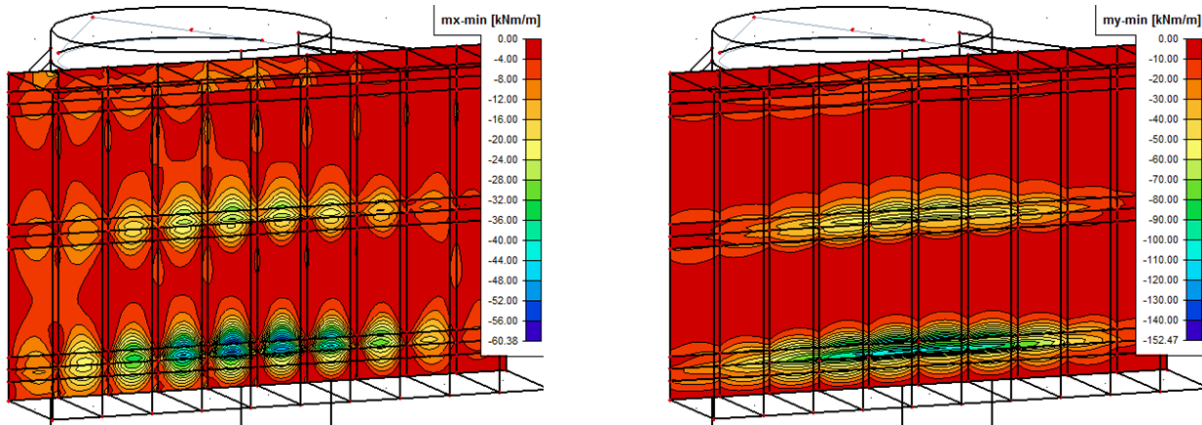
Figure 52 *Left: Mx, Right: My, plots of the rear panel*
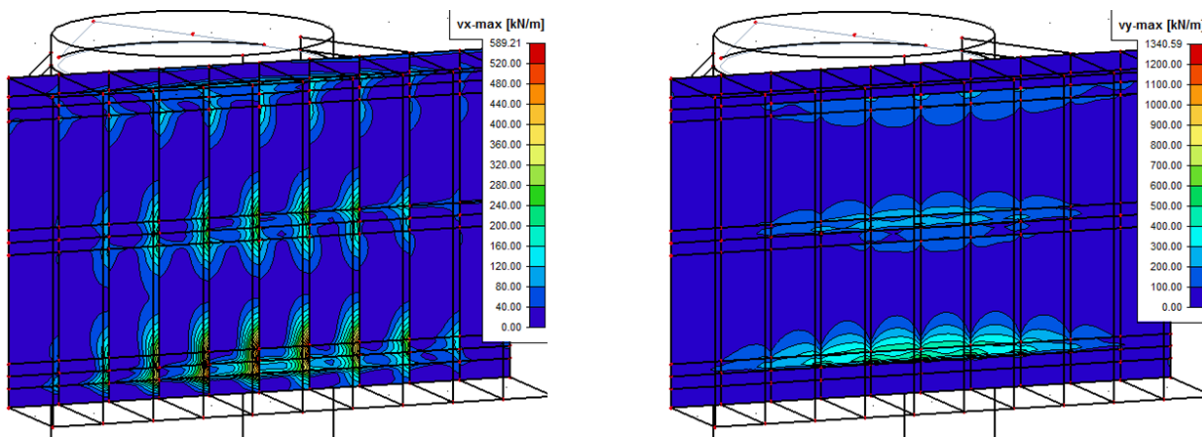
Figure 53 *Left: Vx, Right: Vy, plots of the rear panel*

The most critical location is situated at the connection with the front plates, at the level of the load. On that location the corresponding critical loads are:

Symbol	Maximum value
N_x	+ 789.45 kN/m
N_y	+ 762.83 kN/m
N_{xy}	+ 565.19 kN/m
M_x	- 60.38 kNm/m
M_y	- 152.47 kNm/m
M_{xy}	+ 49.23 kN/m
V_x	+ 589.21 kN/m
V_y	+ 1340.59 kN/m

Table 27 *Critical loads, rear panel*

These forces are converted to maxima strains by means of the ABD-matrix and checked with the strain criterion.

Symbol	Maximum strain	U.C.
ε_x	+ 0.33 %	0.28
ε_y	+ 0.93 %	0.78
γ_{xy}	+ 1.11 %	0.92

Table 28 *Maximum strains rear panel*

The shear capacity of this element is determined by the thickness of the core and is equal to:

$$V_{max} = \tau_c \, b \, h_c = 2.15 * 1000 * 250 = 537.5 kN$$

The shear forces in the rear panel are induced by the horizontal fender load. The maximum values are at the intersection with the horizontal plates, those amount approximately 520kN/m (U.C. = 0.97). However, some extreme peak values are modelled (until v_x = 589.28kN/m). These values can be explained by the fact that SCIA doesn't model the front plates as separate structures, but as a local thickening of the rear-panel. Also, since those values act on such a small area, they are considered negligible for the design.

6.6.3.5   Front panel

The rear panel consists of a sandwich laminate and is characterized by the following stiffness matrix:

$$[ABD] = \begin{bmatrix} 2.0939 \cdot 10^8 & 7.2559 \cdot 10^7 & 0 & 0 & 0 & 0 \\ 7.2559 \cdot 10^7 & 2.0939 \cdot 10^8 & 0 & 0 & 0 & 0 \\ 0 & 0 & 6.8417 \cdot 10^7 & 0 & 0 & 0 \\ 0 & 0 & 0 & 3.0073 \cdot 10^6 & 1.0104 \cdot 10^6 & 0 \\ 0 & 0 & 0 & 1.0104 \cdot 10^6 & 3.0073 \cdot 10^6 & 0 \\ 0 & 0 & 0 & 0 & 0 & 9.9843 \cdot 10^5 \end{bmatrix} N, m$$
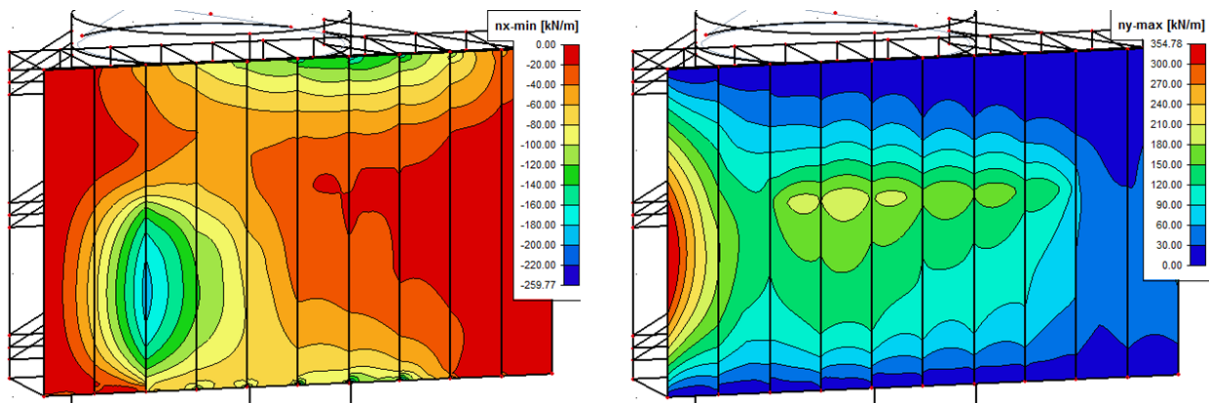
Figure 54 *Left: Nx, Right: Ny, plots of the front panel*
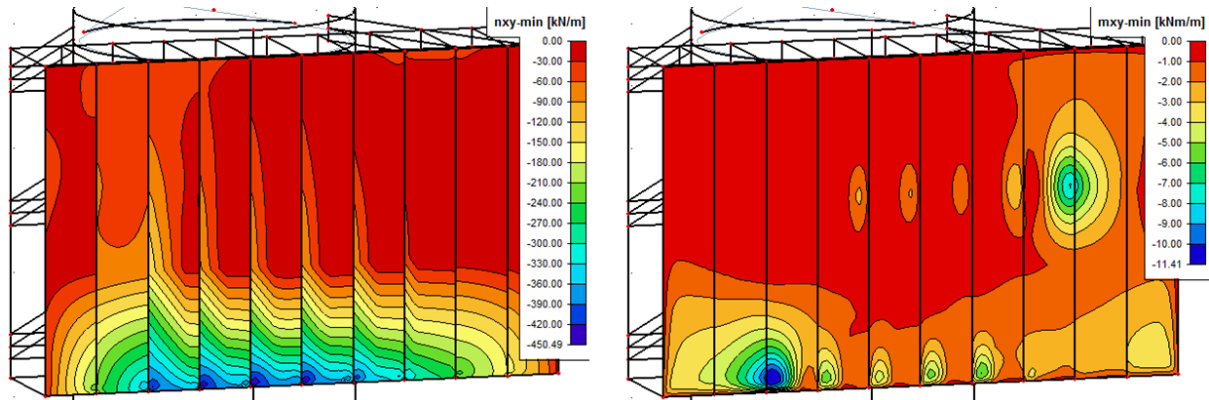
Figure 55 *Left: Nxy, Right: Mxy, plots of the front panel*
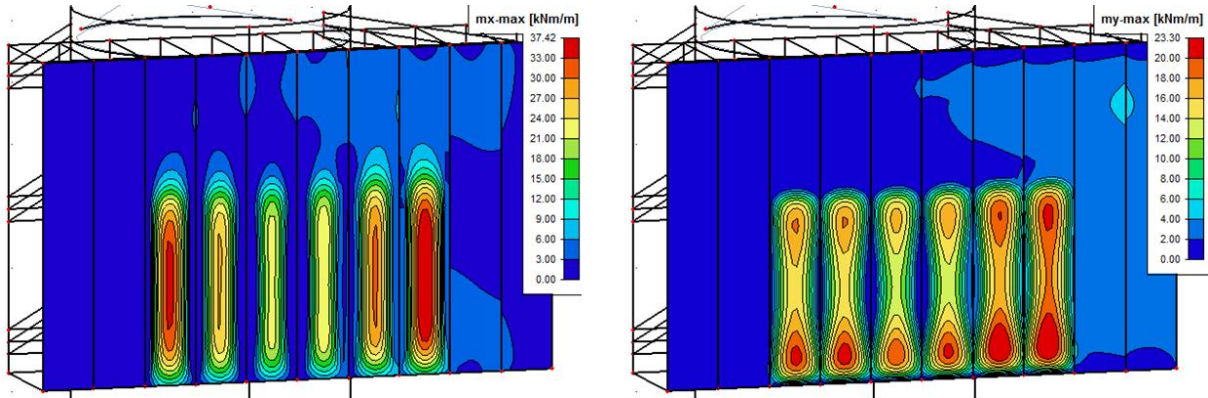
Figure 56 *Left: Mx, Right: My, plots of the front panel*
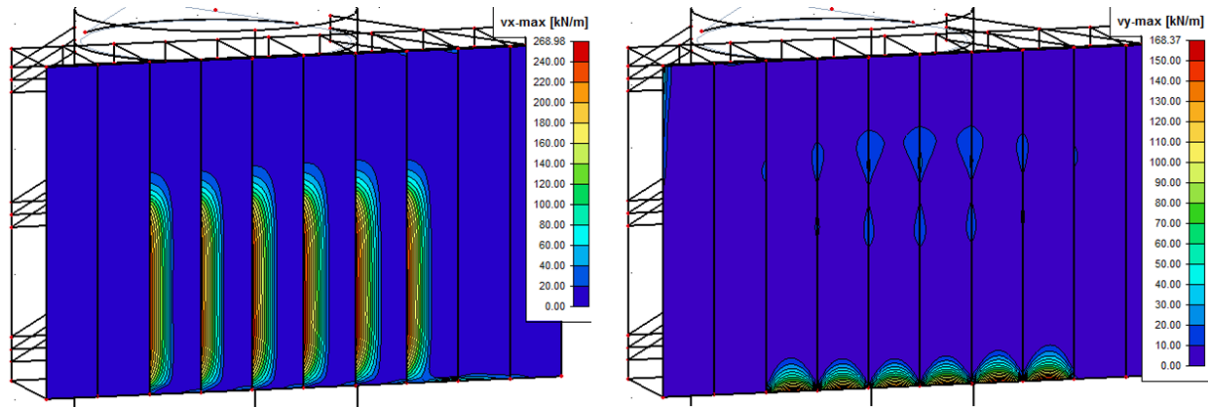
Figure 57 *Left: Vx, Right: Vy, plots of the front panel*

The most critical loads are located at the level where the fender is compressed.

Symbol	Maximum value
N_x	- 259.77 kN/m
N_y	+ 354.78 kN/m
N_{xy}	- 450.49 kN/m
M_x	+ 37.42 kNm/m
M_y	+ 23.30 kNm/m
M_{xy}	- 11.41 kNm/m
V_x	+ 268.96 kN/m
V_y	+ 168.37 kN/m

Table 29 *Critical loads, front panel*

The maxima strains, which are calculated through the ABD-matrix, are checked according the strain criterion of 1.2%.

Symbol	Maximum strain	U.C.
ε_x	- 0.36 %	0.30
ε_y	+ 0.30 %	0.25
γ_{xy}	- 0.48 %	0.40

Table 30 *Maximum strains front panel*

The shear capacity of this element is:

$$V_{max} = \tau_c \, b \, h_c = 2.15 * 1000 * 250 = 537.5 kN$$

The shear forces in the front panel are induced by the horizontal fender load, which result in a maximum shear force within the structure of 268.96kN/m (U.C. = 0.5) and therefore fulfilling the shear requirement.

6.6.3.6   Inner walls

The inner walls consist of monolithic laminates and are therefore checked according to the stress criterion.
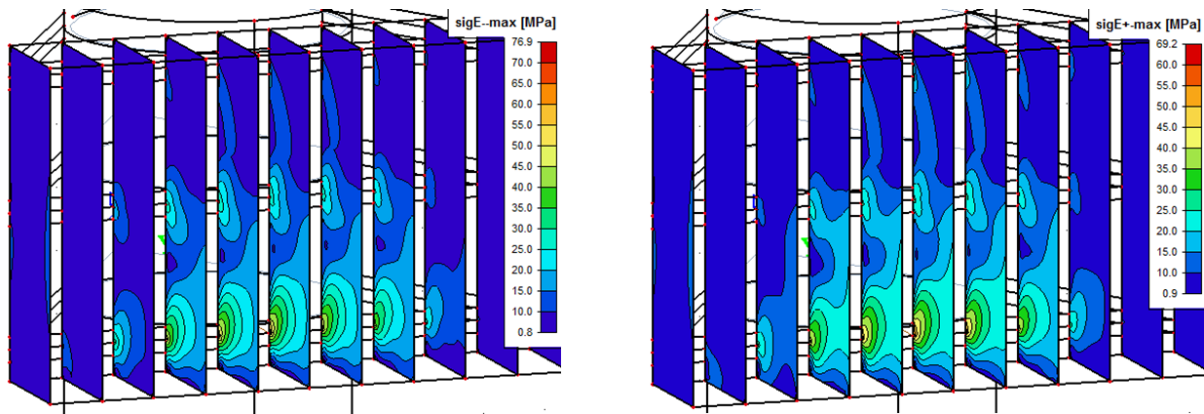
Figure 58 *Left: sigE-, Right: sigE+, plots of the inner walls*

Maximum stresses are at the level of the horizontal plates.

Symbol	Maximum stress	U.C.
σ_{eq} -	76.9 MPa	0.87
σ_{eq} +	69.2 MPa	0.79

Table 31 *Critical stresses, inner walls*

6.6.3.7   Top and bottom plates

The top and bottom plates also consist of monolithic laminates.
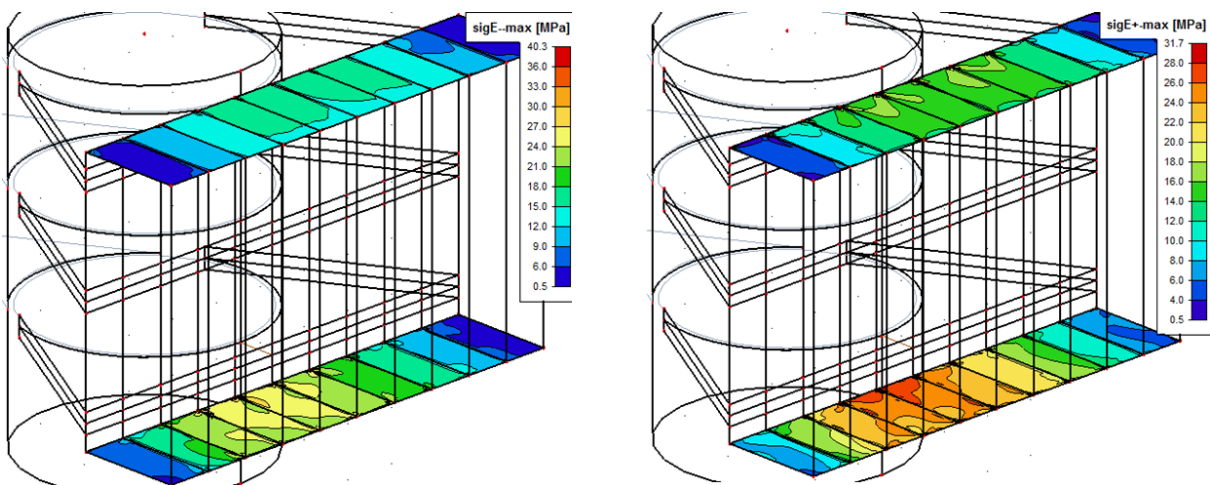
Figure 59 *Left: sigE-, Right: sigE+, plots of the top- & bottom plate*

The contribution of this element to load transfer, compared to the inner walls, is very small. The occurring stresses are therefore insignificant.

Symbol	Maximum stress	U.C.
σ_{eq} -	40.3 MPa	0.46
σ_{eq} +	31.7 MPa	0.36

Table 32 *Critical stresses, top & bottom plates*

6.6.4 Buoyancy

Since a floating structure is chosen, buoyancy is a critical issue in the design. The fender panel must be large enough to provide the whole structure with enough floating capacity. In this section this issue is checked.

Elements of the pile-head	Type of structure	Volume skin [m3]	Volume core [m3]	Weight [kg]
SUPPORT STRUCTURE				
Sleeve element	Monolithic (30mm)	1.499	0	2772
Horizontal plates	Sandwich (340mm)	1.386	10.393	3343
Side plates	Monolithic (30mm)	0.260	0	480
Front plates	Monolithic (40mm)	0.408	0	755
FENDER PANEL				
Rear panel	Sandwich (270mm)	0.901	11.263	2512
Inner walls	Monolithic (30mm)	3.498	0	6471
Upper and lower plates	Monolithic (30mm)	1.020	0	1887
Front panel	Sandwich (270mm)	0.901	11.2625	2512
			Total weight [kg]	20732
			Buoyancy surface [m²]	16
			Draught [m]	1.26

Table 33 *Buoyancy calculations*

The draught is calculated as:

$$d = \frac{F_w}{(b * l * \gamma_w)}$$

Where:

F_w: Total weight of the element

$b*l$:   Buoyancy surface area

γ_w: Specific weight of sea water, according to [10]

As can be seen from Table 33, the structure has a draught of 1.26m and the floating capacity is thus sufficient. If a larger draught is required, extra ballast can be added.

6.6.5 Fatigue analysis

As was mentioned in the "Design conditions", the fatigue strength of FRP composite depends on both the alternating stresses as the mean stresses as creep effect must be taken into consideration. The mean stresses, due to pre-tensioning of the mooring lines, are illustrated in Table 34, followed by the Load Transfer Functions (LTF) which describes the load-stress relationship, and lastly the cumulative damage. This fatigue analysis was performed for different elements of the pile-head.

Element of the pile-head	Pretension [MPa]	LTF [-]	Dd [-]
Horizontal plates	0.4	0.0015	2.58E-12
Front-/side plates	2.0	0.0087	2.23E-05
Rear panel	0.2	0.00115	2.32E-13
Front panel	0.1	0.0004	1.71E-17

Table 34 *Results fatigue assessment pile-head*

The results from above once more show that the fatigue resistance of composite structures is very high as the cumulative damage factors are far below 1. The calculations are included in Appendix XI.

6.6.6 Joints

In general structurally joining composite sections can be achieved in three different manners: mechanically, adhesively and a combination of both [25].

For mechanical joints, fasteners are applied such as rivets or bolts. The main advantage of such type of joints is its well-known behavior to stresses and failure mechanisms. Additionally, mechanical joint can reach high stress capacities. On the other hand, they are very fatigue sensitive as they lead to concentrated stresses and thus to initiation of cracks.

Bonded (adhesive) connections do have a high fatigue- and impact resistance as they have a uniform stress distribution. Their overall capacity, however, is lower than that of a mechanical connection. Also quality control is more difficult and costly.

For combined joints, both mechanical fasteners and adhesive are used. The fatigue stresses can be resisted by the adhesive while high peak stresses, leading to failure of the adhesive, can be taken over by the fasteners to secure the structural integrity.

Critical connection

For this study only the most critical joint will be investigated. For the conceived pile-head this regards the connection between the sleeve member and the horizontal plates. This connection, which connects a flat element to a curved element, is not only geometrically problematic but it is also subjected to high concentrated loads during large impacts. These high concentrated loads make the use of an adhesive-only not possible as its capacity is insufficient without applying a large overlap joint [8].

Next to very large impact loads, fatigue loads are of great importance which makes the use of solely mechanical joints not possible. Furthermore, placements of fasteners within the sleeve-element will hinder the sliding capabilities of the pile-head. For this latter reason the application of a combined joint is also not possible. [20]

The only method which can be applied is thus connecting both elements during the construction process. This can be achieved by extending the fibers out of the sleeve-element as is illustrated in Figure 60. Subsequently those are connected within the horizontal plates creating a stiff connection. Supplementary reinforcement

fibers may be added increasing the strength of the connection and preventing it from becoming a weak spot in the structure. Detailed calculations regarding this issue are however out of the scope of this thesis
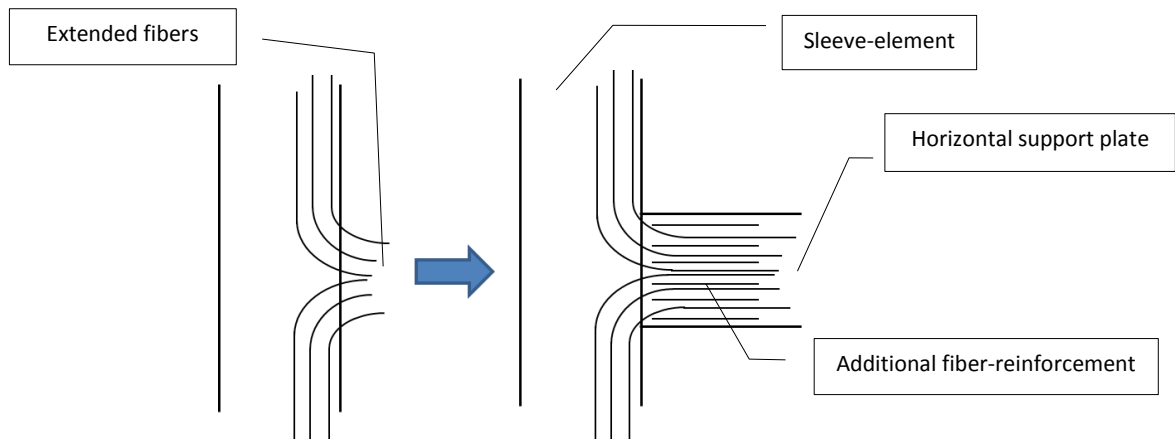
Figure 60 *Fabrication procedure of the critical joint*

6.6.7   Conical transition

The geometrical boundary of the mono-pile's diameter can be overcome by applying a simple conical transition as is illustrated in Figure 61. The range for which a standardized pile-head can be applied therefore increases significantly. Such conical transition, however, is more sensitive to fatigue damage as additional circumferential stresses will occur at the level of that transition. Nevertheless, as the transition-piece will be constructed close to the water level, near the pile-head, large stresses will not be present. Fatigue damage at the location of the conical transition is therefore considered insignificant.
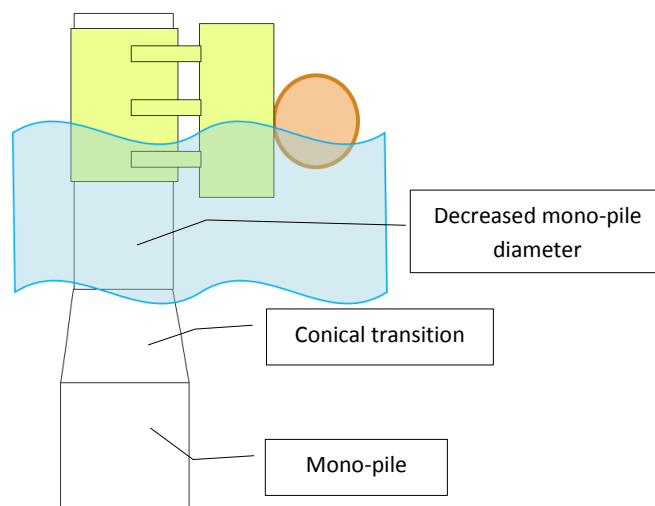
Figure 61 *Conical transition*

7 Discussion of results

In this chapter the results of the previous chapters are summarized and discussed.

7.1 Part 1

In part 1 a method is presented for the estimation of the design loads on the mooring system. The underlying idea behind this method is the separation of the environmental components. The loads on the structure due to wave-action are obtained through a wave height-fender deflection relationship. The loads due to winds and currents are calculated as quasi-static drag forces.

The results of Part 1 are summarized in Table 35. The accuracy of the assessment tool was tested by comparing the outcome of the calculated results to the MPM-results for varying conditions.

Reference project	Stiff fender case	Soft fender case
Aqaba - Storm	+2 %	-
Golar - Storm	+3 %	-
Golar - Wave	+18 %	+5 %
Golar - Wind	+10 %	- 6 %
Golar - Tsunami	- 27 %	- 35%

Table 35 *Error margins, assessment tool*

From the abovementioned table is concluded that the assessment tool can generate rather accurate results. However, some important aspects should be enlightened.

The first one being that stiff fender cases always leads to larger fender loads than softer cases. Relating wave height to fender deflection thus not totally eliminates the influence of the applied fender.

Another interesting aspect is that, in general, the fender loads are slightly overestimated, except for the "Golar – tsunami" case where relatively small values were generated. For larger current velocities the corresponding forces are thus largely underestimated.

The fender loads calculated for larger wave heights are slightly larger than the ones resulting from the DMA runs, thus the positive error margin. This may be explained by the lack of DMA-data for such larger wave heights. The trend line drawn through these data points is therefore not as accurate as for smaller wave heights.

7.2 Part 2

For Part 2 standardization of the mono-piles was researched. This is done by investigating the influence of the soil and of the load on the pile design. From the obtained results, the conclusion is drawn that a generalized pile design is not possible since the dimensions (diameter, thickness and length) differ too much. The limits are consequently redefined.

A strict distinction between stiff- and a soft soil profiles is established, where in reality soil profiles could be a combination soft soil layers and stiff soil layers. In addition a distinction is made between different classes of environmental conditions; mild, moderate and harsh. For each of the abovementioned combinations a standardized pile design is made as is shown in Table 36. Subsequently, for each class, the over-dimensioning costs were calculated.

Soil profile	Dimensions	Environmental condition		
		Mild	Moderate	Harsh
Stiff sand profile	t [mm]	45	50	55
	D [mm]	3300	3800	4100
	L [m]	42.5	45	47.5
Soft clay profile	t [mm]	50	55	60
	D [mm]	3400	3900	4300
	L [m]	65	70	80

Table 36 *Standardized pile designs for varying conditions*

The over dimensioning costs for stiff soil profiles vary between 0 and 0.15 million USD, while those for soft soil profiles vary between 0 and 0.35 million USD. This can be explained by the fact that the variation in pile length is much larger for the softer soils.

	Over-dimensioning costs [million USD]	Ratio over-dimensioning costs/ total costs [%]
Stiff sand profile	0 – 0.15	0 – 0.6 %
Soft clay profile	0 – 0.35	0 – 1.4 %

Table 37 *Over-dimensioning costs compared to the total costs*

In Table 37 the over-dimensioning costs per breasting dolphin are compared to the total costs of an FSRU-project which amounts roughly 25 million USD. For the worst case scenario the over-dimensioning costs of the breasting dolphins are approximately 5.6% (1.4%*4 units) of the total costs which is still considered acceptable for early design stages.

If the FSRU import terminal must be designed for water depths larger than 16m, the standardized pile designs have to be rescaled. This can be achieved by means of the rescaling parameters mentioned in Table 38 which are valid for an increased water depth-case of 26m.

Dimensions	Rescaling parameters for 26m water depth
Thickness	+ 5 mm
Diameter	+ 400 mm
Length	+ 12.5 m

Table 38 *Rescaling parameters for 26m water depth*

The fatigue life of the mono-pile dolphins is assessed by means of a case-study. The calculated cumulative damage factor is far below one (0.0782 << 1); fatigue damage is therefore proven insignificant for the Java Sea without considering pile-driving.

7.3 Part 3

The designed floating pile-head is constructed of two main elements: the fender panel and the support structure. The fender panel consists of an empty box-element which provides floatation capacity for the whole structure and a continuous facing for the compressed fender. The support structure consists of horizontal plate elements, which transfer the loads to the mono-pile, and a sleeve element which slides along the pile shaft.

The pile-head was designed with FRP composite of which two types of laminates were applied: monolithic laminates consisting of a single skin and sandwich laminates which are constructed of two skins separated by a

core in the middle. This latter construction was primarily used for the structural elements which were subjected to large shear forces and bending moments.

The application of FRP composite resulted in a very light weighted construction, only 21 tons. This mostly improves floating issues as the structure reaches a draught of only 1.26m. This lightweight is also favorable for installation operations as low hoisting capacity is required compared to a conventional fixed, steel pile-head.

Fatigue is considered to be insignificant. The fatigue damage was calculated for multiple elements of the pile-head as is listed in Table 39. The cumulative damage numbers (D_D) are far below 1, proving once more the high fatigue resistance of composite structures.

Element of the pile-head	Pretension [MPa]	LTF [-]	D_D [-]
Horizontal plates	0.4	0.0015	2.58E-12
Front-/side plates	2.0	0.0087	2.23E-05
Rear panel	0.2	0.00115	2.32E-13
Front panel	0.1	0.0004	1.71E-17

Table 39 *Fatigue results, pile-head*

Regarding constructability, the sleeve-element and horizontal support plates need to be connected manually during the fabrication process as both bonded- as mechanical connections do not fulfill the mechanical requirements.

The geometrical boundary of the sliding-element, which is the outer diameter of the applied mono-pile, can be overcome by constructing a conical transition. A certain pile-head can therefore be applied for a large range of different pile sizes, enhancing its standardization capabilities.

In the following table a feedback-loop is made, re-evaluating the designed pile-head on the criteria selected for the MCA.

Robustness	Pro	The structure is designed such that the loads are transferred in an efficient and well-distributed manner to the mono-pile. Additionally composite has good impact properties.
Durability	Pro	The application of composite leads to good capabilities of withstanding wear and tear. Creep-effects may play a role; however, the permanent pre-tensioning load is very small and this effect therefore negligible.
Maintenance	Pro	The application of composite results in a structure which require low maintenance works. Corrosion is not an issue.
Reparability	Neutral	The ease to repair broken components may be troublesome, but that's not different for other pile-head structures.
Fatigue resistance	Pro	The structure has very high fatigue resistance and high material damping.
Constructability	Con	Constructability is an issue. Problematic are: the connection between the sleeve-element and the horizontal support plates, and the attachment of the low friction material within the sleeve-element.
Installation	Pro	The low self-weight of the structure facilitates hoisting and installation of the pile-head onto the mono-pile.
Transport	Pro	Light construction, easy transportation

Costs	Neutral	FRP composite has high initial costs. However, since the pile-head is floating, the amount of material required can significantly be reduced for locations with large tidal variations. Furthermore, since the pile-head has good durability properties, it may be re-used for other projects (if still in good condition).
Accessibility	Con	Accessibility of the pile-head for inspection and maintenance works is more difficult for floating pile-heads than for fixed ones
Sustainability	Con	FRP composite has generally a high carbon footprint [9]. Additionally, during fires chemical gasses may be released.

Table 40 *Re-evaluation of the pile-head on the MCA criteria*

8 Conclusions and recommendations

Based on the results discussed in the previous chapter, conclusions are drawn. Furthermore, some recommendations for future research are given.

8.1 Part 1

Part 1 describes a standardized method to visualize the analysis results of the fender loads due to FSRU motions. From the results can be concluded that a standardized assessment tool is possible within certain limits.

However, in order to fully validate such tool, still more DMA-data is required, especially for larger waves ($H_S >$ 1.5m).

The current assessment tool has some restrictions as it is designed for very limited environmental conditions. It would therefore be interesting to investigate expansion possibilities by applying the same design procedure for other type of environmental conditions and see if a similar level of accuracy can be obtained. Interesting environmental conditions to analyze would be, e.g., swell waves or different types of wind loadings.

As was concluded from the results, the fender force due to larger current velocities (2 m/s) is severely underestimated. Additional DMA-runs should be performed and new parameters should be introduced in order to obtain more accurate results. Perhaps find a factor, similar to the gust factor of wind, by which the current velocity can be multiplied.

8.2 Part 2

The main idea behind standardization is to save costs and schedule of the civil structures of a jetty-type mooring system on exposed locations. Part 2 concluded that standardization of the mono-piles can only be achieved to a certain extent, namely in a conceptual design phase.

In this report a standardized work approach is presented. The same starting points and design procedure can be followed in order to reduce the start-up time of the project.

The results discussed in Part 2 can be used in order to get a first indication of pile dimensions. With very little information (soil type and loading) a quick estimate of the design can be made. The over-dimensioning costs of these standardized designs are calculated to be relatively small compared to the total costs of an FSRU-project and therefore considered very acceptable in an early design stage.

More detailed standardization designs can be possible for very site-specific locations, where the geotechnical- and environmental conditions do not differ much. For these limited locations, still, multiple FSRU-projects would be necessary in order to make standardization of its mooring facility feasible. A thorough LNG-market-study is therefore recommended, determining the areas where many FSRU-projects are to be expected before looking into standardization of the civil structures.

For locations with bad soil conditions standardization could be combined with soil improvement, by removing poor soil and replacing it with dense sand. The variation in pile length, due to varying load conditions, would significantly be reduced. An economic feasibility study is recommended comparing the costs of soil improvement to the costs of excess steel.

The fatigue damage of the mono-piles is calculated to be insignificant for the case-study. This calculated value, however, is not so small that fatigue can be neglected for all cases; for a mooring system on exposed locations

a fatigue assessment should always be performed. Nevertheless there are some aspects that can be taken into account in order to significantly reduce this fatigue damage;

- For moorings on exposed locations only foam filled floating fenders should be applied with nearly flat force-deflection curve. The application of other types of fenders will result in a considerable increase of fatigue damage.
- The misalignment between two consecutive pile-sections has to be reduced as much as possible.
- Well executed butt welds should be applied which should be grinded flush.
- For locations where many storms are expected, a threshold can be introduced above which the FSRU should be temporarily relocated.

8.3 Part 3

In Part 3 the pile-head concept is presented which is the most suitable for standardization purposes, namely a FRP composite, floating structure with a slide-bearing sliding system.

The application of composite in exposed marine environment has some major advantages. Its fatigue resistance and high material damping are much desired properties since the exerted load is of cyclic nature. Its lightweight enhances buoyancy and facilitates installation, while its low maintenance and corrosion resistant properties results in a very durable material.

The form of the pile-head is optimized for its application. The slide-bearing system contains at the inner side a fabric of low friction material which allows smooth sliding along the mono-pile. The horizontal support plates transfer the loads in an efficient manner to the mono-pile, while the fender panel provides a continuous facing for the fender and enough buoyancy for the system.

In this study general stability of the structure was looked at, however still some technical details must be further investigated:

- The slide bearing-system requires more detailing, in particular the interface between the low friction material and the steel-mono-pile.
- Accumulation of water will occur on the top of the horizontal plates. A drainage system must therefore be designed.
- The contact between the pile-head and the FSRU-vessel must be investigated. A scale model could give a good insight in whether or not the system (pile-head + vessel) will behave as expected.
- The connection of the fender chains to the fender panel must be designed.
- The corners of the structural elements can be smoothened improving the load distribution and reducing the magnitude of local peak-loads.

Next to technical details it is also advisable to perform a thorough economic feasibility study and compare it to conventional fixed solutions. Not only direct costs should be taken into account, such as material-, construction-, and maintenance costs. But also durability and environmental effects need to be included.

9 References

[1]   API, American Petroleum Institute (2010). API-2A-LRFD, Recommended practice for planning, designing and constructing fixed offshore platforms – Load and Resistance Factor Design.

[2]   Arnout de Pee (2005). Operability of a floating LNG terminal; the influence of operating limits for the approach, transfer and departure cycle on the weather downtime.

[3]   Bangladesh University of Engineering and Technology (2002). Lecture: Undrained and drained shear strength. URL: http://teacher.buet.ac.bd/sid/download/CE341/lecture11_4on1.pdf

[4]   BSI, British Standard Institute (1989). BS 6349 - 6:1989, Code of practice for marine structures, Part 6: design of inshore moorings and floating structures.

[5]   Clarke JL. (1996). Structural Design of Polymer Composites, EUROCOMP Design Code and Handbook.

[6]   CEE, Center for Energy Economics (2006), Offshore LNG receiving terminal.

[7]   CUR-96, Civieltechnisch Centrum Uitvoering Research en Regelgeving, Aanbeveling 96 (2003). Vezelversterkte kunststoffen in civiele draagconstructies.

[8]   Dat Duthinh (2000). Connection of Fiber-Reinforced Polymers (FRP) Structural Members: A Review of the State of the Art.

[9]   Delft University of Technology, Trude Maas, Jarit de Gijt, David Dudok van Heel. Comparison of quay wall designs in concrete, steel, wood and composites with regard to CO2-emisison and the Life Cycle Analysis

[10]   Delft University of Technology (2011). Manual Hydraulic Structures, CT3330.

[11]   Deshpande (2012), The design of sandwich panels with foam cores, Cambridge University.

[12]   DNV, Det Norske Veritas (2008). DNV-OS-C101, Design of offshore steel structures, general (LRFD method).

[13]   DNV, Det Norske Veritas (2010). DNV-RP-C203, Fatigue design of offshore steel structures.

[14]   DNV, Det Norske Veritas (2010). DNV-RP-C205, Environmental conditions and environmental loads, October 2010

[15]   Dr. Ann Schumacher (2010). Lecture: Design of FRP-Profiles and All-FRP-Structures.

[16]   Eindhoven University of Technology, ABD-matrix:
        URL: http://www.mate.nl/~piet/edu/dos/pdf/linlam.pdf

[17]   EN, European Standard (2007). EN 1996-1-6, Euro code 3, Design of steel structures, Part: 1-6 Strength and Stability of Shell Structure, February 2007.

[18]   Ernst & Young (2013), Global LNG - Will new demand and new supply mean new pricing?

[19]   FenderTeam. Product catalogue

[20]   Fiberline (2003). Fiberline Design Manual. URL: www.fiberline.dk

[21]   GL, Germanischer Lloyd (2005). Rules and Guidelines IV, GL Wind Energy.

[22]   Golar. Golar LNG catalogue, Floating Storage and Regasification Unit FSRU

[23]   Gurit. Guide to Composite. URL: http://wwwgurit.com/

[24]   Howard E. Boyer. Atlas of Fatigue Curves

[25]   J.C. Moen (2014). Feasibility Study on Heavy-Traffic FRP Bascule Bridges, Delft University of Technology.

[26]   John W. Gaythwaite. Design of Marine Facilities for the Berthing, Mooring and Repair of Vessels, 2nd Edition

[27]   LNG Floating Storage Regasification Unit International Conference (2014). URL: http://fsru.informa-mea.com/

[28]   NEN, Dutch Standards Insitute (2012). NEN-EN 1993-1-9+C2:2012, Eurocode 3, Design of steel structures, Part: 1-9 Fatigue.

[29]   Novascotia. Wood utilization and Technology; Physical and Mechanical properties wood. URL: http://novascotia.ca/

[30]   OCIMF, Oil Companies International Marine Forum. Mooring Equipment Guidelines, 3rd Edition

[31]   Refitech. Carbon components. URL: http://www.refitech.nl/

[32]   Royal Haskoning (2011). Presentation Golar FSRU West Java Mooring Facilities, 6th of October 2011.

[33]   Royal HaskoningDHV (2012). Aqaba LNG Terminal, Design Basis Report – infrastructure, 7th of November 2012.

[34]   Royal HaskoningDHV (2012). Aqaba LNG Terminal, Preliminary Dynamic Mooring analysis, 31st of January 2012.

[35]   Royal HaskoningDHV (2012). Golar Floating LNG Terminal West Java; Basis of a detailed design of the FSRU Mooring arrangement and gas transfer platform, 13th of April 2012.

[36]   Royal HaskoningDHV (2012). Golar Floating LNG Terminal West Java; Design report breasting dolphins, 13th of April 2012.

[37]   Royal HaskoningDHV (2012). Golar Floating LNG Terminal West Java; Dolphin head design report – breasting dolphin, 13th of April 2012.

[38]   Royal HaskoningDHV (2012). Golar Floating LNG Terminal West Java; Dynamic Mooring Analysis, 13th of April 2012.

[39]   SHELL. Liquefied Natural Gas. URL: http://www.shell.com/

[40]   Ticona. GUR - product brochure, Ultra High Molecular Weight Polyethylene (PE-UHMW)

[41]   Trelleborg Marine Systems. Catalogue, Safe berthing and Mooring

[42]   Unitrove. Natural gas and LNG density calculator. URL: http://www.Unitrove.com/

[43]   Vincent Calard (2011). Formulas and equations for the classical laminate theory.
URL: http://www.aac-research.at/downloads/Formula-collection-for-laminates.pdf

[44]   OTEO Conference (2012). An overview of SBM mooring systems.

10   List of Symbols

Assessment tool

F_{Fender}	Fender load	kN
F_{wave}	Contribution of wave action to fender load	kN
F_{wind}	Contribution of winds to fender load	kN
$F_{current}$	Contribution of currents to fender load	kN
H_S	Significant wave height	m
T_P	Wave period	sec
u_W	Wind velocity	m/s
u_C	Current velocity	m/s
C_W	Wind direction coefficient	-
C_c	Current direction coefficient	-
α	Force-Moment distribution coefficient	-
ρ_W	Density in air (wind)	kg/m³
ρ_c	Density in water (current)	kg/m³
f	Freeboard	m
d	Draught	m
L_{BP}	Length between perpendiculars	m

Geotechnical modelling

c_u	Undrained shear strength	kPa
γ'	Effective unit weight of soil	MN/m³
ε_{50}	Axial strain at one-half of the ultimate soil resistance	-
ϕ'	Angle of internal friction	deg
k	Initial modulus of subgrade reaction	kN/m³
y	Lateral deflection	m
p_u	Ultimate bearing capacity	kN/m

Structural analysis steel mono-piles

D	Pile diameter	m
t	Wall thickness	m
L	Pile length	m
τ_V	Shear stress due to shear force	MPa
V_d	Shear force	kN
R	Outer radius	m
r	Inner radius	m
I_{zz}	Moment of inertia	m⁴
S_z	First moment of area	m³
σ_M	Bending stress due to bending moment	MPa
M_d	Bending moment	kNm
W	Section modulus	m³
σ_N	Normal stress due to normal force	MPa
N_d	Normal force	kN

A	Cross-sectional area	m^2
τ_T	Torsional stress due to torsional moment	MPa
T_d	Torsional moment	kNm
I_p	Polar moment of inertia	m^4
σ_d	Meridional stresses	MPa
τ_d	Shear stresses	MPa
$\sigma_{vm,d}$	Von Mises equivalent yield strength	MPa
f_{yd}	Design yield strength	MPa
σ_{Rd}	Design buckling strength	MPa
χ	Buckling reduction factor	-

Structural analysis composite pile-head

E	Elastic modulus	MPa
v	Poisson's ratio	-
G	Modulus of rigidity	MPa
F_{VER}	Vertical friction force	kN
F_{HOR}	Horizontal friction force	kN
ε^o	Mid-plain strains	-
κ	Mid-plain curvatures	m^{-1}
N	Resultant normal force	kN/m
M	Resultant bending moment	kNm/m
V	Resultant shear force	kN/m

Fatigue analysis

ΔF	Alternating fatigue load	kN
$\sigma_{nominal}$	Nominal fatigue stress	MPa
$n_{life\ time}$	Number of cycles during design life time	-
$n_{DMA-run}$	Number of cycles during DMA-run	-
$p_\%$	Probability of occurrence	-
δ_m	Maximum allowable misalignment	m
n_c	Actual number of cycles	-
N_c	Allowable number of cycles	-
D_D	Cumulative damage factor	-
m	Slope parameter of the S-N curve	

Factors

γ_M	Material factor	-
γ_C	Conversion factor	-

11   List of Abbreviations

ALS	*Accidental Limit State*
API	*American Petroleum Institute*
BD	*Breasting Dolphin*
BS	*British Standards*
CAPEX	*Capital Expenditure*
CBM	*Conventional Buoy Mooring System*
CD	*Chart Datum*
CUR	*Civieltechnisch Centrum Uitvoering Research en Regelgeving*
DFF	*Design Fatigue Factor*
DMA	*Dynamic Mooring Analysis*
DNV	*Det Norske Veritas*
EN	*European Standard*
FLS	*Fatigue Limit State*
FSRU	*Floating Storage and Regasification Unit*
FRP	*Fiber Reinforced Polymers*
GL	*Germanischer Lloyd*
IEA	*International Energy Agency*
LNG	*Liquefied Natural Gas*
LNGC	*LNG Carrier*
LTF	*Load Transfer Function*
MBL	*Minimum Breaking Load*
MCA	*Multi Criteria Analysis*
MD	*Mooring Dolphin*
MPM	*Most Probable Maximum*
NEN	*Dutch Standards Institute*
OCIMF	*Oil Companies International Marine Forum*
PTFE	*Polytetrafluoroethylene (= Teflon)*
RAO	*Response Amplitude Operators*
RP	*Return Period*
SCF	*Stress Concentration Factor*
SLS	*Serviceability Limit State*
SPM	*Single Point Mooring Systems*
UHMWPE	*Ultra High Molecular Weight Polyethylene*
ULS	*Ultimate Limit State*
USD	*United States Dollar*

12   List of Figures

13 List of Tables

14   Appendix I: FSRU operations

14.1 Introduction

In this Appendix first a closer look is taken in the FSRU operations (14.1), namely the offloading process, the storage of LNG and finally the regasification process and delivery of the LNG. Then the main components of the FSRU will be described (14.2) and finally the main components of the FSRU mooring system will be dealt with (14.3).

14.2 FSRU operations

14.2.1   The offloading process (LNG transfer from LNGC to FSRU)

Once the LNG has been transported overseas to its final destination, the gas must be transferred from the LNGC to the FSRU. This will be referred to as the offloading process and consists of the berthing of the LNGC alongside the FSRU, offloading the LNG and finally disconnecting and un-berthing.

After the LNGC arrives at the FSRU's location, it will be positioned parallel to the FSRU aligning the manifolds of both vessels. With the assistance from tugs the LNGC is maneuvered alongside the FSRU for the offloading of the cargo in a so-called side-by-side mooring configuration. After berthing a combination of transverse mooring lines and spring lines will be used to limit horizontal relative motions.

After the LNGC is securely moored, the offloading of the LNG can begin by means of 'loading arms'. After the offloading operations 5 to 10% of the cargo will be kept onboard. This is referred to as the heel and this is required for tank cooling during the return voyage.

On completion of offloading, the loading arms are disconnected and the LNGC can be un-berthed. Tugs will then secure the LNGC while the mooring lines and spring lines are released. Thereafter the LNGC will be pulled away by tugs until sufficient distance is reached in order to sail away safely.

Operation with two LNG arms will ensure a loading time of 16 hours. Berthing, loading and un-berthing will take approximately 24 hours. [22]

14.2.2   The storage of LNG

An LNG import terminal (in this case an FSRU) must be able to receive and store the delivered amount of LNG. The storage of the LNG will be in storage tanks of the FSRU and is based on standard design LNGC storage tank systems; using membrane- or self-supporting tanks.

The storage tanks of the FSRU not only serve as immediate storage of LNG when a carrier is offloading, but also works as a buffer in case the supply and demand of LNG fails. The storage capacity of the FSRU must therefore be sufficient in order to supply natural gas for base load operations[3] in a continuous matter and supply for some peak demand events. Furthermore enough storage capacity is required to compensate delays in shipments and limit demurrage[4].

14.3 The regasification process and the delivery of LNG from FSRU to land

When the consumer demands the gas, the LNG has to processed back into its gaseous state and transported by pipeline to its desired location.

---

[3] *Base load operations = natural gas supply that must always be delivered on a daily basis [6]*
[4] *Demurrage = detention or delay of a tanker due to loading or unloading [6]*

LNG is sent from the tanks to the regasification unit situated forward, see Figure 62. The regasification unit essentially comprises booster pumps and steam heated vaporizers. The booster pumps will increase the pressure, before the high pressure LNG is vaporized after which the gas is sent to the subsea pipeline via jumpers and flexible risers. [22]
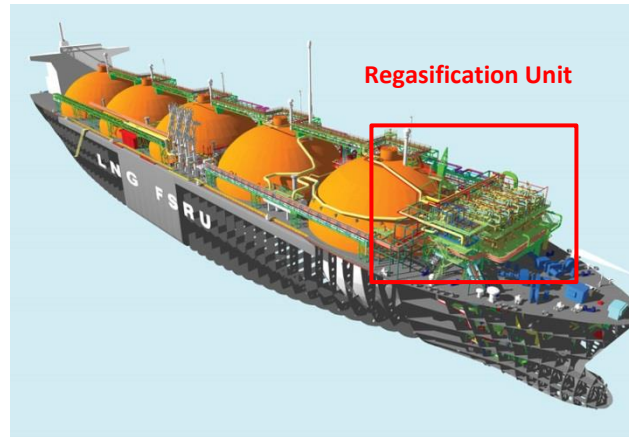
Figure 62 *Regasification unit on the FSRU*

In the vaporization units, heat needs to be added to the LNG so that it can change to its gaseous state. Since the FSRU are located on sea, seawater is available in unlimited quantities compared to other sources of heat, and is therefore the preferred heat source.

14.4 The FSRU

The main components of an FSRU are described in this section.

LNG storage tank systems

When considering FSRU's which have been converted from LNGC four LNG tank systems can be distinct; two self-supporting tank systems and two membrane tank systems.

Membrane tanks, unlike self-supporting tanks, are embedded in the ship structure utilizing the hull shape more efficiently and thus having less space between the storage tanks for the LNG and the ballast tanks. As a result membrane tank systems are cheaper than self-supporting tank systems. The two membrane types are the GTT Mark III and the GTT No.9

On the other hand, self-supporting tank systems are far more robust and have greater resistance to sloshing forces. Membrane types may break due to sloshing impact, therefore destroying the ship's hull. The self-supporting tank systems are thus the preferred type where rough environmental conditions are a significant factor. The two self-supporting types are the Moss (spherical) and the IHI-SPB (prismatic). The storage tank systems are depicted in Figure 63. The membrane type systems have the same shape and are therefore illustrated as one.
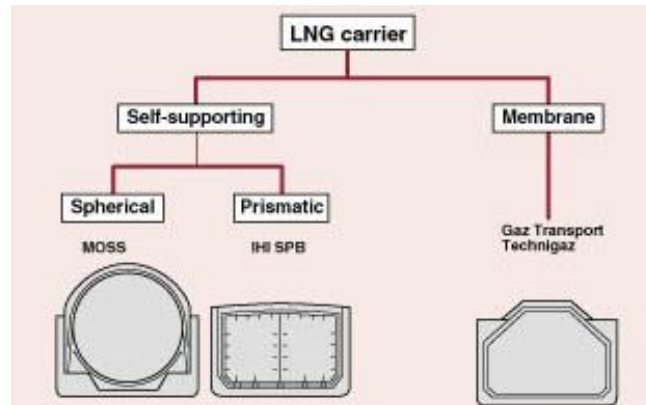
Figure 63 *LNG storage tank systems*

Regasification system

The main components of the regasification system are listed below:

- Sea water pumps which are used to pump seawater to the vaporizers
- Vaporizers warm up the LNG so that it can be transformed back to its natural gaseous state.
- Booster pumps pump the LNG under high pressure into the vaporizers
- Boil of Gas (BOG) compressors, compresses gas that boils off (resulting in vaporization of the LNG). This compressed boil-off gas is typically added to the natural gas send-out. It may also be re-liquefied and returned to the LNG storage tanks.

Loading arms

Loading arms are used to transfer the LNG from the LNGC to the FSRU. Standard loading arms are placed on one side of the FSRU and allow side-by-side transfer of LNG and vapor return[5]. The loading arms will be quite similar to the type that is used on onshore terminals however modified to account for relative motions between LNGC and FSRU [22].

Ballasting tanks

By using ballasting tanks the freeboard is kept constant which improves the mooring integrity and limits the operating range necessary for the loading arms. Also the ballasting tanks may improve the general stability of the FSRU when it is not loaded with LNG.

---

[5] *Vapor return = transfer of boil-off-gas back to the LNGC while it is being unloaded. The boil-off-gas fills the void being created in the ship's tanks thereby preventing tank collapse and the introduction of oxygen into the system.*

15 Appendix II: Other FSRU mooring systems

15.1 Tower Yoke Mooring System

The tower yoke mooring system includes a ''soft-yoke'' for mooring of a vessel directly to a fixed tower. A turntable is fastened to the tower with a roller bearing to allow the vessel to freely weathervane around the tower. A yoke arm is connected to the turntable with pitch and roll joints to allow the vessel to pitch and to roll. [39]

Figure 64 *Picture of a Tower Yoke Mooring System*

15.2 Conventional Buoy Mooring System (CBM)

For A CBM the mooring function is achieved by a spread mooring system of four mooring buoys secured to the seabed. Each buoy incorporates a quick release mooring hook and navigation aids. The transfer of the LNG is achieved by a subsea hose connected to a Pipeline End Manifold [44]

Figure 65 *Picture of a Conventional Buoy Mooring system*

15.3 Single Point Mooring Systems (SPM)

The single point mooring buoy consists of a buoy that is permanently moored to the seabed by means of multiple mooring lines. In opposition to a fixed CBM system, the SPM allows the moored tanker to weathervane. With this principle, the tanker offers the environment (waves, current and wind), the least resistance, thus the system can operates in much higher conditions than fixed systems. [44]

Figure 66 *Picture of a Single Point Mooring System*

15.4 Turrets Mooring Systems

The turret mooring system consists of an integrated Mooring SPM into the vessel. The vessel is anchored at the seabed via the Turret by means of mooring legs and anchor points, and is equipped with a turntable which allows 360° continuous rotation of the FSRU. The turret may be externally fixed (for mild to medium environments) or internally fixed (for harsh environments). [44]

Figure 67 *Picture of a Turrets Mooring System*

16 Appendix III: Dynamic Mooring Analysis

16.1 Introduction

In this appendix first some general background information is given regarding the Dynamic Mooring Analyses (16.2). Subsequently the parameters of the reference projects will be mentioned: Golar (16.3) and Aqaba (16.4). Finally some drawn conclusions from the DMA-analysis will be presented (16.5).

16.2 General information

For a DMA, varying environmental conditions from all directions are considered. Multiple, realistic combinations of those environmental conditions are used as input for such a DMA. The variables which are included in the DMA are wind, waves and currents. Besides additional input is required which is mainly dependent on characteristics of the FSRU and the mooring system. Also, location bounded variables must be defined such as water depth and spectral shapes (for waves and winds). Each run consists of a combination of all the above mentioned input.

The output of a DMA run is: a time series of the vessels motions in the 6 Degrees Of Freedom (6-DOF) and of the mooring forces for that particular run. For the mooring system considered in this study, the output mooring forces are: 4 fender forces and 20 mooring line forces. The maximum motions and maximum mooring forces are subsequently calculated by processing the DMA output.

All input and output parameters are listed in Table 41.

Input	Output
Environmental conditions • Current: velocity, direction • Wind: velocity, direction • Waves: Height, period, direction • Spectral shapes Additional input • Mooring configuration: FSRU-only, side-by-side • Ship: type, dimensions, condition • Lines: diameter, material allocation • Fenders: type, size position • Water depth • Pile-stiffness	• Time series ship motions: surge, sway, heave, roll, pitch, yaw • Time series mooring forces: mooring line forces, fender forces

Table 41 *Input- and output parameters a DMA*

Initial runs

As a first step the varying environmental conditions from all directions are considered in the so-called 'initial DMA runs'. From the results of these runs, the critical runs can be defined which contain the maximum mooring loads as well as the maximum vessel motions. Those 'critical runs' are than considered in more detail by looking at the Most Probable Maximum (MPM).

Most Probable Maximum (MPM)

Since DMA runs in time domain, the maxima of a run are influenced by the length of the run. The longer the run, the more likely a larger maximum is found. The MPM method is therefore introduced. A certain critical case will be simulated various times with different random seeds in order to arrive at a distribution of the maxima. Subsequently the mean and standard deviation of the distribution can be established. The Most Probable Maximum of that distribution can then be derived at the peak of the probability density function.

Determination of Maximum Dolphin Loads

As indicated previously, the critical cases for mooring loads (breast line, spring line and fender loads) are considered in more detail in order to determine the Most Probable Maximum of the loads. The MPM line and fenders loads are used to determine the maximum loads on the breasting and mooring dolphins. Those maximum forces are determined as follows:

- The maximum mooring dolphin (MD) load is determined by adding the MPM loads of the breast lines which are attached to one single mooring dolphin.

$$F_{MD,max} = \sum F_{breasting\ line}$$

- The maximum breasting dolphin (BD) load is determined by combining the MPM fender load with the fender friction and the spring line load. The fender load and spring line load are taken from the same run but act perpendicular to each other.

$$F_{BD,max} = \sqrt{F_{fender}^2 + \left(F_{friction} + F_{spring\ line}\right)^2}$$

16.3 DMA reference project Golar

A FSRU will be located offshore approximately 15km north of Jakarta in the Java Sea. The import of LNG will be done in side-by-side mooring configuration between FSRU and LNGC. Mooring facility required for the mooring and operating of the FSRU consists of mooring and breasting dolphins.

The mooring loads and vessel motion are assessed with the aid of numerical simulation, DMA.

16.3.1 Mooring configuration
Vessels

The FSRU is a converted 125.000m3 spherical LNGC.

Parameters	Unit	FSRU 125,000 m3	
Length over all (Loa)	m	292	
Length between perpendiculars (Lpp)	m	282	
Breadth (Bs)	m	41,6	
Depth to upper deck	m	25	
Loading conditions	-	*Loaded*	*Ballasted*
Displacement	m³	100000	82500
Draught	m	11,8	9,6
Freeboard	m	13,2	15,4
Front wind area/ Side wind area	m²	1400/7850	1500/8500
Height of Center of Gravity (above keel)	m	14	13
Transverse radius of inertia	m	14,5	14,5
Distance of center of Gravity (to midship)	m	0,4	0,2

Table 42 *Dimensions 125.000m3 spherical LNGC*

FSRU mooring arrangement

The mooring arrangement of the FSRU, including the dolphin/bollard locations is illustrated below. The bow of the vessel is directed towards the north.
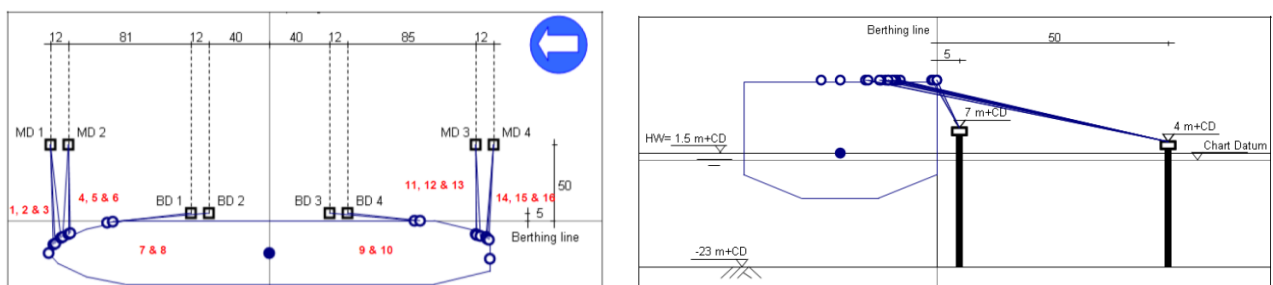
Figure 68 *FSRU mooring arrangement - Golar project*

The bollard level of the breasting dolphins (BD) is CD+7.0m and the bollard level of the mooring dolphin (MD) is CD+4.0m. The total number of mooring lines of the FSRU is 20:

- 6 breast lines at the bow and 6 at the stern
- 4 spring line at the bow and 4 at the stern

Mooring lines (between FSRU and dolphins)

Parameter	Unit	Breast lines	Spring lines
Type of mooring lines	-	Steel wire	Steel wire
Diameter	mm	56	36
Minimum Breaking Load	kN	2220	918
Max permitted line load (55% MBL)	kN	1221	504.9
Stiffness	kN	122,700	50,700
Type of tail	-	Double braided	Double braided
Diameter	mm	129.4	80.9
Minimum Breaking Load	kN	3335	1354

Table 43 *Mooring lines, Golar project*

Fenders (between FSRU and dolphins)

- Foam fender Sea Guard [41] or Ocean Guard [19]
- Extra High Capacity (EHC, foam grade factor 1.9)
- Fender diameter 3300 mm
- Fender length 6500 mm
- Maximum rated reaction force of 5189 kN at 60% deflection (1.98m)
- Maximum fender force of 5967 kN (Taking into account a 15% manufactory tolerance) which results in a higher stiffness and higher fender loads
- The fender friction coefficient is 0.5

16.3.2 Environmental conditions
Currents

Direction	RP =1 yr	RP =10 yr	RP =100 yr
0	0,6	0,7	0,8
30	0,7	0,7	0,8
45	0,7	0,7	0,8
60	0,7	0,7	0,8
90	0,7	0,8	0,9
120	0,6	0,7	0,8
135	0,6	0,7	0,8
150	0,6	0,7	0,7
180	0,5	0,6	0,6
210	0,6	0,7	0,7
225	0,7	0,7	0,8
240	0,8	0,8	0,9
270	0,9	1	1,1
300	0,8	0,9	1
315	0,8	0,9	0,9
330	0,8	0,9	0,9

Table 44 *Current conditions, Golar project*

Waves

Direction	RP = 1 yr		RP = 10 yr		RP = 100 yr	
	Hs [m]	Tm [sec]	Hs [m]	Tm [sec]	Hs [m]	Tm [sec]
0	1,6	6,2	1,7	6,6	1,8	7,1
30	1,5	6	1,6	6,4	1,7	6,8
45	1,5	6	1,5	6,3	1,6	6,6
60	1,4	5,6	1,4	5,9	1,5	6,1
90	1,2	4,8	1,3	5	1,4	5
120	1	3,8	1,2	4	1,3	4
135	0,9	3,2	1,1	3,5	1,2	3,6
150	0,8	3	1	3,2	1,1	3,3
180	0,7	2,6	0,8	2,8	0,9	2,9
210	0,8	3	1	3,1	1,1	3,2
225	0,9	3,2	1,1	3,3	1,2	3,4
240	1	3,7	1,2	3,9	1,3	4
270	1,3	4,9	1,4	5	1,5	5,1
300	1,5	5,5	1,6	5,8	1,6	6,2
315	1,6	5,9	1,7	6,2	1,7	6,8
330	1,6	6	1,7	6,3	1,7	6,9

Table 45 *Wave conditions, Golar project*

Wind

Direction	RP = 1 yr		RP = 10 yr		RP = 100 yr	
	Storm [m/s]	Squall [m/s]	Storm [m/s]	Squall [m/s]	Storm [m/s]	Squall [m/s]
0	13	21	14	27	16	33
30	11,7	21	13,3	27	14,7	33
45	11	21	13	27	14	33
60	11,7	20,7	13,3	26,7	14,7	32,3
90	13	20	14	26	16	31
120	13	19,3	14	25,3	16	30,3
135	13	19	14	25	16	30
150	12,7	19,3	13,7	25,3	15,7	30,3
180	12	20	13	26	15	31
210	13,3	20,7	15	26,7	16,3	32,3
225	14	21	16	27	17	33
240	14,3	21	16,7	27	18	33
270	15	21	18	27	20	33
300	15	20,3	16,7	26,3	18,7	31,7
315	15	20	16	26	18	31
330	14,3	20,3	15,3	26,3	17,3	31,7

Table 46 *Wind conditions, Golar project*

16.4 DMA reference project Aqaba

The Aqaba project consists of designing a single berth jetty for an FSRU. This jetty will be situated close to the Jordan's coast line on the Red Sea near the city of Aqaba. The import of LNG will be done in side-by-side mooring configuration between FSRU and LNGC. The mooring facility required for the mooring and operating of the FSRU consists of mooring and breasting dolphins. The mooring loads and vessel motion are assessed with the aid of numerical simulation, DMA.

16.4.1 Mooring configuration
Vessels

The FSRU is a 170,000m3 converted LNGC. Further specifications are listed below.

Parameters	Unit	FSRU 170,000 m3	
Length over all (Loa)	m	292	
Length between perpendiculars (Lpp)	m	284	
Breadth (Bs)	m	46,4	
Depth to upper deck	m	25	
Loading conditions	-	*Loaded*	*Ballasted*
Displacement	m³	108100	80500
Draught	m	11,5	8,8
Freeboard	m	13,5	16,2
Front wind area/ Side wind area	m²	1692/6560	1860/7510
Height of Center of Gravity (above keel)	m	17,5	14
Transverse radius of inertia	m	18	18
Distance of center of Gravity (to midship)	m	0	0

Table 47 *Dimensions 170.000m3 LNGC*

FSRU mooring arrangement

The mooring arrangement of the FSRU, including the dolphin/bollard locations is illustrated below. The bow of the vessel is directed towards the NNE (-25⁰N)
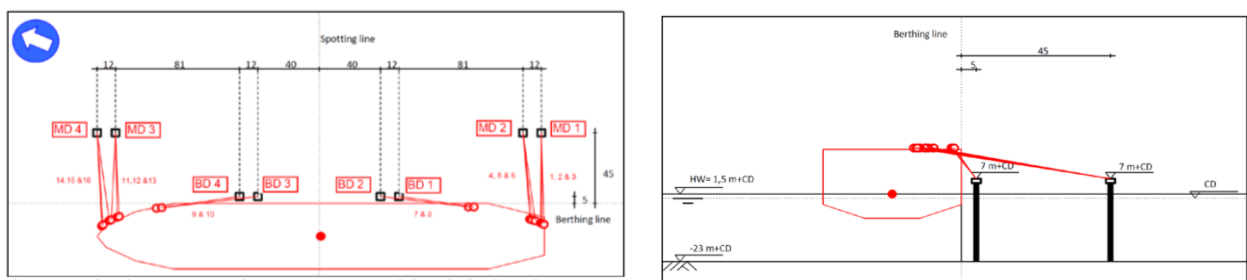
Figure 69 *FSRU mooring arrangement – Aqaba project*

The bollard level of the breasting dolphins (BD) is CD+7.0m and the bollard level of the mooring dolphin (MD) is CD+7.0m. The total number of mooring lines of the FSRU is 20:

- 6 breast lines at the bow and 6 at the stern
- 4 spring line at the bow and 4 at the stern

Mooring lines (between FSRU and dolphins)

Parameter	Unit	Breasting lines	Spring lines
Type of mooring lines	-	Steel wire	Steel wire
Diameter	mm	44	44
Minimum Breaking Load	kN	1350	1350
Max permitted line load (55% MBL)	kN	742.5	742.5
Stiffness	kN	75,700	75,700
Type of tail	-	Double braided	Double braided
Diameter	mm	97	97
Minimum Breaking Load	kN	1913	1913

Table 48 *Mooring Lines, Aqaba project*

Fenders (between FSRU and dolphins)

- Foam fender Sea Guard [41] or Ocean Guard [19]
- Extra High Capacity (EHC, foam grade factor 1.9)
- Fender diameter 3300 mm
- Fender length 4500 mm
- Maximum rated reaction force of 3211 kN at 60% deflection (1.98m)
- Maximum fender reaction force of 3693 kN (Taking into account a 15% manufactory tolerance)
- The fender friction coefficient is 0.5

16.4.2 Environmental conditions
Currents

For this case the recommendations of the OCIMF guidelines have been adopted. A current of 0.5m/s with an approximate direction of 10° and 170° with respect to the ships center line has been taken into account

Waves

Direction	RP = 1 yr		RP = 2 yr		RP = 5 yr		RP = 10 yr	
	Hs [m]	Tp [sec]	Hs [m]	Tp [sec]	Hs [m]	Tp [sec]	Hs [m]	Tp [sec]
S	0,9	5,9	1	6,1	1,1	6,4	1,2	6,6
SSW	1,3	6	1,5	6,4	1,7	6,6	1,8	6,9
SW	1,4	5,5	1,6	5,9	1,8	6,3	2	6,5
WSW	1,2	4,9	1,4	5	1,7	5,4	1,8	5,5
W	1,1	4,2	1,2	4,3	1,4	4,5	1,6	4,6
WNW	0,9	3,7	0,9	3,8	1	3,9	1,1	4
NW	0,8	3,6	0,8	3,7	0,9	3,8	0,9	3,8
NNW	0,7	3,6	0,7	3,6	0,8	3,7	0,8	3,8
N	0,5	3,2	0,5	3,3	0,6	3,5	0,6	3,5

RP = 20 yr		RP = 50 yr		RP = 100 yr	
Hs [m]	Tp [sec]	Hs [m]	Tp [sec]	Hs [m]	Tp [sec]
1,3	6,9	1,4	7,1	1,5	7,3
2	7,1	2,1	7,4	2,3	7,6
2,1	6,7	2,4	7	2,5	7,1
2	5,8	2,2	6	2,4	6,2
1,7	4,8	1,9	5	2	5
1,2	4,1	1,2	4,2	1,3	4,2
0,9	3,8	1	3,9	1	3,9
0,8	3,8	0,9	3,8	0,9	3,9
0,7	3,6	0,7	3,8	0,7	3,8

Table 49 *Wave conditions, Aqaba project*

Wind

Direction	RP = 1 yr	RP = 2 yr	RP = 5 yr	RP = 10 yr	RP = 20 yr	RP = 50 yr	RP = 100 yr
S	13,3	14,5	16	17	18	19,3	20,2
SSW	14,5	15,8	17,5	18,7	19,8	21,2	22,2
SW	13,4	14,9	16,7	17,9	19,2	20,8	21,9
WSW	12,9	14,4	16,3	17,7	19,1	20,8	22
W	13,7	15,1	16,9	18,2	19,5	21,1	22,3
WNW	12,6	13,5	14,6	15,4	16,2	17,1	17,8
NW	12,2	12,7	13,3	13,8	14,2	14,8	15,1
NNW	11,5	12	12,7	13,2	13,7	14,3	14,8
N	9,4	10,1	11	11,6	12,3	13,1	13,8
NNE	5,9	7,2	8,8	10,1	11,3	13	14,2
NE	6	6,5	7,2	9	10,8	13,1	14,8
ENE	5,1	5,7	6,5	7,1	7,7	8,5	9,1
E	6,7	7,1	7,5	7,8	8,1	8,4	8,7
ESE	7,8	8,2	8,7	9,1	9,5	9,9	10,3
SE	7	7,6	8,4	8,9	9,5	10,3	10,9
SSE	8,5	9,2	10,1	10,7	11,2	11,9	12,4

Table 50 *Wind conditions, Aqaba project*

16.5 Drawn conclusions from DMA analysis

16.5.1 Fender deflection mainly dominated by sway motion

From the analysis of the different DMA data can be concluded that the fender deflection is dominated by the sway motion. For waves coming perpendicular towards the ships axis (270°), the fender deflection is nearly due to sway only. If the waves are coming from an angle, the yaw motion becomes more significant. The contribution of roll to fender deflection is minor and can therefore be neglected. The runs which are represented below are all from the Golar project. The runs which have been performed for waves and winds coming from 270° (marked in orange), lead to the largest fender forces.

Run name	Wind/ Wave Direction	Wave height	Wave period	Wind Speed	Current direction	Current velocity	MAX Fd1 (DMA) [kN]	MAX u1 [m]	Sway (DMA) [m]	Contribution of sway	Contribution of other motions
					ULS STORM CELL FENDER						
Run0010B	330	1.1	3.5	16.3	330	0.7	726	0.38	-0.29	76.1%	23.9%
Run0011B	315	1.2	3.7	17	315	0.8	1260	0.66	-0.46	70.2%	29.8%
Run0012B	300	1.3	4.3	18	300	0.9	1842	0.97	-0.68	69.9%	30.1%
Run0013B	270	1.5	5.5	20	270	1.1	2751	1.56	-1.50	96.0%	4.0%
Run0014B	240	1.6	6.7	18.7	240	1	1781	0.94	-1.02	91.2%	8.8%
Run0015B	225	1.7	7.3	18	225	0.9	1328	0.70	-0.76	91.1%	8.9%
Run0016B	210	1.7	7.4	17.3	210	0.9	770	0.40	-0.43	92.5%	7.5%
					ULS SQUALL CELL FENDER						
Run0210B	330	0.8	3.2	32.3	330	0.6	1224	0.64	-0.44	68.6%	31.4%
Run0211B	315	0.9	3.4	33	315	0.7	2061	1.10	-0.75	68.6%	31.4%
Run0212B	300	1	4	33	300	0.8	2668	1.48	-1.04	70.3%	29.7%
Run0213B	270	1.3	5.3	33	270	0.9	2945	1.75	-1.73	99.1%	0.9%
Run0214B	240	1.5	6	31.7	240	0.8	1831	0.97	-1.32	64.0%	36.0%
Run0215B	225	1.6	6.3	31	225	0.8	1311	0.69	-1.00	54.0%	46.0%
Run0216B	210	1.6	6.4	31.7	210	0.8	800	0.42	-0.59	57.7%	42.3%
					ULS STORM FOAM FENDER						
Run0010B	330	1.1	3.2	16.3	330	0.7	849	0.31	-0.23	72.0%	28.0%
Run0011B	315	1.2	3.4	17	315	0.8	1523	0.56	-0.38	68.1%	31.9%
Run0012B	300	1.3	4	18	300	0.9	2035	0.75	-0.53	70.5%	29.5%
Run0013B	270	1.5	5.1	20	270	1.1	3333	1.19	-1.12	94.7%	5.3%
Run0014B	240	1.6	6.2	18.7	240	1	1755	0.65	-0.70	92.0%	8.0%
Run0015B	225	1.7	6.8	18	225	0.9	1462	0.54	-0.58	92.9%	7.1%
Run0016B	210	1.7	6.9	17.3	210	0.9	842	0.31	-0.32	98.0%	2.0%
					ULS SQUALL FOAM FENDER						
Run0210B	330	0.8	3	32.3	330	0.6	1322	0.49	-0.33	67.9%	32.1%
Run0211B	315	0.9	3.2	33	315	0.7	2200	0.81	-0.55	67.8%	32.2%
Run0212B	300	1	3.7	33	300	0.8	2868	1.05	-0.73	69.3%	30.7%
Run0213B	270	1.3	4.9	33	270	0.9	4255	1.46	-1.36	92.6%	7.4%
Run0214B	240	1.5	5.5	31.7	240	0.8	1648	0.61	-0.90	52.6%	47.4%
Run0215B	225	1.6	5.9	31	225	0.8	1281	0.47	-0.73	46.5%	53.5%
Run0216B	210	1.6	6	31.7	210	0.8	812	0.30	-0.45	49.6%	50.4%

Table 51 *Contribution of vessel motions to fender deflection*

16.5.2 Fender deflections more accurate than fender forces

In order to determine whether comparison of the fender deflections or fender forces is more accurate, the DMA results of two different types of fenders are compared: a very soft CELL fender and a Foam fender. Their Reaction Force/Deflection-curve is shown in Figure 70.
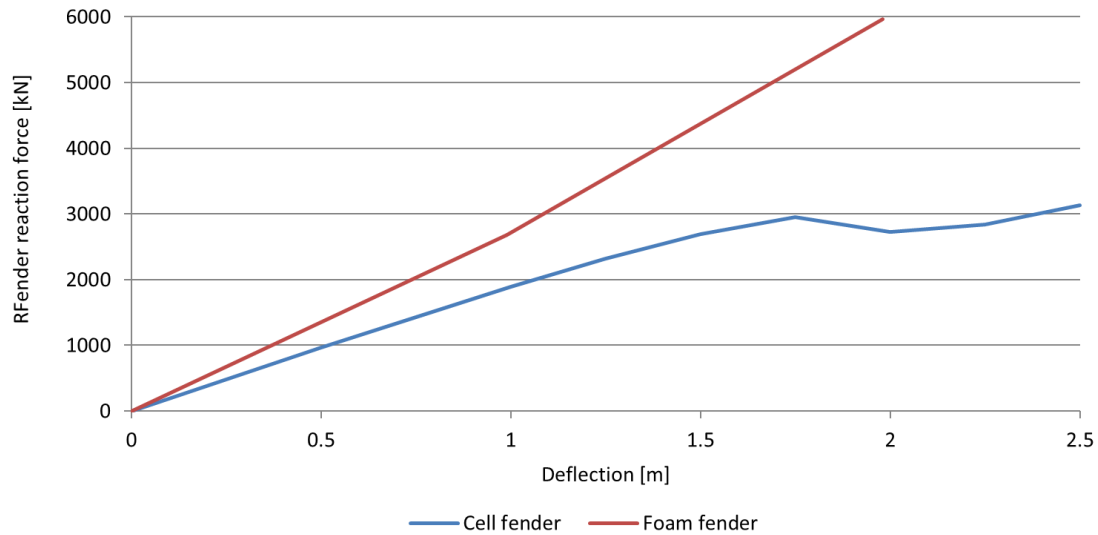
Figure 70 *Fender curves applied for the comparison*

For the DMA's which are performed for both fenders, (nearly) similar environmental conditions are applied. This gives the opportunity to compare both fenders solely on their characteristics since all other input variables are the same.

The maximum fender forces (MAX Fd1) are direct output of the DMA's. The resultant fender force (RES Fd1) is calculated by subtracting the contribution of wind and currents to "MAX Fd1". "RES Fd1" represents the fender force due to wave action only. The corresponding fender deflections are calculated by means of the Force-Deflection curves. For this study only the environmental conditions coming from portside direction (330⁰ - 210 ⁰) are considered, since those lead to the maximum fender forces.

Input parameters						Foam fender			Cell fender			Fender force		Fender deflection	
Run Name	Wind/ Wave Direction	Wave height	Wave period	Wind speed	Current direction	Current velocity	MAX Fd1 [kN]	RES Fd1 [kN]	RES u1 [m]	MAX Fd1 [kN]	RES Fd1 [kN]	RES u1 [m]	Δ RES Fd1 [kN]	Margin of Error	Δ RES u1 [m]	Margin of Error
Run 0010B	330	1.1	3.4	16.3	330	0.7	849	562	0.21	726	445	0.18	117	21%	0.03	14%
Run 0011B	315	1.2	3.6	17	315	0.8	1523	942	0.35	1260	692	0.32	251	27%	0.03	8%
Run 0012B	300	1.3	4.2	18	300	0.9	2035	1176	0.43	1842	982	0.44	193	16%	-0.01	1%
Run 0013B	270	1.5	5.3	20	270	1.1	3333	2393	0.88	2751	1825	0.86	567	24%	0.02	2%
Run 0014B	240	1.6	6.5	18.7	240	1	1755	1239	0.46	1781	1239	0.56	0	0%	-0.10	22%
Run 0015B	225	1.7	7.1	18	225	0.9	1462	1083	0.40	1328	949	0.41	134	12%	-0.01	3%
Run 0016B	210	1.7	7.2	17.3	210	0.9	842	628	0.23	770	554	0.24	75	12%	0.00	2%
Run 0030B	330	1.1	3.4	16.3	90	0.9	296	320	0.12	319	334	0.16	-14	4%	-0.04	34%
Run 0031B	315	1.2	3.6	17	90	0.9	525	365	0.13	820	630	0.28	-266	73%	-0.15	109%
Run 0032B	300	1.3	4.2	18	90	0.9	888	540	0.20	1274	877	0.40	-337	62%	-0.20	99%
Run 0033B	270	1.5	5.3	20	90	0.9	2161	1734	0.64	2281	1820	0.80	-86	5%	-0.16	24%
Run 0034B	240	1.6	6.5	18.7	90	0.9	1246	1015	0.37	1498	1248	0.57	-232	23%	-0.19	51%
Run 0035B	225	1.7	7.1	18	90	0.9	1075	950	0.35	1070	944	0.49	6	1%	-0.13	38%
Run 0036B	210	1.7	7.2	17.3	90	0.9	514	536	0.20	633	652	0.25	-116	22%	-0.05	28%
Run 0050B	330	1.1	3.4	16.3	270	1.1	1255	691	0.26	992	427	0.19	263	38%	0.07	26%
Run 0051B	315	1.2	3.6	17	270	1.1	1723	943	0.35	1447	656	0.30	287	30%	0.05	14%
Run 0052B	300	1.3	4.2	18	270	1.1	2112	1140	0.42	1922	924	0.42	216	19%	0.01	1%
Run 0053B	270	1.5	5.3	20	270	1.1	3333	2393	0.88	2751	1825	0.86	567	24%	0.02	2%
Run 0054B	240	1.6	6.5	18.7	270	1.1	1930	1313	0.48	1883	1239	0.52	74	6%	-0.04	8%
Run 0055B	225	1.7	7.1	18	270	1.1	1640	1109	0.41	1581	1041	0.39	68	6%	0.02	5%
Run 0056B	210	1.7	7.2	17.3	270	1.1	1145	732	0.27	1011	618	0.25	114	16%	0.02	8%

Table 52 *Comparison between fender force and fender deflection*

The conclusion which can be drawn from this study is that; comparing the fender forces is much less accurate then comparing the fender deflections. This can be explained by the fact that the fenders have a different Force-Deflection relationship as can be seen from the graph. In this case the Cell fender is more advantageous as it is much more flexible and may allow larger movements of the vessel for similar fender reaction forces. This can also be seen from the DMA results; for similar environmental conditions the Foam fender lead to much larger fender forces than the Cell fender.

From this study can be assumed that the motions of the vessel are not significantly restrained by the choice of the fender. The vessel will move due to certain environmental conditions. Those movements are only very little restrained/influenced by the type of fender. It is therefore recommended to analyze the lateral movements of the ship and link them afterwards to a fender force based on a certain fender type (through the Force-Deflection curves).

16.5.3 Squall conditions governing over storm conditions

Squalls are peaked winds which are modeled as a constant 1-minute mean wind speed. Storms are modeled as a spectrum and are represented by a constant 1-hourly mean wind speed.

Based on DMA result can be concluded that; squall conditions always lead to larger fender forces than storm conditions. Even if for the storm conditions somewhat larger waves are applied within the DMA's. When considering wind and wave conditions coming beam-on the maximum fender force due to squall may be up to 40% higher than for storm conditions. This can also be seen in Figure 71.

The following graph shows the fender force per incoming wind/wave direction, for both storm and squall conditions. The directions are according the reference system described in the introduction.
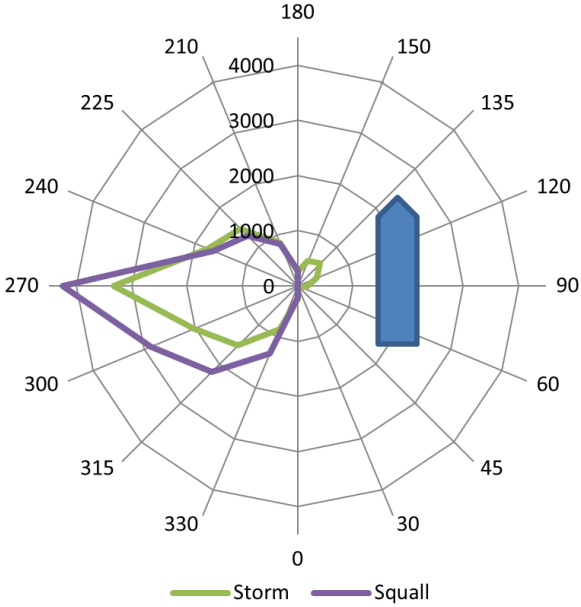
Figure 71 *Maximum fender force [kN] per incoming direction, Golar project, Foam fender*

17 Appendix IV: Application assessment tool example

In this appendix an example is shown of how the assessment tool should be applied to calculate the fender loads on the mooring system.

It starts off with the definition of the input variables; environmental conditions, vessel dimensions and fender characteristics.

Input parameters	Input values
Environmental conditions	
Wave direction	270 deg
H_S	1.4 m
T_P	5 sec
Wind direction	270 deg
U_W	18 m/s
Current direction	270 deg
U_C	1 m/s
Vessel dimensions	
f	15.4 m
d	9.6 m
L	282 m
Fender characteristic	
Type	Ocean Guard - Stiff
$F_{reaction}$	5967 kN

Table 53 *Input variables applied in calculation example*

Fender force due to wave action

For the calculation of the fender force due to wave action, the fender deflection should be determined. This is achieved by translating a design wave height to a fender deflection by means of the graph illustrated in Figure 72.
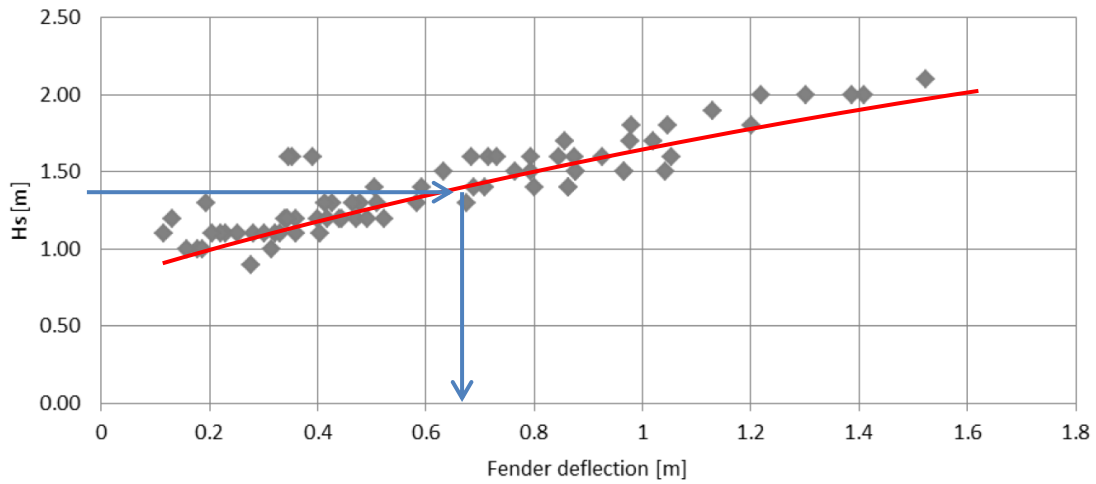
Figure 72 *Hs / fender deflection*

For a wave height of 1.4m, the fender deflection reads approximately 0.68m. Subsequently, this deflection can be translated to a fender reaction force with a fender-curve corresponding to the chosen fender. In this case the fender force due to waves (F$_{wave}$) is 1850kN.
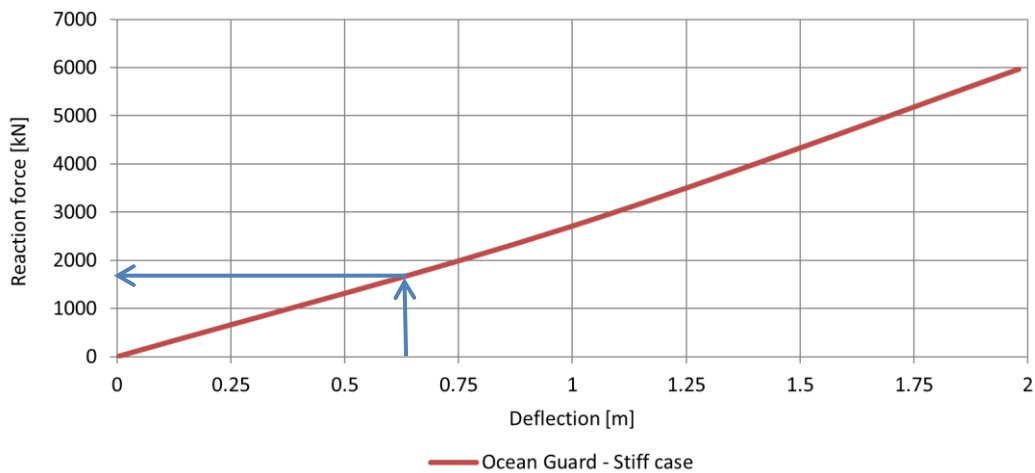
Figure 73 *Fender curve for the Ocean Guard-type with a maximum reaction force of 5967 kN*

Fender force due to winds

The winds were assumed quasi-static. Their corresponding fender force can calculated with the following equation:

$$Fwind = \alpha \; \frac{1}{2} \; C_w \; \rho_w \; v_w^2 \; L_{BP} \; f/1000 = 0.27 * \frac{1}{2} * 1.165 * 1.28 * (1.37 * 18)^2 * 15.4 * \frac{282}{1000} = 532$$

A gust factor of 1.37 is applied. The C_w coefficient is described in the OCIMF guidelines, where the alpha-coefficient is obtained through Figure 74 and is dependent on the incoming direction of winds according to the Cartesian convention.
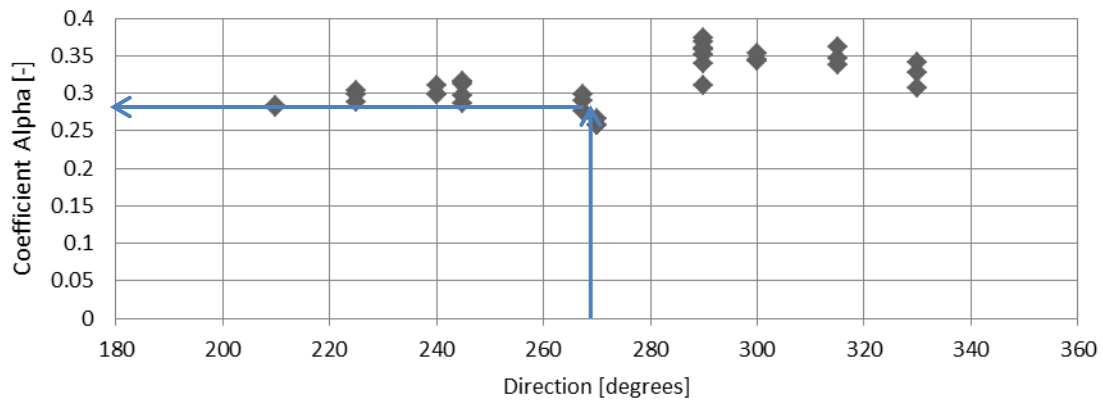
Figure 74 *Coefficient alpha / incoming direction*

Fender force due to currents

In a similar manner the fender force due to currents is obtained.

$$Fcurrent = \alpha \; \frac{1}{2} \; C_c \; \rho_c \; v_c^2 \; L_{BP} \; \frac{d}{1000} = 0.27 * \frac{1}{2} * 0.653 * 1025 * (1)^2 * 9.6 * \frac{282}{1000} = 245 kN$$

Total fender force

The total fender force is then a simple summation of the three terms:

$$Ffender = \; Fwave + \; Fwind + \; Fcurrent = \; 1850 + 532 + 245 = 2626 \; kN$$

Subsequently, the calculated value shall be multiplied with a load factor in order to have the design load.

18 Appendix V: Other method for visualization of the design fender loads

18.1 Introduction

In this appendix another method is presented for the visualization of the design fender loads. It must be noted that this method is not yet optimized and still need some research before generating reliable results. The underlying idea behind this method is described in Section (18.2). The current results and conclusions are presented in Section (18.3).

18.2 Method

For this method, as well as for the one presented in the main report, the three environmental components are separated: wind, wave and current. This is considered a safe assumption as foam filled floating fenders are applied with a, nearly, linear force-deflection curve. The calculation of the fender loads due to winds and currents is performed in the same manner as for the method presented in the main report (Section 4.3.2). The fender forces due to wave action are obtained through a dimensionless fender force – fender deflection relationship. Such relationship is normally described by the fender curves and represents the stiffness of the system.

The dimensionless fender force is determined by dividing the actual fender force (F) by the maximum fender force if the vessel was fully fixed to a system of infinite stiffness (F*).

> ➢ *E.g. if the FSRU would be attached directly to a caisson (without the resonance effects of the waves being reflected against the wall). The mooring system would be infinitely stiff and there would be little to no energy dissipation. The load would therefore be maximal and the displacement zero. (see Figure 75 top)*

The dimensionless fender deflection is determined by dividing the actual fender deflection (u) by the largest possible motion if the vessel was completely free in its movements (u*), thus attached to a system of zero stiffness.

> ➢ *E.g. if the FSRU would be attached to very loose anchor lines. The vessel would be completely unrestrained in its movements and therefore the displacement would be maximal while and the force zero. (see Figure 75 bottom)*

The stiffness of the mooring system considered in this study, which is a fender combined with a flexible mono-pile, must be situated somewhere in between the two abovementioned extremes (see Figure 75 middle). By analyzing where the position of the considered mooring system is in the dimensionless graph, an insight can be gained into the stiffness of this system.
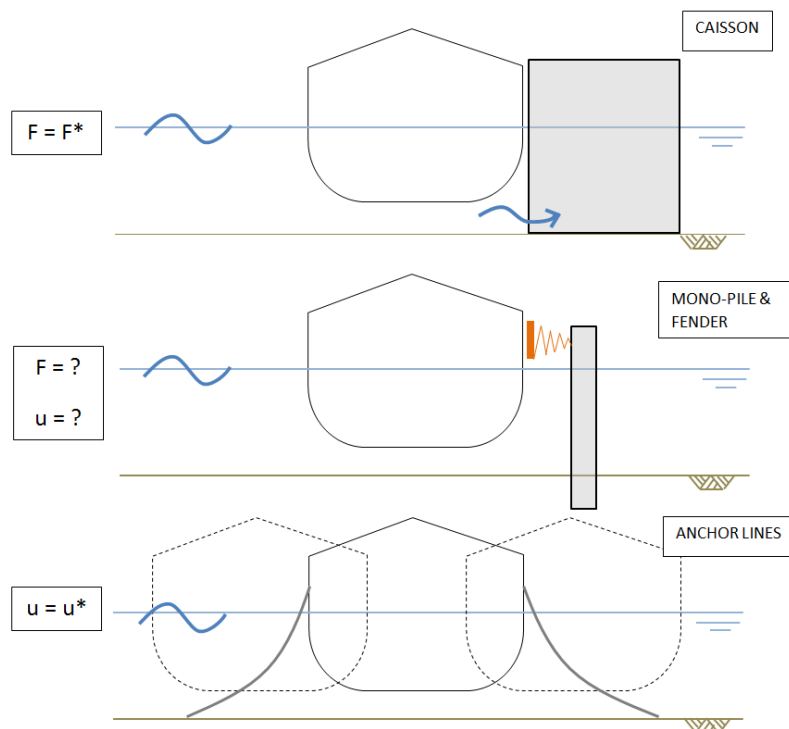
Figure 75 *Schematic representation of systems with different rigidities*

Calculation of F*

The maximum force on the structure if the vessel would be completely fixed, F*, is calculated by means of 'wave force transfer functions' which can be found in the so-called hydrodynamic files (HYD-files) of a vessel. Those files describe the hydrodynamics of an object, in this case the LNG carriers. A HYD-file contains the results of diffraction calculations: added masses, potential damping, and first and second order wave force transfer functions.

By means of the wave force transfer function the force can be calculated resulting from an incoming wave. The force amplitude response (FAMP) which follows from the wave transfer functions depends on: wave period, -direction and the motion of the vessel being considered. Each of the 6 Degrees of Freedom (6 DOF) has its own corresponding transfer function.

The first order wave transfer functions are the direct response to an incoming wave. The second order wave transfer function regards secondary drift forces. Those occur due to the fact that the waves at one side of the vessel are larger than the transmitted waves at the other side of the vessel (partly damped), which leads to a net force in the same direction as the wave field. For the results presented in the following section, F* was only calculated as a result of the first order wave force transfer functions. For accurate results the secondary drift forces should be taken into account.

The calculation of F* are done for sway and yaw:

$$F_Y^* = FAMP_Y * \zeta_a$$

$$F_\psi^* = FAMP_\psi * \zeta_a / X_{CoG-fender}$$

$$F^* = F_Y^* + F_\psi^*$$

$FAMP_Y = \frac{F_a}{\zeta_a} \left[\frac{kN}{m}\right]$ Force Amplitude response for sway

$FAMP_\psi = \frac{M_a}{\zeta_a} \left[\frac{kNm}{m}\right]$ Force Amplitude response for yaw

ζ_a [m]   Wave amplitude

$X_{CoG-fender}[m]$ Distance, in x-direction, between Center of Gravity (COG) and fender

Calculation of u*

This maximum displacement (in Y-direction according to the Cartesian convention, Figure 5) of the vessel when being completely free to move, u*, is calculated by means of so-called RAO's (Response Amplitude Operators).

RAOs are transfer functions used to determine the effect that a sea state will have upon the motion of a ship through the water. RAO's are computed in tandem with the generation of a hydrodynamic database (HYD-files). The RAO's can be found for the 6 DOF. Furthermore, they are dependent on wave period and –direction. In must be noted that, also in these calculations only the oscillatory component of the waves are taken into account. The drift component is neglected.

The calculation of u* are done in the following manner:

$$u_Y^* = RAO_Y * \zeta_a$$

$$u_\psi^* = sin\ (\psi) * X_{CoG-fender}$$

$$\psi\ [deg] = RAO_\psi * \zeta_a$$

$$u^* = u_Y^* + u_\psi^*$$

$RAO_Y = \frac{Y_a}{\zeta_a} \left[\frac{m}{m}\right]$ Response Amplitude Operator for sway

$RAO_\psi = \frac{\psi_a}{\zeta_a} \left[\frac{deg}{m}\right]$ Response Amplitude Operator for yaw

ζ_a [m]   Wave amplitude

$\psi[deg]$ Yaw angle

$X_{CoG-fender}[m]$ Distance between COG and fender in x-direction

The motions of a vessel as a result to a certain sea state are described by an amplitude and a phase angle:

$$Incoming\ wave: \qquad \zeta\ (t) = \zeta_a \sin(\omega t)$$

$$Sway\ motion: \qquad Y(t) = Y_a \sin(\omega t + \varepsilon_{y\zeta})$$

$$Yaw\ motion: \qquad \psi(t) = \psi_a \sin(\omega t + \varepsilon_{\psi\zeta})$$

For the calculations made in this section, the phase angles are neglected. The assumption is made that the maxima of the motions (and forces), for sway and yaw, will occur simultaneously. This is an overestimation.

18.3 Results and conclusions

As mentioned in the introduction the method is not yet optimized: the second order drift component should be taken into account, wind and current forces should also be implemented in this method (currently seen as quasi static forces) and more DMA data is required in order to see whether the method generates reliable results or not. In the graph below the method was tested with the available DMA data.
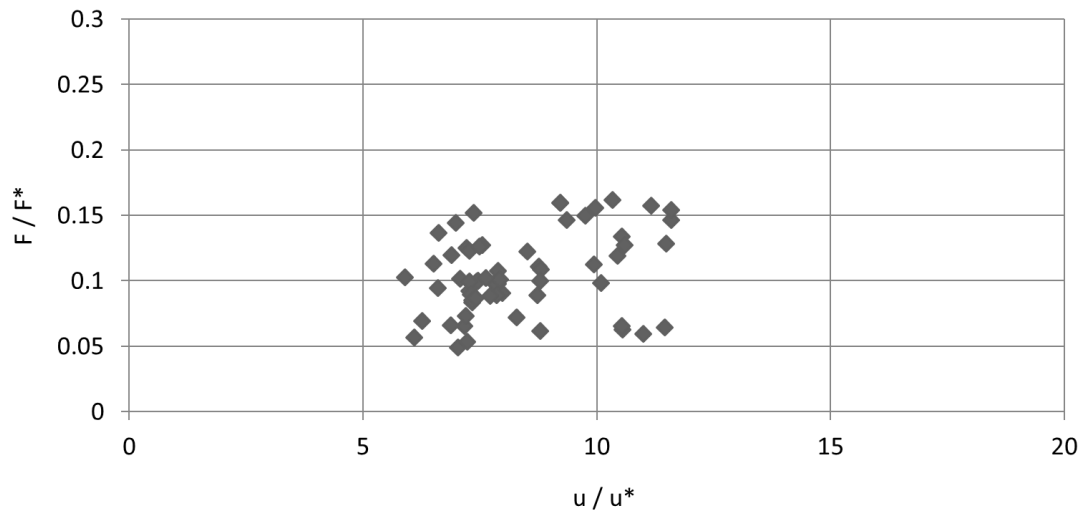
Figure 76 *Results of the method for determination of design fender loads*

As can be observed, the results are clustered which indicate that this method may generate reliable results. The horizontal axis, however, is not rightly scaled; both axes should range between 0 and 1. This can mainly be explained by the fact that the second order drift component is not yet implemented in the method. The vertical axis does show good results; the processed DMA data is ranging between 0.05 and 0.15, already giving some indication on the stiffness of the system.

19 Appendix VI: Lateral bearing capacity mono-piles, p-y curves

19.1 Introduction

Different p-y curves applied for the lateral bearing capacity of the piles are described in this Appendix. Since the loads are of cyclic nature, the modified p-y curves are used. These curves are implemented within the program LPile v6.0 with which the laterally loaded pile calculations are made. In (19.2) the p-y curves for soft clay are discusses, in (19.3) the p-y curves for stiff clay and in (19.4) the p-y curves for sand.

19.2 P-y curves for soft clay (Below Water Table)

The p-y curves for soft clay are determined based on the Matlock theory (1970).

The ultimate soil resistance for soft clays depends on the depth below the surface and can be calculated using the smaller of the values calculated by the following equations:

$$p_u = 3c + \gamma X + J\frac{cX}{D}$$

$$p_u = 9c \ for \ X \ \geq \ X_R$$

p_u: ultimate resistance [kPa]

c: undrained shear strength for undisturbed clay soil samples [kPa]

D: pile diameter [mm]

γ: effective unit weight of soil [MN/m³]

J: dimensionless empirical constant with values ranging between from 0.25 to 0.5

X: depth below soil surface [mm]

X_R: depth below soil surface to bottom reduced resistance zone [mm]. For a condition of constant strength with depth, the two above equations are solved simultaneously to give:

$$X_R = \frac{6D}{\frac{\gamma D}{c} + J}$$

With the ultimate soil resistance determined, the deflection y_{50}, at one-half of the ultimate soil resistance will be determined by:

$$y_{50} = 2.5 \ \varepsilon_{50} \ D \ [mm]$$

Where ε_{50} is the axial strain.

The p-y curve for soft clay is given in Figure 77. The first branch of the curve (0 < y < $3y_{50}$) is given by:

$$\frac{p}{p_u} = 0.5 \ \left(\frac{y}{y_{50}}\right)^{\frac{1}{3}}$$

The other branches are linear. For $y/y_{50} > 3$ two lines can be distinguished, namely one line (for depth: $X > X_R$) where the flow around failure governs and one (for depth: $X < X_R$) where wedge failure occurs.
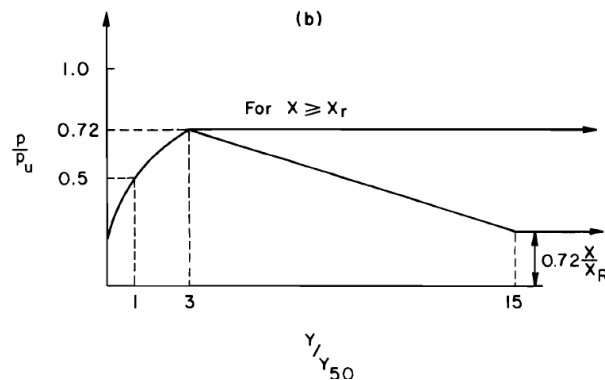
Figure 77 *Characteristic shapes of p-y curves for soft clay below water table: cyclic loading (Matlock)*

Correction for large diameter piles

It has to be noted that the determination of the p-y curves for soft sand are based on results of lateral load tests of piles with a diameter of 0.15m to 0.60m. In a study of Stevens and Audibert it was concluded that the adaptation theory on larger diameter piles (up to 1.50m) will overestimate the deflection and maximum moment of the piles. So a correction factor of the y_c value is suggested, according to the following relation:

$$y_c = 2.5 \, \varepsilon_c \, D^{0.5} \, [inches]$$

With 1 inch = 25.4mm this formula can be written as:

$$y_c = 45 \, \varepsilon_c \, D^{0.5} \, [mm]$$

As LPile uses the original theory of Matlock without compensation of large diameter piles a correction factor will be used defined as follows:

$$c = \frac{45 \, \varepsilon_c \, D^{0.5}}{2.5 \, \varepsilon_c \, D} = \frac{45}{2.5 \, D^{0.5}}$$

The correction factor will be applied on the y-values in the LPile program for the correction of the p-y curves for soft clay. The correction factor (c) for different pile diameters (D) is illustrated in Figure 78.
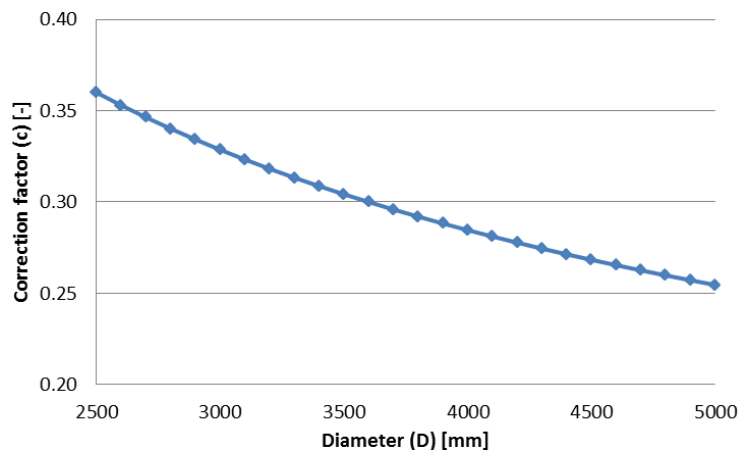
Figure 78 *Relation between pile diameter (d) and correction factor (c)*

19.3 P-y curves for stiff clay (Below Water Table)

The p-y curves for stiff clay are determined on the Reese, Cox and Koop theory (1975). Reese developed separate expressions for the ultimate soil resistance for two distinct mechanisms by which the pile was assumed to move through the soil. Based on the failure wedge of the soil in front of the pile and on the plastic flow of soil around the pile in an horizontal plane, the ultimate lateral soil resistance p,u per unit length of the pile is determined as the lesser of the following equations.

$$p_u = 2c_a + \gamma X + 2.83 \frac{c_a X}{D}$$

$$p_u = 11c \ for \ X \ \geq \ X_N$$

p_u: ultimate resistance [kPa]

c: undrained shear strength for undisturbed clay soil samples [kPa]

c_a: average undrained shear strength over depth X [kPa]

D: pile diameter [mm]

γ: effective unit weight of soil [MN/m³]

X: depth below soil surface [mm]

X_N: depth below soil surface to bottom reduced resistance zone [mm]. For a condition of constant strength with depth, the two above equations are solved simultaneously to give:

$$X_N = \frac{6 \, D}{\frac{\gamma \, D}{c} + J}$$

The p-y curve for stiff clay below the water table is illustrated in Figure 79.
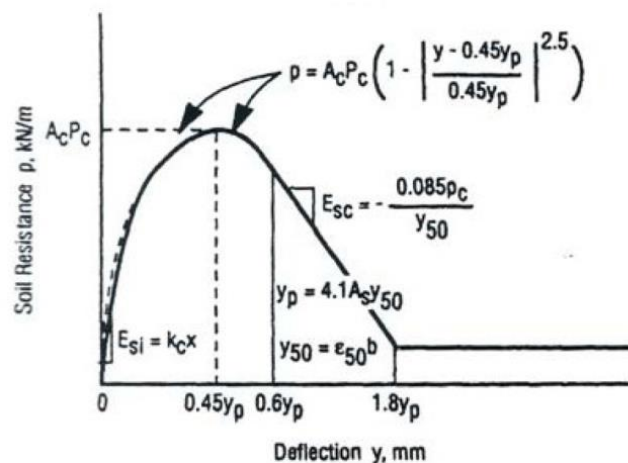
Figure 79 *Characteristic shapes of p-y curves for stiff clay below water table: cyclic loading (Reese et al)*

For stiff clay the appropriate value of Ac (cyclic loading) has to be chosen from Figure 80, with on the vertical axis the non –dimensional depth following from the depth X divided by the pile diameter.
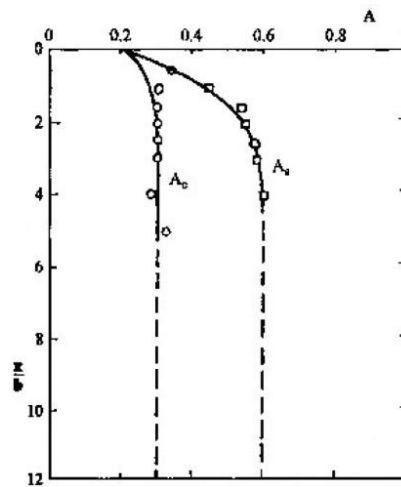
Figure 80 *Values of constants As (static loading) and Ac (cyclic loading)*

19.4 P-y curves for sand

For sand the p-y curves are evaluated by O'Neill and Murchison (1983) and is adopted ion the API standards.

The ultimate bearing capacity for sand depends on the depth below the surface and can be calculated using the smaller of the values calculated by the following equations:

$$p_{us} = (C_1 X + C_2 D) \gamma X$$

$$p_{ud} = C_3 D \gamma X$$

p_u: ultimate resistance [kPa] (s = shallow, d = deep)

γ: effective unit weight of soil [MN/m³]

X: depth below soil surface [mm]

ϕ': angle of internal friction of sand [deg]

C_1, C_2, C_3: Coefficients determined from Figure 81

D: pile diameter [mm]
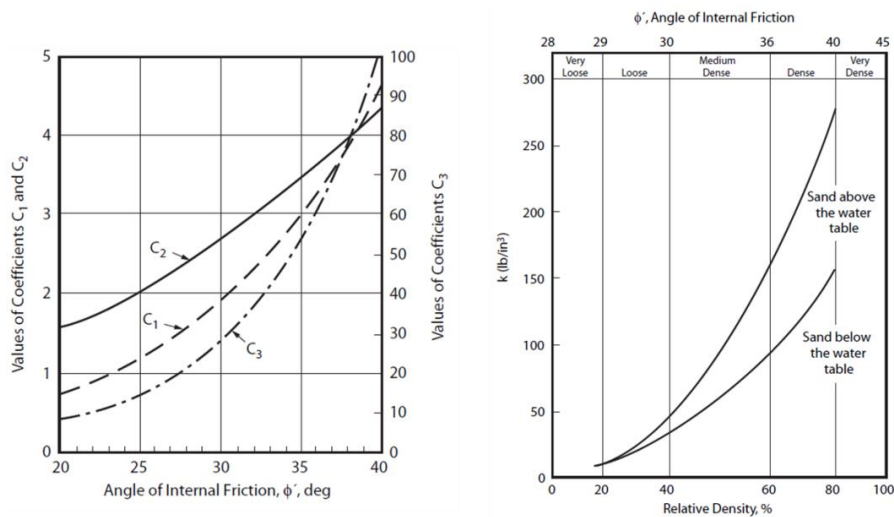
Figure 81 *Left: values C1, C2, C3; Right: Initial modulus of subgrade reaction*

The p-y relationship for sand is described by the following expression:

$$P = A\, p_u \tanh\left(\frac{k\,H}{A\, p_u}\, y\right)$$

p_u: ultimate bearing capacity at depth H [kN/m]

A: factor to account for cyclic or static conditions evaluated by:

- A = 0.9   for cyclic loading
- A = (3 − 0.8 H/D) ≥ 0.9   for static loading

k: initial modulus of subgrade reaction [kN/m³] determined from Figure 81 as a function of angle   of internal friction φ'

y: lateral deflection [m]

H: depth [m]

20 Appendix VII: Local buckling mono-piles, calculation methods

20.1 Introduction

Three different approaches were considered regarding local buckling of shell structures: the DNV standard, the European Standard and the API. The method presented by DNV, however, was too vague and therefore considered not applicable. In the following section both the European-method (20.2) as the API-method (20.3) is presented. It must be noted that the European- approach is at all times governing.

20.2 European Standard (EN 1993-1-6)

Buckling resistance (buckling strength)

The design buckling stresses are obtained from:

$$\sigma_{x,Rd} = \frac{\sigma_{x,Rk}}{\gamma_{M1}} = \frac{\chi_x \, f_{yk}}{\gamma_{M1}}$$

$\sigma_{x,Rd}$:   meridional design buckling stress

$\sigma_{x,Rk}$:   meridional characteristic buckling stress

χ_x: buckling reduction factor

γ_{M1}:   partial factor is 1.15 based on the DNV-OS-C101

The buckling reduction factor χ_x should be determined as a function of the relative slenderness of the shell $\bar{\lambda}$ from:

$$\chi = 1 \; when \; \bar{\lambda} \leq \overline{\lambda_0}$$

$$\chi = 1 - \beta \left(\frac{\bar{\lambda} - \overline{\lambda_0}}{\overline{\lambda_p} - \overline{\lambda_0}} \right)^\eta \; when \; \lambda_0 < \bar{\lambda} \leq \overline{\lambda_p}$$

$$\chi = \frac{\alpha_x}{\bar{\lambda}^2} \; when \; \overline{\lambda_p} \leq \bar{\lambda}$$

Where:

α: elastic imperfection reduction factor

β: plastic range factor

η: interaction exponent.

$\overline{\lambda_0}$:   squash limit relative slenderness

The values from the plastic limit relative slenderness should be determined from:

$$\overline{\lambda_p} = \sqrt{\frac{\alpha}{1 - \beta}}$$

The relative shell slenderness parameters for different stress components should be determined from:

$$\overline{\lambda_x} = \sqrt{\frac{f_{yk}}{\sigma_{x,Rcr}}}$$

Critical meridional buckling stresses

The length of the shell segment is characterized in terms of the dimensionless length parameter ω:

$$\omega = \frac{l}{r}\sqrt{\frac{r}{t}}$$

The elastic meridional buckling stress, using a value of C_x depending on the length of the cylinder, should be obtained from:

$$\sigma_{x,Rcr} = 0.605\, E\, C_x \frac{t}{r}$$

For this case C_x= 1.00

Meridional buckling parameters

The meridional imperfection reduction factor α_x should be obtained through:

$$\alpha_x = \frac{0.62}{1 + 1.91(\Delta w_k l\, t)^{1.44}}$$

Where Δw_k is the characteristic imperfection amplitude:

$$\Delta w_k = \frac{1}{Q}\sqrt{\frac{r}{t}}t$$

Where Q is the meridional compression fabrication quality parameter.

The fabrication quality parameter Q should be taken from Table 54 for the specified fabrication tolerance quality class. For this case Q is taken as 25.

Fabrication tolerance quality class	Description	Q
Class A	Excellent	40
Class B	High	25
Class C	Normal	16

Table 54 *Fabrication quality parameter Q*

The meridional squash limit $\overline{\lambda_{x0}}$ the plastic range factor β and the interaction exponent η should be taken as:

$$\overline{\lambda_{x0}} = 0.20\,;\ \beta = 0.60\,;\ \eta = 1.0$$

For long cylinders (which are defined by: $\omega > 0.5\frac{r}{t}$; $with\ \omega = \frac{l}{r}\sqrt{\frac{r}{t}}$) the meridional squash limit slenderness $\overline{\lambda_{x0}}$ may be obtained from:

$$\overline{\lambda_{x0}} = 0.20 + 0.10 \left(\frac{\sigma_{xE,M}}{\sigma_{xE}} \right)$$

σ_{xE}:   design value of meridional stress σ_{xEd}

$\sigma_{xE,M}$:   component of σ_{xEd} that derives from tubular global bending (peak value of the circumferentially varying component)

Cylinders need not to be checked against meridional shell buckling if they satisfy:

$$\frac{r}{t} \le 0.03 \frac{E}{f_{yk}}$$

20.2.1 API

In the API standards a nominal inelastic buckling strength F_{xc} is determined which the design stress shall not exceed:

$$F_{xc} = f_y \ for \ D/t \le 60$$

$$F_{xc} = f_y * \left(1.64 - 0.23 \left(\frac{D}{t} \right)^{0.25} \right) for \ D/t > 60$$

21 Appendix VIII: Structural analysis mono-piles, calculation example

In this appendix an example of a structural pile calculation is shown. In this example the calculations are made with a stiff soil profile and a design load of 8000kN.

The calculations are only shown for the first 16 meters of the pile, extending from CD+6.0m until approximately CD-10.0m. The load acts at a level of CD+2.5m. Additional parameters are listed below.

Input parameters		
Material properties		
Density Steel	78.5	kN/m^3
E_S	210000	MPa
X60 (f,yield)	448	Mpa
Factors		
gm,yield	1.15	-
gm,e.g	1.3	-
Loads		
Design Load	8000	kN
Weight Pile head	1500	kN
Output parameters		
Length	47.5	m
D	3.8	m
t	0.055	m
R,outer	1.900	m
R,inner	1.873	m

	INPUT										STEEL STRESSES							VON MISES			YIELD STRENGTH		BUCKLING STRENGTH			
Level [m]	Md [kNm]	Vd [kN]	Uhor [m]	OD [mm]	t [m]	A [m^2]	W [m^3]	Section Weight [kN]	Nd [kN]	Td [kNm]	σ,M(Md) [MPa]	σ,M(Uhor) [MPa]	σ,N [MPa]	τ,V [MPa]	τ,T [MPa]	σ,max [MPa]	τ,max [MPa]	σ,vm1 [MPa]	σ,vm2 [MPa]	σ,vmd [MPa]	f,yd [MPa]	U.C. [-]	EN1993-1- [MPa]	API [MPa]	U.C. [-]	
6.0	0	0	0.801	3.8	0.055	0.647	0.597	1500.0	1500.0	7600.0	0.00	0.00	2.32	0.00	12.45	2.3	12.5	21.7	21.7	21.7	389.6	0.06	351.67	380.56	0.06	ok
5.5	0	0	0.789	3.8	0.055	0.647	0.597	31.4	1531.4	7600.0	0.00	0.03	2.37	0.00	12.45	2.4	12.5	21.7	21.7	21.7	389.6	0.06	351.67	380.56	0.06	ok
5.1	0	0	0.776	3.8	0.055	0.647	0.597	31.4	1562.7	7600.0	0.00	0.06	2.42	0.00	12.45	2.5	12.5	21.7	21.7	21.7	389.6	0.06	351.67	380.56	0.06	ok
4.6	0	0	0.764	3.8	0.055	0.647	0.597	31.4	1594.1	7600.0	0.00	0.10	2.46	0.00	12.45	2.6	12.5	21.7	21.7	21.7	389.6	0.06	351.67	380.56	0.06	ok
4.1	0	0	0.751	3.8	0.055	0.647	0.597	31.4	1625.5	7600.0	0.00	0.13	2.51	0.00	12.45	2.6	12.5	21.7	21.7	21.7	389.6	0.06	351.67	380.56	0.06	ok
3.6	0	0	0.739	3.8	0.055	0.647	0.597	31.4	1656.8	7600.0	0.00	0.16	2.56	0.00	12.45	2.7	12.5	21.7	21.7	21.7	389.6	0.06	351.67	380.56	0.06	ok
3.2	0	0	0.726	3.8	0.055	0.647	0.597	31.4	1688.2	7600.0	0.00	0.20	2.61	0.00	12.45	2.8	12.5	21.7	21.7	21.7	389.6	0.06	351.67	380.56	0.06	ok
2.7	0	1250	0.714	3.8	0.055	0.647	0.597	31.4	1719.6	7600.0	0.00	0.24	2.66	7.67	12.45	2.9	20.1	21.8	35.0	35.0	389.6	0.09	351.67	380.56	0.10	ok
2.2	1188	4400	0.702	3.8	0.055	0.647	0.597	31.4	1750.9	7600.0	1.99	0.27	2.71	27.00	12.45	5.0	39.5	22.1	68.4	68.4	389.6	0.18	351.67	380.56	0.19	ok
1.7	4180	7150	0.689	3.8	0.055	0.647	0.597	31.4	1782.3	7600.0	7.00	0.31	2.75	43.87	12.45	10.1	56.3	23.8	97.6	97.6	389.6	0.25	351.67	380.56	0.28	ok
1.3	7980	8000	0.677	3.8	0.055	0.647	0.597	31.4	1813.7	7600.0	13.36	0.35	2.80	49.09	12.45	16.5	61.5	27.2	106.6	106.6	389.6	0.27	351.67	380.56	0.30	ok
0.8	11780	8000	0.664	3.8	0.055	0.647	0.597	31.4	1845.0	7600.0	19.73	0.38	2.85	49.09	12.45	23.0	61.5	31.5	106.6	106.6	389.6	0.27	351.67	380.56	0.30	ok
0.3	15580	8000	0.652	3.8	0.055	0.647	0.597	31.4	1876.4	7600.0	26.09	0.42	2.90	49.09	12.45	29.4	61.5	36.5	106.6	106.6	389.6	0.27	351.67	380.56	0.30	ok
-0.2	19380	8000	0.639	3.8	0.055	0.647	0.597	31.4	1907.8	7600.0	32.45	0.46	2.95	49.09	12.45	35.9	61.5	41.8	106.6	106.6	389.6	0.27	351.67	380.56	0.30	ok
-0.7	23180	8000	0.627	3.8	0.055	0.647	0.597	31.4	1939.1	7600.0	38.81	0.50	3.00	49.09	12.45	42.3	61.5	47.5	106.6	106.6	389.6	0.27	351.67	380.56	0.30	ok
-1.1	26980	8000	0.614	3.8	0.055	0.647	0.597	31.4	1970.5	7600.0	45.18	0.54	3.05	49.09	12.45	48.8	61.5	53.3	106.6	106.6	389.6	0.27	351.67	380.56	0.30	ok
-1.6	30780	8000	0.602	3.8	0.055	0.647	0.597	31.4	2001.9	7600.0	51.54	0.58	3.09	49.09	12.45	55.2	61.5	59.3	106.6	106.6	389.6	0.27	351.67	380.56	0.30	ok
-2.1	34580	8000	0.590	3.8	0.055	0.647	0.597	31.4	2033.2	7600.0	57.90	0.63	3.14	49.09	12.45	61.7	61.5	65.3	106.6	106.6	389.6	0.27	351.67	380.56	0.30	ok
-2.6	38380	8000	0.577	3.8	0.055	0.647	0.597	31.4	2064.6	7600.0	64.27	0.67	3.19	49.09	12.45	68.1	61.5	71.5	106.6	106.6	389.6	0.27	351.67	380.56	0.30	ok
-3.0	42180	8000	0.565	3.8	0.055	0.647	0.597	31.4	2096.0	7600.0	70.63	0.71	3.24	49.09	12.45	74.6	61.5	77.6	106.6	106.6	389.6	0.27	351.67	380.56	0.30	ok
-3.5	45980	8000	0.553	3.8	0.055	0.647	0.597	31.4	2127.3	7600.0	76.99	0.75	3.29	49.09	12.45	81.0	61.5	83.9	106.6	106.6	389.6	0.27	351.67	380.56	0.30	ok
-4.0	49780	8000	0.541	3.8	0.055	0.647	0.597	31.4	2158.7	7600.0	83.36	0.80	3.34	49.09	12.45	87.5	61.5	90.1	106.6	106.6	389.6	0.27	351.67	380.56	0.30	ok
-4.5	53580	8000	0.529	3.8	0.055	0.647	0.597	31.4	2190.1	7600.0	89.72	0.84	3.38	49.09	12.45	93.9	61.5	96.4	106.6	106.6	389.6	0.27	351.67	380.56	0.30	ok
-4.9	57380	8000	0.517	3.8	0.055	0.647	0.597	31.4	2221.5	7600.0	96.08	0.89	3.43	49.09	12.45	100.4	61.5	102.7	106.6	106.6	389.6	0.27	351.67	380.56	0.30	ok
-5.4	61180	8000	0.505	3.8	0.055	0.647	0.597	31.4	2252.8	7600.0	102.45	0.93	3.48	49.09	12.45	106.9	61.5	109.0	106.7	109.0	389.6	0.28	351.67	380.56	0.31	ok
-5.9	64980	8000	0.493	3.8	0.055	0.647	0.597	31.4	2284.2	7600.0	108.81	0.98	3.53	49.09	12.45	113.3	61.5	115.4	106.7	115.4	389.6	0.30	351.67	380.56	0.33	ok
-6.4	68780	8000	0.481	3.8	0.055	0.647	0.597	31.4	2315.5	7600.0	115.17	1.02	3.58	49.09	12.45	119.8	61.5	121.7	106.7	121.7	389.6	0.31	351.67	380.56	0.35	ok
-6.8	72580	8000	0.469	3.8	0.055	0.647	0.597	31.4	2346.9	7600.0	121.53	1.07	3.63	49.09	12.45	126.2	61.5	128.1	106.7	128.1	389.6	0.33	351.67	380.56	0.36	ok
-7.3	76380	8000	0.457	3.8	0.055	0.647	0.597	31.4	2378.3	7600.0	127.90	1.12	3.68	49.09	12.45	132.7	61.5	134.4	106.7	134.4	389.6	0.35	351.67	380.56	0.38	ok
-7.8	80180	8000	0.445	3.8	0.055	0.647	0.597	31.4	2409.6	7600.0	134.26	1.17	3.72	49.09	12.45	139.1	61.5	140.8	106.7	140.8	389.6	0.36	351.67	380.56	0.40	ok
-8.3	83980	8000	0.434	3.8	0.055	0.647	0.597	31.4	2441.0	7600.0	140.62	1.21	3.77	49.09	12.45	145.6	61.5	147.2	106.7	147.2	389.6	0.38	351.67	380.56	0.42	ok
-8.7	87780	8000	0.422	3.8	0.055	0.647	0.597	31.4	2472.4	7600.0	146.99	1.26	3.82	49.09	12.45	152.1	61.5	153.6	106.7	153.6	389.6	0.39	351.67	380.56	0.44	ok
-9.2	91580	8000	0.411	3.8	0.055	0.647	0.597	31.4	2503.7	7600.0	153.35	1.31	3.87	49.09	12.45	158.5	61.5	160.0	106.7	160.0	389.6	0.41	351.67	380.56	0.45	ok
-9.7	95380	8000	0.399	3.8	0.055	0.647	0.597	31.4	2535.1	7600.0	159.71	1.36	3.92	49.09	12.45	165.0	61.5	166.4	106.7	166.4	389.6	0.43	351.67	380.56	0.47	ok
-10.2	99180	8000	0.388	3.8	0.055	0.647	0.597	31.4	2566.5	7600.0	166.08	1.41	3.97	49.09	12.45	171.4	61.5	172.8	106.7	172.8	389.6	0.44	351.67	380.56	0.49	ok
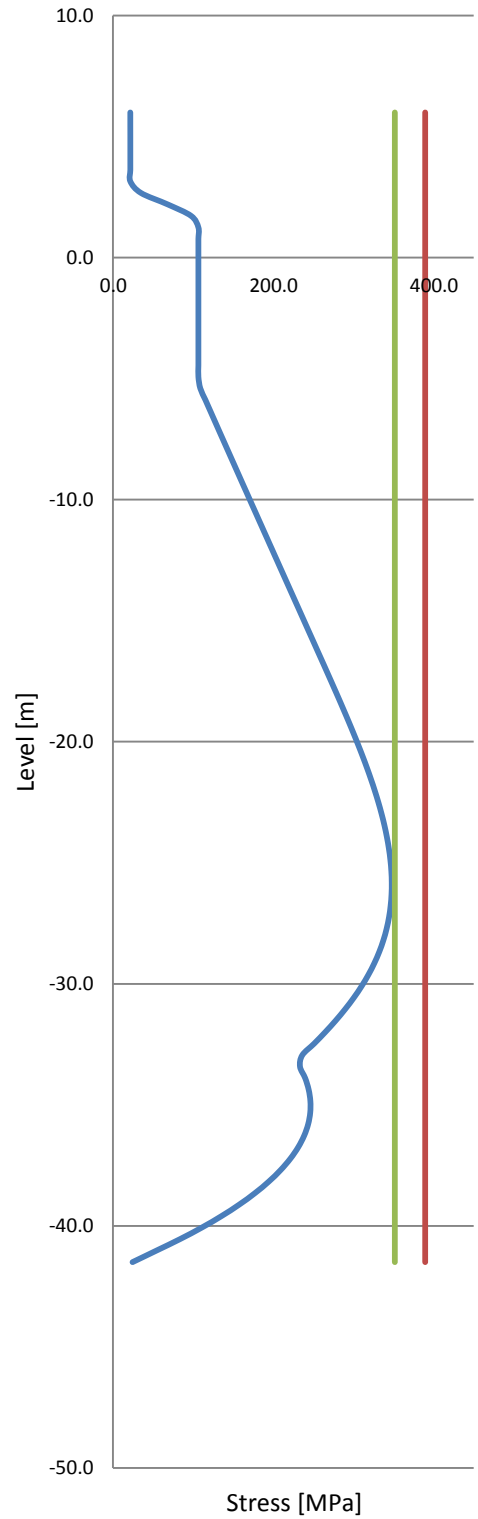
Chart — y-axis: Level [m] (10.0, 0.0, -10.0, -20.0, -30.0, -40.0, -50.0); x-axis: Stress [MPa] (0.0, 200.0, 400.0). Legend: sigma,vmd; f,yd; f,bucd

22 Appendix IX: Pile designs for larger water depths

22.1 Introduction

One of the main assumptions made in the design of the mono-piles was a constant water depth of 16m. It was rationalized that, for the considered mooring system, the FSRU import terminal would always be located as close as possible to the shoreline reducing pipe-laying costs. The water depth would therefore always be a few meters larger than the maximum draught of the FSRU. In case a larger water depth is to be expected, the standardized pile designs presented in Section (5.4.1) should be rescaled to an appropriate design for that specific situation. In this Appendix this rescaling has been investigated by making pile designs for a water depth of 26 meters, 10 meter larger than was assumed in the design considerations of Part 2. These are subsequently compared to the designs made for a 16m water depth.

A distinction was made between two "extreme" soil profiles: a soft clay profile and a stiff sand profile. In Section (22.2) the pile designs are presented for the soft clay profile, in Section (22.3) for the stiff sand profile. Drawn conclusions regarding this matter are mentioned in Section (22.4).

For each combination of fender load and soil profile a pile design is made characterized by its dimensions: diameter (D), wall thickness (t) and length (L). For each combination two pile designs are possible; one with an optimized diameter, the other with an optimized wall thickness. For a few combinations, however, the designs were outside the chosen D/t range (65 < D/t < 85) and considered unsuitable.

22.2 Soft clay profile

The light blue dots represent the 16 meter water depth case, the dark blue dots the 26 meter water depth case. The lines represent an approximated upper- and lower bound.

F,d [kN]	CLAY 16 m water depth					CLAY 26 m water depth				
	L [m]	D [m]	t [m]	D/t [-]	Check [-]	L [m]	D [m]	t [m]	D/t [-]	Check [-]
2000	52.5	2.6	0.030	86.67	no	65	2.9	0.035	82.86	yes
	55	2.5	0.035	71.43	yes	67.5	2.7	0.040	67.50	yes
3000	57.5	3.1	0.035	88.57	no	70	3.3	0.040	82.50	yes
	57.5	2.9	0.040	72.50	yes	70	3.1	0.045	68.89	yes
4000	60	3.3	0.040	82.50	yes	72.5	3.7	0.045	82.22	yes
	62.5	3.1	0.045	68.89	yes	72.5	3.5	0.050	70.00	yes
5000	62.5	3.6	0.045	80.00	yes	75	3.9	0.050	78.00	yes
	65	3.4	0.050	68.00	yes	77.5	3.7	0.055	67.27	yes
6000	67.5	3.7	0.050	74.00	yes	77.5	4.3	0.050	86.00	no
	67.5	3.6	0.055	65.45	yes	77.5	4.1	0.055	74.55	yes
7000	70	3.9	0.055	70.91	yes	80	4.5	0.055	81.82	yes
	72.5	3.8	0.060	63.33	no	82.5	4.3	0.060	71.67	yes
8000	75	4.2	0.055	76.36	yes	82.5	4.6	0.060	76.67	yes
	77.5	4	0.060	66.67	yes	85	4.4	0.065	67.69	no
9000	77.5	4.4	0.055	80.00	yes	85	4.9	0.060	81.67	yes
	80	4.3	0.060	71.67	yes	87.5	4.7	0.065	72.31	yes

Table 55 *Soft clay profile - Pile designs for varying design loads and water depths*
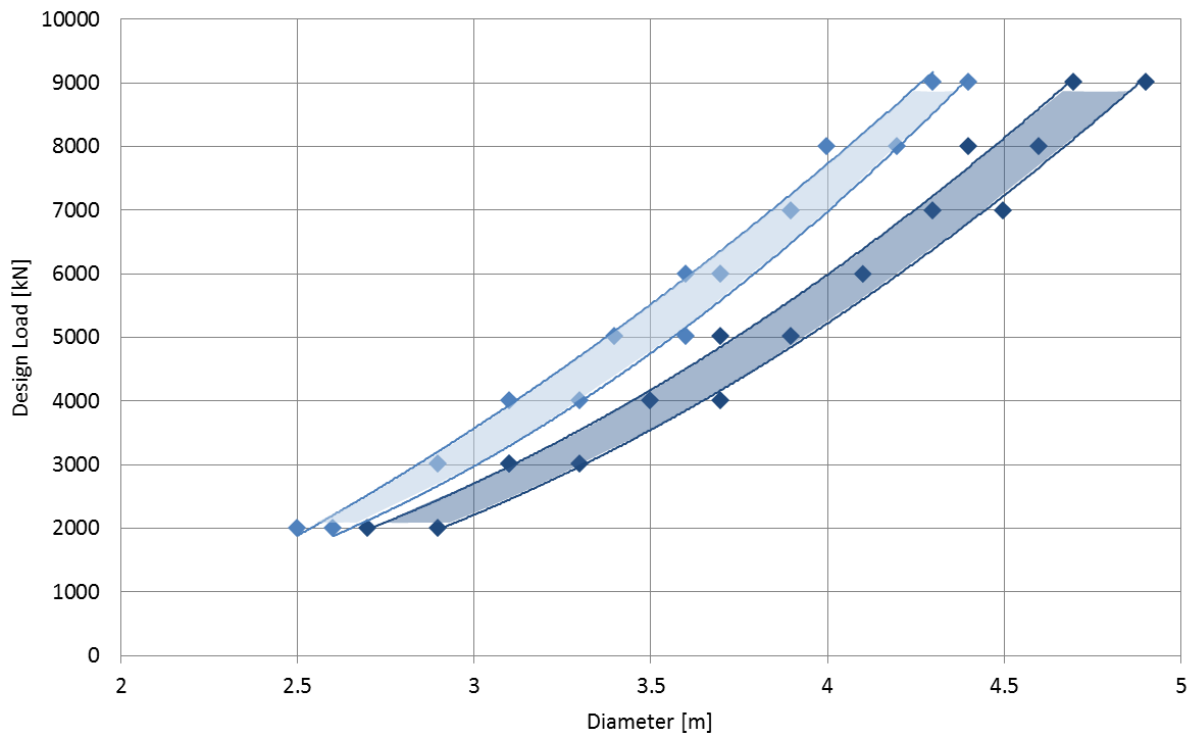
Figure 82 *Soft clay profile - Design load / Pile diameter; light blue: 16m water depth, dark blue: 26m water depth*
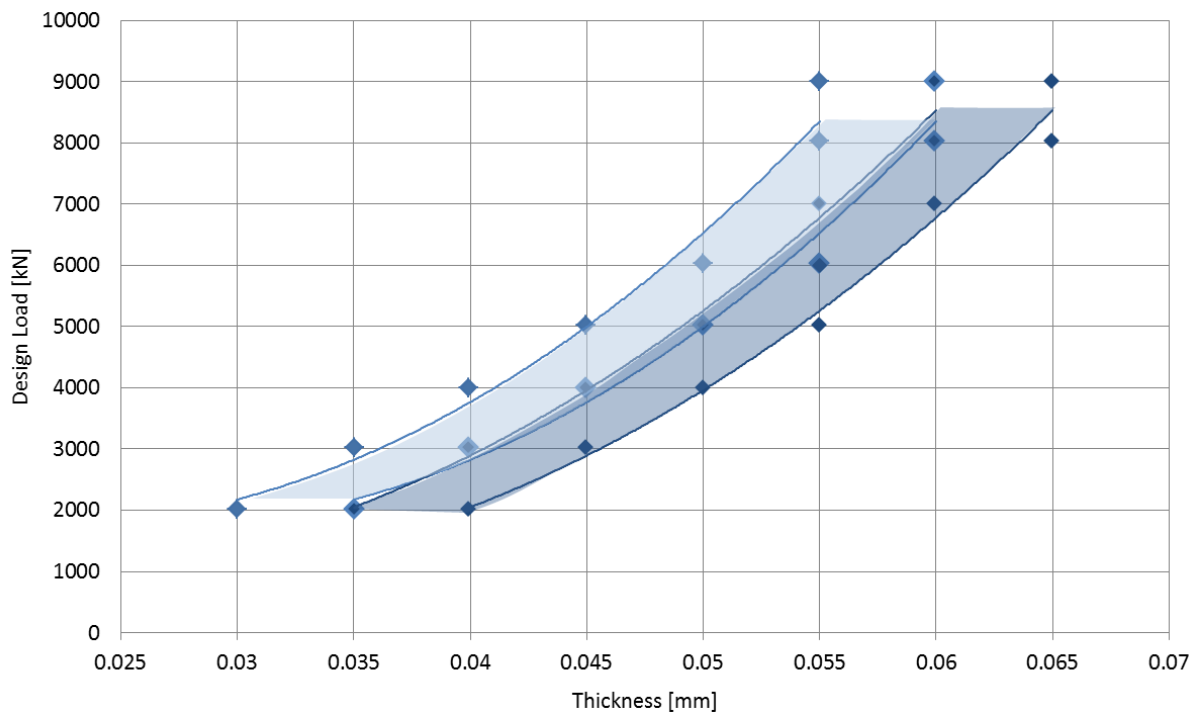
Figure 83 *Soft clay profile - Design load / Wall thickness; light blue: 16m water depth, dark blue: 26m water depth*
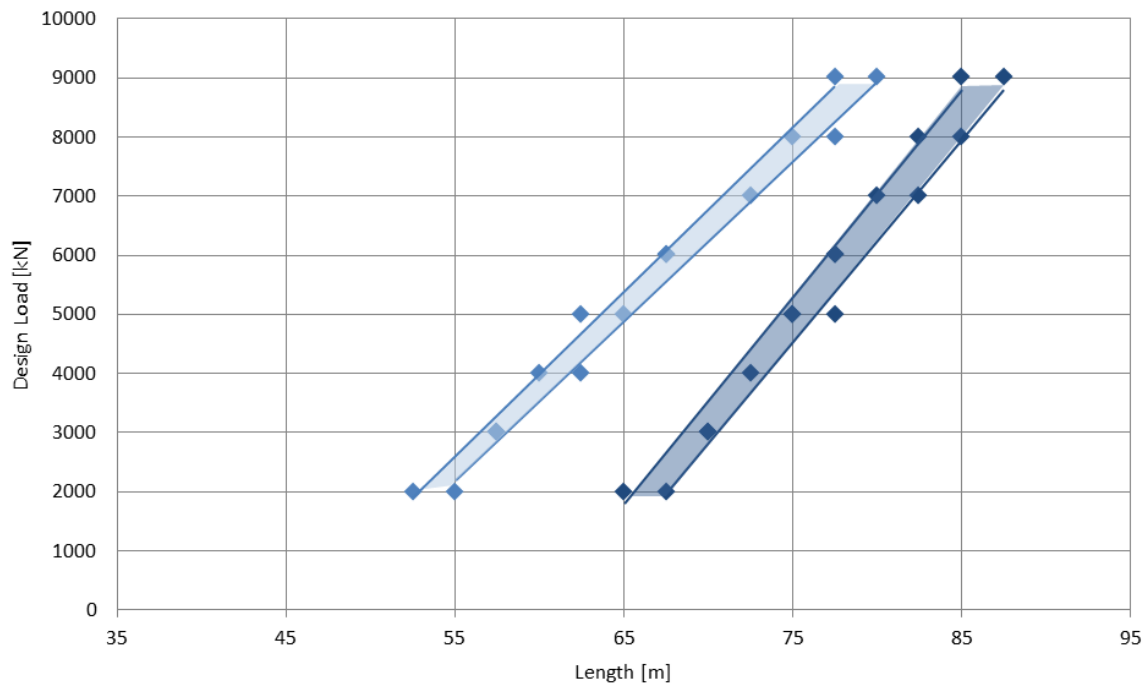
Figure 84 *Soft clay profile - Design load / Pile length; light blue: 16m water depth, dark blue: 26m water depth*

22.3 Stiff sand profile

In the following graphs, the light-green dots represent the 16m water depth case, the dark-green the 26m water depth case.

F,d [kN]	SAND 16 m water depth					SAND 26 m water depth				
	L	D	t	D/t	Check	L	D	t	D/t	Check
	[m]	[m]	[m]	[-]	[-]	[m]	[m]	[m]	[-]	[-]
2000	40	2.5	0.030	83.33	yes	50	2.8	0.035	80.00	yes
	40	2.3	0.035	65.71	yes	52.5	2.6	0.040	65.00	yes
3000	40	2.9	0.035	82.86	yes	52.5	3.2	0.040	80.00	yes
	40	2.7	0.040	67.50	yes	52.5	3	0.045	66.67	yes
4000	42.5	3.1	0.040	77.50	yes	52.5	3.5	0.045	77.78	yes
	42.5	2.9	0.045	64.44	no	55	3.3	0.050	66.00	yes
5000	42.5	3.3	0.045	73.33	yes	55	3.7	0.050	74.00	yes
	42.5	3.1	0.050	62.00	no	55	3.5	0.055	63.64	no
6000	45	3.6	0.045	80.00	yes	57.5	4.1	0.050	82.00	yes
	45	3.4	0.050	68.00	yes	57.5	3.9	0.055	70.91	yes
7000	45	3.8	0.050	76.00	yes	57.5	4.2	0.055	76.36	yes
	45	3.6	0.055	65.45	yes	57.5	4	0.060	66.67	yes
8000	45	4.1	0.050	82.00	yes	57.5	4.3	0.060	71.67	yes
	47.5	3.8	0.055	69.09	yes	57.5	4.1	0.065	63.08	no
9000	47.5	4.1	0.055	74.55	yes	60	4.6	0.060	76.67	yes
	47.5	3.9	0.060	65.00	yes	60	4.4	0.065	67.69	yes

Table 56 *Stiff sand profile - Pile designs for varying design loads and water depths*
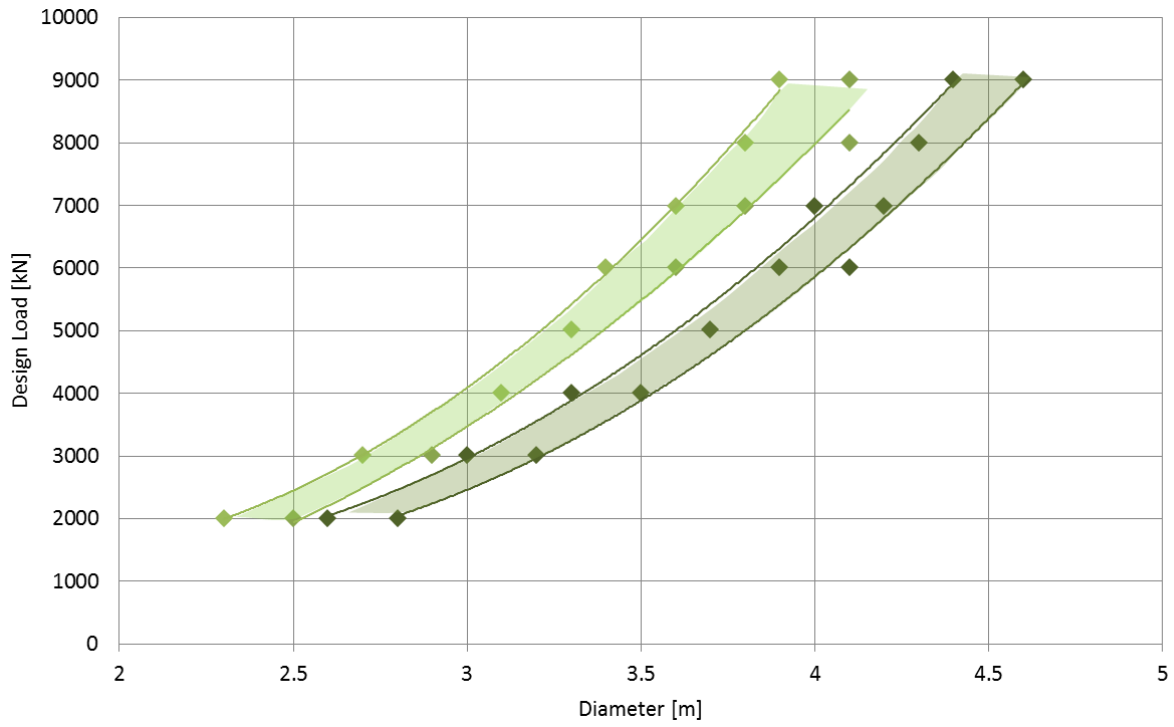
Figure 85 *Stiff sand profile - Design load / Pile diameter; light green: 16m water depth, dark green: 26m water depth*
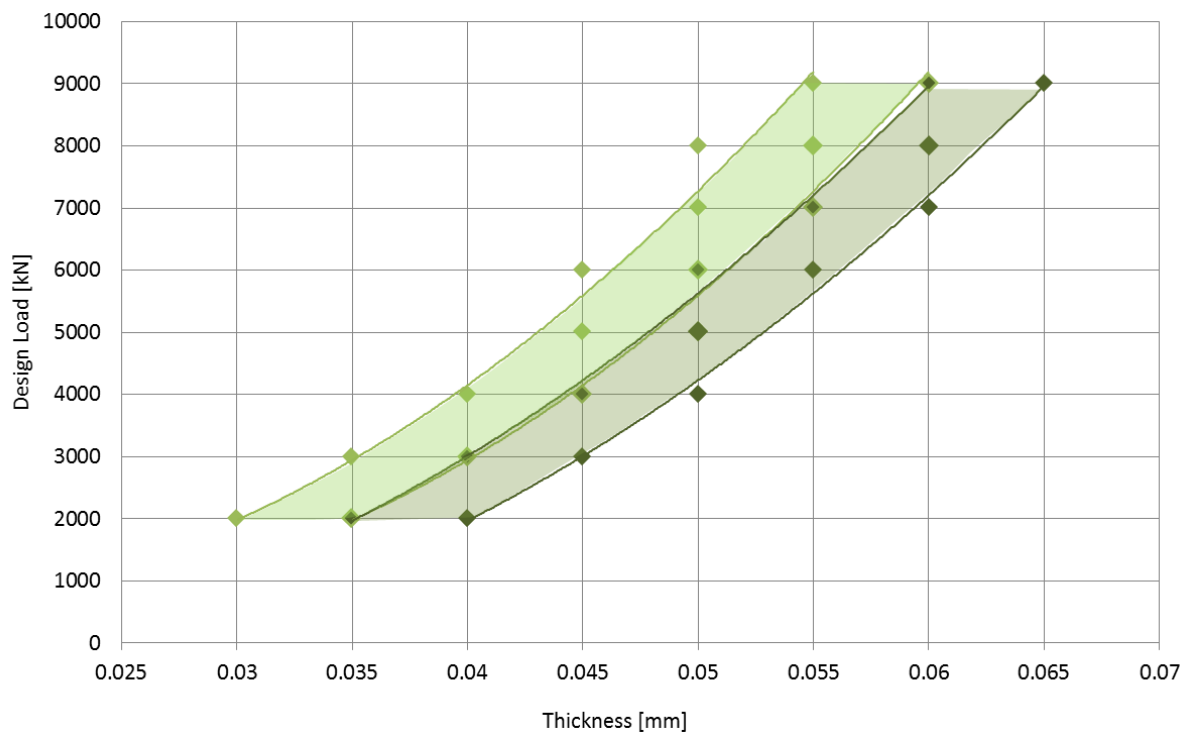
Figure 86 *Stiff sand profile - Design load / Wall thickness; light green: 16m water depth, dark green: 26m water depth*
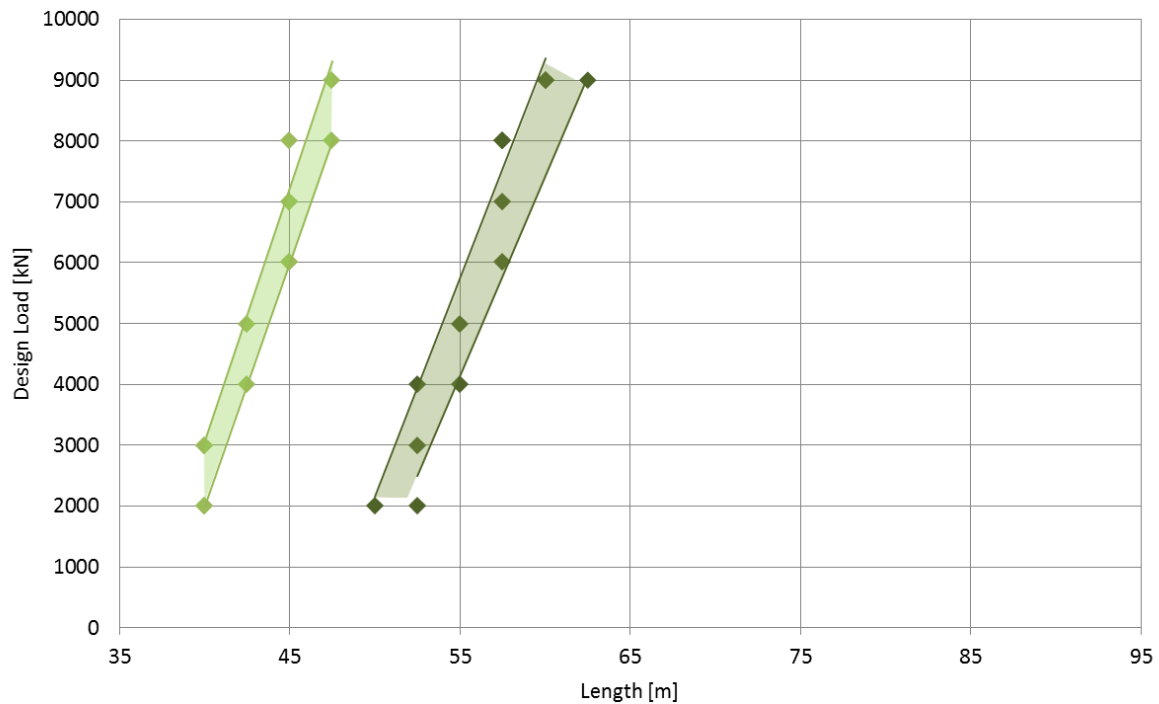
Figure 87 *Stiff sand profile - Design load / Pile length; light green: 16m water depth, dark green: 26m water depth*

22.4 Conclusions

In the graphs showed above can be observed how the pile diameters, wall thicknesses and pile lengths increase for increasing water depth (from 16m to 26m).

Pile diameter

For both soil profiles the same phenomena has been observed. The difference in diameter, between the two water depth cases, increases for increasing load. The difference in pile diameter increases:

- from 0.3m to 0.4m for the soft clay case
- from 0.4m to 0.5m for the stiff sand case

Wall thickness

For a 10m increase of the water depth, the wall thicknesses of the piles increase with 5mm for both soil profiles.

Pile length

For the stiff sand profile; the length of the piles increases with 12.5m. For the soft clay profile, the difference in pile length is 12.5m for small loads and decreases linearly to 10m for larger loads.

The standardized pile designs presented in Section (5.4.1) can quite easily be rescaled in the following manner:

Soil profile	Dimensions	Environmental condition		
		Mild	Moderate	Harsh
Stiff sand profile	t [mm]	45 +5	50 + 5	55 + 5
	D [mm]	3300 + 400	3800 + 400	4100 + 500
	L [m]	42.5 + 12.5	45 + 12.5	47.5 + 12.5
Soft clay profile	t [mm]	50 + 5	55 + 5	60 + 5
	D [mm]	3400 + 300	3900 + 400	4300 + 400
	L [m]	65 + 12.5	70 + 12.5	80 + 10

Table 57 *Rescaling of the standardized pile designs for a 10m increased water depth*

The change in pile dimension is nearly similar for all six cases listed above. Since the standardized pile designs are meant for a conceptual design stage, it is concluded acceptable to define generalized rescaling parameters.

Dimensions	Rescaling parameters
Thickness (t)	+ 5 mm
Diameter (D)	+ 400 mm
Length (L)	+ 12.5 m

Table 58 *Generalized rescaling parameters for a 10m increased water depth*

23 Appendix X: Structural analysis pile-head, summary results

23.1 Introduction

In this appendix the FEA-results from SCIA Engineer are presented for both ULS loading cases: ULS1 and ULS2. For each element the critical loads are listed and their corresponding unity checks are performed. A distinction is made between elements built up of sandwich laminates (23.2), and the ones built up from monolithic laminates (23.3) as other design checks are required.

23.2 Sandwich laminates

The elements constructed of sandwich laminates are; the horizontal plates of the support structure and the front- and rear fender panel. Those elements are checked on the strain- and shear criterion.

As can be seen some of the shear strength (V) unity checks are below 1 (marked in red). Those are shear forces resulting from an incorrect modelling of the connection between the rear fender panel and the front plates of the support structure. Furthermore those shear forces act on very small surfaces and are therefore considered negligible for the design.

Parameters	HORIZONTAL PLATES				REAR PANEL				FRONT PANEL			
	ULS 1		ULS 2		ULS 1		ULS 2		ULS 1		ULS 2	
	Value	U.C.	Value	U.C.	Value	U.C.	Value	U.C.	Value	U.C.	Value	U.C.
N_X [kN/m]	- 2634.20	-	- 2717.15	-	789.45	-	508.97	-	- 259.77	-	- 150.81	-
N_Y [kN/m]	- 650.00	-	425.36	-	762.83	-	785.84	-	364.32	-	177.85	-
N_{XY} [kN/m]	- 1149.62	-	-398.47	-	565.19	-	305.57	-	- 418.84	-	229.65	-
M_X [kNm/m]	238.41	-	223.84	-	-60.38	-	-60.86	-	37.42	-	41.43	-
M_Y [kNm/m]	102.08	-	103.66	-	-152.47	-	-148.39	-	23.30	-	22.95	-
M_{XY} [kNm/m]	- 49.86	-	52.70	-	49.23	-	21.74	-	- 11.41	-	- 10.72	-
ε_x [-]	- 0.88	0.73	- 0.99	0.83	0.33	0.28	0.18	0.15	-0.36	0.30	0.06	0.05
ε_y [-]	0.08	0.06	0.41	0.34	0.93	0.78	0.98	0.82	0.30	0.25	0.08	0.07
γ_{xy} [-]	- 0.99	0.83	- 0.20	0.17	1.11	0.92	0.53	0.44	- 0.48	0.40	0.32	0.27
V [kN/m]	732.00	1.13	750.01	1.16	589.28	1.10	495.49	0.92	265.89	0.49	274.41	0.51

Table 59 *Summary results; structural analysis of the sandwich laminates*

23.3 Monolithic laminates

The elements constructed of monolithic laminates are; the side- and front plates of the support structures and the inner walls, bottom/top plates of the fender panel. Those elements are checked on the stress criterion and are all below a unity check of 1.

Parameters	SIDE PLATES				FRONT PLATES				INNER WALLS				BOTTOM- & TOP PLATES			
	ULS 1		ULS 2		ULS 1		ULS 2		ULS 1		ULS 2		ULS 1		ULS 2	
	Value	U.C.	Value	U.C.	Value	U.C.	Value	U.C.	Value	U.C.	Value	U.C.	Value	U.C.	Value	U.C.
sigE- [MPa]	24.30	0.28	60.10	0.68	37.10	0.42	34.70	0.39	76.90	0.87	73.50	0.84	40.30	0.46	13.10	0.15
sigE+ [MPa]	28.90	0.33	71.40	0.81	36.70	0.42	31.70	0.36	69.20	0.79	76.80	0.87	31.70	0.36	18.00	0.20

Table 60 *Summary results; structural analysis of the monolithic laminates*

24 Appendix XI: Fatigue calculations, case study

24.1 Introduction

The fatigue assessments for both the pile-head as the mono-piles have been performed based on a case study, the Golar project. In this assessment 6 different wave heights, coming from all directions (16 in total), are considered. The load signals were obtained by means of DMA software. These were subsequently processed in order to obtain the alternating fatigue loads (ΔF) and the corresponding number of cycles (n). The alternating loads for every combination of wave height and incoming direction are depicted in section (24.2). These values are also the basis of the fatigue calculations.

The alternating loads are described by "Delta F". These are translated to alternating stresses by means a linear load-stress relation, described by so-called load transfer functions (LTF's). E.g., a Delta F of 10 represents the load variations 0-10kN / 10-20kN/ 20-30kN / 30-40kN. The corresponding stress variations are described as s1 / s2 / s3 /s4. For the fatigue calculations of the mono-piles, these are then multiplied with a Stress Concentration Factor (SCF) to obtain the hot-spot stresses ("s,hot").

The actual number of cycles for each alternating stress range is represented by "n", while the allowable number of cycles is abbreviated with "N". The final cumulative damage number is the summation of all the damage factors (Dd) which can be found in the last column of the table.

In section (24.3) the S-N curve for steel and composite are plotted in one figure in order to illustrate their difference.

In section (24.4) the fatigue calculations of a mono-pile are showed. The considered mono-pile is designed for stiff soil conditions and an ULS design load of 5000kN.

In section (24.5) the fatigue calculations of the critical pile-head element are illustrated, namely the front- and side plates.

24.2 S-N curves: steel vs. composite

The S-N curves are plotted for steel class C1 according to the DNV-standard and composite class glass/polyester according to the CUR-standard.
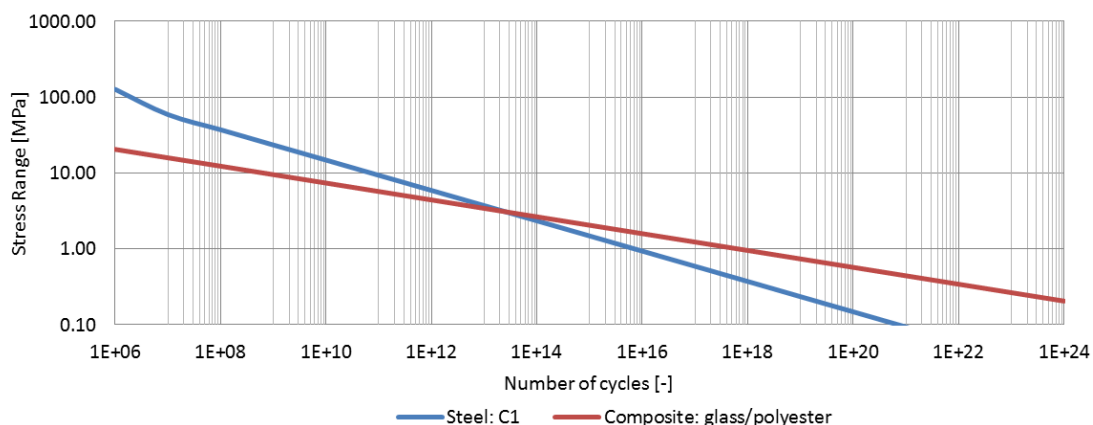
Figure 88 *S-N curve; steel vs. composite*

As can be seen, composite is much more fatigue resistant for smaller alternative stresses, up to 3MPa.

24.3 Alternating loads

Incoming directions	Hs = 0.5m		Hs = 0.7m		Hs = 0.9m		Hs = 1.1m		Hs = 1.3m	
	ΔF [kN]	Number of cycles	ΔF [kN]	Number of cycles	ΔF [kN]	Number of cycles	ΔF [kN]	Number of cycles	ΔF [kN]	Number of cycles
North 0°	0 - 5	1800	0 - 5	1800	0 - 5	1800	0 - 5	1789	0 - 5	1601
	5 - 10	0	5 - 10	0	5 - 10	0	5 - 10	11	5 - 10	198
	10 - 15	0	10 - 15	0	10 - 15	0	10 - 15	0	10 - 15	1
	15 - 20	0	15 - 20	0	15 - 20	0	15 - 20	0	15 - 20	0
NNE 22.5°	0 - 5	1641	0 - 5	1246	0 - 25	1458	0	0	0	0
	5 - 10	159	5 - 10	538	25 - 50	340	0	0	0	0
	10 - 15	0	10 - 15	16	50 -75	2	0	0	0	0
	15 - 20	0	15 - 20	0	75 - 100	0	0	0	0	0
NE 45°	0 - 10	1260	0 - 25	1304	0 - 50	1397	0 - 50	877	0	0
	10 - 20	529	25 - 50	482	50 - 100	395	50 - 100	835	0	0
	20 - 30	11	50 -75	14	100 - 150	8	100 - 150	82	0	0
	30 - 40	0	75 - 100	0	150 - 200	0	150 - 200	6	0	0
ENE 67.5°	0 - 10	913	0 - 25	834	0 -75	1103	0 - 100	521	0 - 150	509
	10 - 20	822	25 - 50	888	75 - 150	676	100 - 200	843	150 - 300	913
	20 - 30	65	50 -75	75	150 - 225	21	200 - 300	410	300 -450	356
	30 - 40	0	75 - 100	3	225 - 300	0	300 - 400	26	450 - 600	22
East 90°	0 -75	1140	0 -100	361	0 - 150	239	0 - 200	729	0 -350	1071
	75 - 150	625	100 - 200	868	150 - 300	1066	200 - 400	980	350 - 700	672
	150 - 225	35	200 - 300	501	300 -450	484	400 - 600	89	700 - 1050	55
	225 - 300	0	300 - 400	70	450 - 600	11	600 - 800	2	1050 -1400	2
ESE 112.5°	0 - 25	1306	0 - 25	391	0 - 50	616	0	0	0	0
	25 - 50	493	25 - 50	988	50 - 100	1005	0	0	0	0
	50 -75	1	50 -75	371	100 - 150	174	0	0	0	0
	75 - 100	0	75 - 100	50	150 - 200	5	0	0	0	0
SE 135°	0 - 10	1053	0 - 25	1145	0 - 50	1320	0	0	0	0
	10 - 20	706	25 - 50	638	50 - 100	474	0	0	0	0
	20 - 30	41	50 -75	17	100 - 150	6	0	0	0	0
	30 - 40	0	75 - 100	0	150 - 200	0	0	0	0	0
SSE 157.5°	0 - 5	1730	0 - 10	1668	0	0	0	0	0	0
	5 - 10	70	10 - 20	131	0	0	0	0	0	0
	10 - 15	0	20 - 30	1	0	0	0	0	0	0
	15 - 20	0	30 - 40	0	0	0	0	0	0	0
South 180°	0 - 5	1800	0	0	0	0	0	0	0	0
	5 - 10	0	0	0	0	0	0	0	0	0
	10 - 15	0	0	0	0	0	0	0	0	0
	15 - 20	0	0	0	0	0	0	0	0	0
SSW 202.5°	0 - 5	1800	0	0	0	0	0	0	0	0
	5 - 10	0	0	0	0	0	0	0	0	0
	10 - 15	0	0	0	0	0	0	0	0	0
	15 - 20	0	0	0	0	0	0	0	0	0
SW 225°	0 - 10	1333	0 - 25	1206	0	0	0	0	0	0
	10 - 20	458	25 - 50	580	0	0	0	0	0	0
	20 - 30	9	50 -75	14	0	0	0	0	0	0
	30 - 40	0	75 - 100	0	0	0	0	0	0	0
WSW 247.5°	0 - 15	776	0 - 25	389	0 -75	1259	0 -75	533	0	0
	15 - 30	916	25 - 50	1018	75 - 150	536	75 - 150	968	0	0
	30 - 45	108	50 -75	357	150 - 225	5	150 - 225	274	0	0
	45 - 60	0	75 - 100	36	225 - 300	0	225 - 300	25	0	0
West 270°	0 -75	1500	0 - 125	838	0 - 200	600	0 - 300	564	0 - 500	567
	75 - 150	299	125 - 250	847	200 - 400	921	300 - 600	904	500 -1000	940
	150 - 225	1	250 - 375	113	400 - 600	253	600 - 900	312	1000 - 1500	283
	225 - 300	0	375 - 500	2	600 - 800	26	900 - 1200	20	1500 - 2000	10
WNW 292.5°	0 - 10	1066	0 - 25	1292	0 - 50	1207	0 -100	1115	0 - 150	753
	10 - 20	711	25 - 50	502	50 - 100	581	100 - 200	670	150 - 300	898
	20 - 30	23	50 -75	6	100 - 150	12	200 - 300	15	300 -450	148
	30 - 40	0	75 - 100	0	150 - 200	0	300 - 400	0	450 - 600	1
NW 315°	0 - 10	1637	0 -15	943	0 - 25	784	0 - 50	1167	0 - 50	601
	10 - 20	163	15 - 30	797	25 - 50	886	50 - 100	610	50 - 100	928
	20 - 30	0	30 - 45	59	50 -75	123	100 - 150	23	100 - 150	246
	30 - 40	0	45 - 60	1	75 - 100	7	150 - 200	0	150 - 200	25
NNW 337.5°	0 - 5	1775	0 - 10	1489	0 -15	1073	0 - 25	1070	0 - 50	1508
	5 - 10	25	10 - 20	310	15 - 30	678	25 - 50	684	50 - 100	291
	10 - 15	0	20 - 30	1	30 - 45	48	50 -75	45	100 - 150	1
	15 - 20	0	30 - 40	0	45 - 60	1	75 - 100	1	150 - 200	0

24.4 Fatigue mono-pile: soft soil profile, Fd = 5000kN

Hs = 0.5

Hs = 0.5	DeltaF	s1 [MPa]	s2 [MPa]	s3 [MPa]	s4 [MPa]	p %					n1	n2	n3	n4	SCF	s,hot1 [MPa]	s,hot2 [MPa]	s,hot3 [MPa]	s,hot4 [MPa]	N1	N2	N3	N4	n/N1	n/N2	n/N3	n/N4	Dd
North	5	0.340	0.680	1.020	1.360	0.13	1800	159			6.9E+04	0.0E+00	0.0E+00	0.0E+00	1.21	0.41	0.41	1.23	1.65	8.4E+17	3.9E+16	5.1E+15	8.3E+14	8.2E-14	0.0E+00	0.0E+00	0.0E+00	8.2E-13
NNE	5	0.340	0.680	1.020	1.360	0.14	1641				6.6E+04	6.4E+03	0.0E+00	0.0E+00	1.21	0.41	0.41	0.82	1.65	8.4E+17	3.9E+16	5.1E+15	8.3E+14	7.9E-14	1.6E-13	0.0E+00	0.0E+00	2.4E-12
NE	10	0.680	1.360	2.040	2.720	0.43	1260	529	11		1.6E+05	6.7E+04	1.4E+03	0.0E+00	1.21	0.82	0.82	2.47	3.29	3.9E+16	8.3E+14	9.2E+13	3.8E+13	4.0E-12	8.0E-11	1.5E-11	0.0E+00	9.9E-10
ENE	10	0.680	1.360	2.040	2.720	2.28	913	822	65		6.1E+05	5.5E+05	4.3E+04	0.0E+00	1.21	0.82	1.65	2.47	3.29	3.9E+16	8.3E+14	9.2E+13	3.8E+13	1.5E-11	6.6E-10	4.7E-10	0.0E+00	1.1E-08
East	75	5.100	10.200	15.300	20.400	5.63	1140	625	35		1.9E+06	1.0E+06	5.8E+04	0.0E+00	1.21	6.17	6.17	18.51	24.68	9.3E+11	5.1E+10	6.2E+09	9.2E+08	2.0E-06	2.0E-05	9.3E-06	0.0E+00	3.2E-04
ESE	25	1.700	3.400	5.100	6.800	5.22	1306	493	1		2.0E+06	7.5E+05	1.5E+03	0.0E+00	1.21	2.06	4.11	6.17	8.23	4.0E+14	8.4E+12	9.3E+11	3.9E+11	4.9E-09	9.0E-08	1.6E-09	0.0E+00	9.6E-07
SE	10	0.680	1.360	2.040	2.720	2.77	1053	706	41		8.5E+05	5.7E+05	3.3E+04	0.0E+00	1.21	0.82	1.65	2.47	3.29	3.9E+16	8.3E+14	9.2E+13	3.8E+13	2.2E-11	6.9E-10	3.6E-10	0.0E+00	1.1E-08
SSE	5	0.340	0.680	1.020	1.360	0.38	1730	70			1.9E+05	7.8E+03	0.0E+00	0.0E+00	1.21	0.41	0.82	1.23	1.65	8.4E+17	3.9E+16	5.1E+15	8.3E+14	2.3E-13	2.0E-13	0.0E+00	0.0E+00	4.3E-12
South	5	0.340	0.680	1.020	1.360	0.08	1800				4.3E+04	0.0E+00	0.0E+00	0.0E+00	1.21	0.41	0.41	1.23	1.65	8.4E+17	3.9E+16	5.1E+15	8.3E+14	5.1E-14	0.0E+00	0.0E+00	0.0E+00	5.1E-13
SSW	5	0.340	0.680	1.020	1.360	0.08	1800				4.3E+04	0.0E+00	0.0E+00	0.0E+00	1.21	0.41	0.41	1.23	1.65	8.4E+17	3.9E+16	5.1E+15	8.3E+14	5.1E-14	0.0E+00	0.0E+00	0.0E+00	5.1E-13
SW	10	0.680	1.360	2.040	2.720	0.37	1333	458	9		1.4E+05	4.9E+04	9.6E+02	0.0E+00	1.21	0.82	1.65	2.47	3.29	3.9E+16	8.3E+14	9.2E+13	3.8E+13	3.6E-12	5.9E-11	1.0E-11	0.0E+00	7.3E-10
WSW	15	1.020	2.040	3.060	4.080	1.11	776	916	108		2.5E+05	3.0E+05	3.5E+04	0.0E+00	1.21	1.23	2.47	3.70	4.94	5.1E+15	9.2E+13	1.1E+13	5.0E+12	4.9E-11	3.2E-09	3.1E-09	0.0E+00	6.3E-08
West	75	5.100	10.200	15.300	20.400	2.25	1500	299	1		9.9E+05	2.0E+05	6.6E+02	0.0E+00	1.21	6.17	12.34	18.51	24.68	9.3E+11	5.1E+10	6.2E+09	9.2E+08	1.1E-06	3.9E-06	1.1E-07	0.0E+00	5.0E-05
WNW	10	0.680	1.360	2.040	2.720	2.57	1066	711	23		8.0E+05	5.3E+05	1.7E+04	0.0E+00	1.21	0.82	1.65	2.47	3.29	3.9E+16	8.3E+14	9.2E+13	3.8E+13	2.0E-11	6.4E-10	1.9E-10	0.0E+00	8.5E-09
NW	10	0.680	1.360	2.040	2.720	1.51	1637	163			7.2E+05	7.2E+04	0.0E+00	0.0E+00	1.21	0.82	1.65	2.47	3.29	3.9E+16	8.3E+14	9.2E+13	3.8E+13	1.8E-11	8.6E-11	0.0E+00	0.0E+00	1.0E-09
NNW	5	0.340	0.680	1.020	1.360	0.39	1775	25			2.0E+05	2.9E+03	0.0E+00	0.0E+00	1.21	0.41	0.82	1.23	1.65	8.4E+17	3.9E+16	5.1E+15	8.3E+14	2.4E-13	7.3E-14	0.0E+00	0.0E+00	3.1E-12

Hs = 0.7

Hs = 0.7	DeltaF	s1 [MPa]	s2 [MPa]	s3 [MPa]	s4 [MPa]	p %					n1	n2	n3	n4	SCF	s,hot1 [MPa]	s,hot2 [MPa]	s,hot3 [MPa]	s,hot4 [MPa]	N1	N2	N3	N4	n/N1	n/N2	n/N3	n/N4	Dd
North	5	0.340	0.680	1.020	1.360	0.09	1800				4.7E+04	0.0E+00	0.0E+00	0.0E+00	1.21	0.41	0.41	1.23	1.65	8.4E+17	3.9E+16	5.1E+15	8.3E+14	5.6E-14	0.0E+00	0.0E+00	0.0E+00	5.6E-13
NNE	10	0.680	1.360	2.040	2.720	0.03	1246	538	16		1.2E+04	5.1E+03	1.5E+02	0.0E+00	1.21	0.82	1.65	2.47	3.29	3.9E+16	8.3E+14	9.2E+13	3.8E+14	3.0E-13	6.2E-12	1.7E-12	0.0E+00	8.1E-11
NE	25	1.700	3.400	5.100	6.800	0.21	1304	482	14		8.1E+04	3.0E+04	8.7E+02	0.0E+00	1.21	2.06	4.11	6.17	8.23	4.0E+14	8.4E+12	9.3E+11	3.9E+11	2.0E-10	3.6E-09	9.3E-10	0.0E+00	4.7E-08
ENE	25	1.700	3.400	5.100	6.800	1.74	834	888	75		4.2E+05	4.5E+05	3.8E+04	1.5E+03	1.21	2.06	4.11	6.17	8.23	4.0E+14	8.4E+12	9.3E+11	3.9E+11	1.1E-09	5.4E-08	4.1E-08	3.9E-09	1.0E-06
East	100	6.800	13.600	20.400	27.200	3.80	361	868	501	70	4.0E+05	9.6E+05	5.6E+05	7.8E+04	1.21	8.23	16.46	24.68	32.91	3.9E+11	8.3E+09	9.2E+08	3.8E+08	1.0E-06	1.2E-04	6.0E-04	2.0E-04	9.2E-03
ESE	25	1.700	3.400	5.100	6.800	2.09	391	988	371	50	2.4E+05	6.0E+05	2.3E+05	3.0E+04	1.21	2.06	4.11	6.17	8.23	4.0E+14	8.4E+12	9.3E+11	3.9E+11	5.9E-10	7.2E-08	2.4E-07	7.7E-08	3.9E-06
SE	25	1.700	3.400	5.100	6.800	0.42	1145	638	17		1.4E+05	7.7E+04	2.1E+03	0.0E+00	1.21	2.06	4.11	6.17	8.23	4.0E+14	8.4E+12	9.3E+11	3.9E+11	3.4E-10	9.2E-09	2.2E-09	0.0E+00	1.2E-07
SSE	10	0.680	1.360	2.040	2.720	0.03	1668	131	1		1.6E+04	1.2E+03	9.5E+00	0.0E+00	1.21	0.82	1.65	2.47	3.29	3.9E+16	8.3E+14	9.2E+13	3.8E+13	4.0E-13	1.5E-12	1.0E-13	0.0E+00	2.0E-11
South	0	0.000	0.000	0.000	0.000	0.00					0.0E+00	0.0E+00	0.0E+00	0.0E+00	1.21	0.00	0.00	0.00	0.00	0.0E+00	0.0E+00	0.0E+00	0.0E+00	0.0E+00	0.0E+00	0.0E+00	0.0E+00	0.0E+00
SSW	0	0.000	0.000	0.000	0.000	0.00					0.0E+00	0.0E+00	0.0E+00	0.0E+00	1.21	0.00	0.00	0.00	0.00	0.0E+00	0.0E+00	0.0E+00	0.0E+00	0.0E+00	0.0E+00	0.0E+00	0.0E+00	0.0E+00
SW	25	1.700	3.400	5.100	6.800	0.05	1206	580	14		1.7E+04	8.3E+03	2.0E+02	0.0E+00	1.21	2.06	4.11	6.17	8.23	4.0E+14	8.4E+12	9.3E+11	3.9E+11	4.3E-11	9.9E-10	2.1E-10	0.0E+00	1.2E-08
WSW	25	1.700	3.400	5.100	6.800	0.42	389	1018	357	36	4.8E+04	1.3E+05	4.4E+04	4.5E+03	1.21	2.06	4.11	6.17	8.23	4.0E+14	8.4E+12	9.3E+11	3.9E+11	1.2E-10	1.5E-08	4.8E-08	1.1E-08	7.4E-07
West	125	8.500	17.000	25.500	34.000	1.21	838	847	113	2	3.0E+05	3.0E+05	4.0E+04	7.0E+02	1.21	10.29	20.57	30.86	41.14	8.5E+10	4.0E+09	5.2E+08	8.4E+07	3.5E-06	7.4E-05	7.7E-05	8.4E-06	1.6E-03
WNW	25	1.700	3.400	5.100	6.800	1.92	1292	502	6		7.3E+05	2.8E+05	3.4E+03	0.0E+00	1.21	2.06	4.11	6.17	8.23	4.0E+14	4.0E+12	1.1E+08	3.9E+11	1.8E-09	3.4E-08	3.6E-09	3.4E-08	3.9E-07
NW	15	1.020	2.040	3.060	4.080	1.28	943	797	59	1	3.5E+05	3.0E+05	2.2E+04	3.7E+02	1.21	1.23	2.47	3.70	4.94	5.1E+15	9.2E+13	1.1E+13	5.0E+12	6.9E-11	3.2E-09	1.9E-09	7.5E-11	5.3E-08
NNW	10	0.680	1.360	2.040	2.720	0.28	1489	310	1		1.2E+05	2.5E+04	8.1E+01	0.0E+00	1.21	0.82	1.65	2.47	3.29	3.9E+16	8.3E+14	9.2E+13	3.8E+13	3.1E-12	3.0E-11	8.8E-13	0.0E+00	3.4E-10

Hs = 0.9

Hs = 0.9	DeltaF	s1 [MPa]	s2 [MPa]	s3 [MPa]	s4 [MPa]	p %					n1	n2	n3	n4	SCF	s,hot1 [MPa]	s,hot2 [MPa]	s,hot3 [MPa]	s,hot4 [MPa]	N1	N2	N3	N4	n/N1	n/N2	n/N3	n/N4	Dd
North	5	0.340	0.680	1.020	1.360	0.05	1800				2.6E+04	0.0E+00	0.0E+00	0.0E+00	1.21	0.41	0.41	1.23	1.65	8.4E+17	3.9E+16	5.1E+15	8.3E+14	3.1E-14	0.0E+00	0.0E+00	0.0E+00	3.1E-13
NNE	25	1.700	3.400	5.100	6.800	0.01	1458	340	2		3.5E+03	8.1E+02	4.8E+00	0.0E+00	1.21	2.06	4.11	6.17	8.23	4.0E+14	8.4E+12	9.3E+11	3.9E+11	8.6E-12	9.6E-11	5.1E-12	0.0E+00	1.1E-09
NE	50	3.400	6.800	10.200	13.600	0.05	1397	395	8		2.0E+04	5.6E+03	1.1E+02	0.0E+00	1.21	4.11	8.23	12.34	16.46	8.4E+12	3.9E+11	5.1E+10	8.3E+09	2.4E-09	1.4E-08	2.2E-09	0.0E+00	1.9E-07
ENE	75	5.100	10.200	15.300	20.400	0.56	1103	676	21		1.8E+05	1.1E+05	3.4E+03	0.0E+00	1.21	6.17	12.34	18.51	24.68	9.3E+11	5.1E+10	6.2E+09	9.2E+08	1.9E-07	2.2E-06	5.6E-07	0.0E+00	2.9E-05
East	150	10.200	20.400	30.600	40.800	0.83	239	1066	484	11	5.8E+04	2.6E+05	1.2E+05	2.7E+03	1.21	12.34	24.68	37.03	49.37	5.1E+10	9.2E+08	1.1E+08	5.0E+07	1.1E-06	2.8E-04	1.0E-03	5.4E-05	1.4E-02
ESE	50	3.400	6.800	10.200	13.600	0.14	616	1005	174	5	2.5E+04	4.1E+04	7.0E+03	2.0E+02	1.21	4.11	8.23	12.34	16.46	8.4E+12	3.9E+11	5.1E+10	8.3E+09	3.0E-09	1.0E-07	1.4E-07	2.4E-08	2.7E-06
SE	50	3.400	6.800	10.200	13.600	0.02	1320	474	6		9.4E+03	3.4E+03	4.3E+01	0.0E+00	1.21	4.11	8.23	12.34	16.46	8.4E+12	3.9E+11	5.1E+10	8.3E+09	1.1E-09	8.6E-09	8.4E-10	0.0E+00	1.1E-07
SSE	0	0.000	0.000	0.000	0.000	0.00					0.0E+00	0.0E+00	0.0E+00	0.0E+00	1.21	0.00	0.00	0.00	0.00	0.0E+00	0.0E+00	0.0E+00	0.0E+00	0.0E+00	0.0E+00	0.0E+00	0.0E+00	0.0E+00
South	0	0.000	0.000	0.000	0.000	0.00					0.0E+00	0.0E+00	0.0E+00	0.0E+00	1.21	0.00	0.00	0.00	0.00	0.0E+00	0.0E+00	0.0E+00	0.0E+00	0.0E+00	0.0E+00	0.0E+00	0.0E+00	0.0E+00
SSW	0	0.000	0.000	0.000	0.000	0.00					0.0E+00	0.0E+00	0.0E+00	0.0E+00	1.21	0.00	0.00	0.00	0.00	0.0E+00	0.0E+00	0.0E+00	0.0E+00	0.0E+00	0.0E+00	0.0E+00	0.0E+00	0.0E+00
SW	0	0.000	0.000	0.000	0.000	0.00					0.0E+00	0.0E+00	0.0E+00	0.0E+00	1.21	0.00	0.00	0.00	0.00	0.0E+00	0.0E+00	0.0E+00	0.0E+00	0.0E+00	0.0E+00	0.0E+00	0.0E+00	0.0E+00
WSW	75	5.100	10.200	15.300	20.400	0.10	1259	536	5		3.6E+04	1.5E+04	1.4E+02	0.0E+00	1.21	6.17	12.34	18.51	24.68	9.3E+11	5.1E+10	6.2E+09	9.2E+08	3.9E-08	3.0E-07	2.3E-08	0.0E+00	3.6E-06
West	200	13.600	27.200	40.800	54.400	0.34	600	921	253	26	6.0E+04	9.2E+04	2.5E+04	2.6E+03	1.21	16.46	32.91	49.37	65.82	8.3E+09	3.8E+08	5.0E+07	8.2E+06	7.2E-06	2.4E-04	5.1E-04	3.2E-04	1.1E-02
WNW	50	3.400	6.800	10.200	13.600	0.89	1207	581	12		3.1E+05	1.5E+05	3.1E+03	0.0E+00	1.21	4.11	8.23	12.34	16.46	8.4E+12	3.9E+11	5.1E+10	8.3E+09	3.7E-08	3.8E-07	6.1E-08	6.1E-08	4.8E-06
NW	25	1.700	3.400	5.100	6.800	0.74	784	886	123	7	1.7E+05	1.9E+05	2.7E+04	1.5E+03	1.21	2.06	4.11	6.17	8.23	4.0E+14	8.4E+12	9.3E+11	3.9E+11	4.2E-10	2.3E-08	2.9E-08	3.8E-09	5.6E-07
NNW	15	1.020	2.040	3.060	4.080	0.24	1073	678	48	1	7.4E+04	4.7E+04	3.3E+03	6.9E+01	1.21	1.23	2.47	3.70	4.94	5.1E+15	9.2E+13	1.1E+13	5.0E+12	1.5E-11	5.1E-10	2.9E-10	1.4E-11	8.3E-09

Hs = 1.1

Hs = 1.1	Delta F	s1 [MPa]	s2 [MPa]	s3 [MPa]	s4 [MPa]	p %					n1	n2	n3	n4	SCF	s.hot1 [MPa]	s.hot2 [MPa]	s.hot3 [MPa]	s.hot4 [MPa]	N1	N2	N3	N4	n/N1	n/N2	n/N3	n/N4	Dd
North	5	0.340	0.680	1.020	1.360	0.02	1789	11			8.5E+03	5.2E+01	0.0E+00	0.0E+00	1.21	0.41	0.82	1.23	1.65	8.4E+17	3.9E+16	5.1E+15	8.3E+14	1.0E-14	1.3E-15	0.0E+00	0.0E+00	1.1E-13
NNE	0	0.000	0.000	0.000	0.000	0.00					0.0E+00	0.0E+00	0.0E+00	0.0E+00	1.21	0.00	0.00	0.00	0.00	0.0E+00	0.0E+00	0.0E+00	0.0E+00	0.0E+00	0.0E+00	0.0E+00	0.0E+00	0.0E+00
NE	50	3.400	6.800	10.200	13.600	0.01	877	835	82	6	2.1E+03	2.0E+03	2.0E+02	1.4E+01	1.21	4.11	8.23	12.34	16.46	8.4E+12	3.9E+11	5.1E+10	8.3E+09	2.5E-10	5.0E-09	3.8E-09	1.7E-09	1.1E-07
ENE	100	6.800	13.600	20.400	27.200	0.10	521	843	410	26	1.5E+04	2.4E+04	1.2E+04	7.4E+02	1.21	8.23	16.46	24.68	32.91	3.9E+11	8.3E+09	9.2E+08	3.8E+08	3.8E-08	2.9E-06	1.3E-05	1.9E-06	1.8E-04
East	250	17.000	34.000	51.000	68.000	0.08	729	980	89	2	1.7E+04	2.3E+04	2.1E+03	4.8E+01	1.21	20.57	41.14	61.71	82.28	4.0E+09	8.4E+07	9.3E+06	3.9E+06	4.3E-06	2.8E-04	2.3E-04	1.2E-05	5.2E-03
ESE	0	0.000	0.000	0.000	0.000	0.00					0.0E+00	0.0E+00	0.0E+00	0.0E+00	1.21	0.00	0.00	0.00	0.00	0.0E+00	0.0E+00	0.0E+00	0.0E+00	0.0E+00	0.0E+00	0.0E+00	0.0E+00	0.0E+00
SE	0	0.000	0.000	0.000	0.000	0.00					0.0E+00	0.0E+00	0.0E+00	0.0E+00	1.21	0.00	0.00	0.00	0.00	0.0E+00	0.0E+00	0.0E+00	0.0E+00	0.0E+00	0.0E+00	0.0E+00	0.0E+00	0.0E+00
SSE	0	0.000	0.000	0.000	0.000	0.00					0.0E+00	0.0E+00	0.0E+00	0.0E+00	1.21	0.00	0.00	0.00	0.00	0.0E+00	0.0E+00	0.0E+00	0.0E+00	0.0E+00	0.0E+00	0.0E+00	0.0E+00	0.0E+00
South	0	0.000	0.000	0.000	0.000	0.00					0.0E+00	0.0E+00	0.0E+00	0.0E+00	1.21	0.00	0.00	0.00	0.00	0.0E+00	0.0E+00	0.0E+00	0.0E+00	0.0E+00	0.0E+00	0.0E+00	0.0E+00	0.0E+00
SSW	0	0.000	0.000	0.000	0.000	0.00					0.0E+00	0.0E+00	0.0E+00	0.0E+00	1.21	0.00	0.00	0.00	0.00	0.0E+00	0.0E+00	0.0E+00	0.0E+00	0.0E+00	0.0E+00	0.0E+00	0.0E+00	0.0E+00
SW	0	0.000	0.000	0.000	0.000	0.00					0.0E+00	0.0E+00	0.0E+00	0.0E+00	1.21	0.00	0.00	0.00	0.00	0.0E+00	0.0E+00	0.0E+00	0.0E+00	0.0E+00	0.0E+00	0.0E+00	0.0E+00	0.0E+00
WSW	75	5.100	10.200	15.300	20.400	0.01	533	968	274	25	1.3E+03	2.3E+03	6.5E+02	5.9E+01	1.21	6.17	12.34	18.51	24.68	9.3E+11	5.1E+10	6.2E+09	9.2E+08	1.4E-09	4.5E-08	1.1E-07	6.5E-08	2.2E-06
West	300	20.400	40.800	61.200	81.600	0.07	564	904	312	20	1.1E+04	1.7E+04	5.9E+03	3.8E+02	1.21	24.68	49.37	74.05	98.74	9.2E+08	5.0E+07	6.1E+06	9.6E+05	1.2E-05	3.4E-04	9.8E-04	4.0E-04	1.7E-02
WNW	100	6.800	13.600	20.400	27.200	0.30	1115	670	15		9.8E+04	5.9E+04	1.3E+03	0.0E+00	1.21	8.23	16.46	24.68	32.91	3.9E+11	8.3E+09	9.2E+08	3.8E+08	2.5E-07	7.1E-06	1.4E-06	0.0E+00	8.8E-05
NW	50	3.400	6.800	10.200	13.600	0.57	1167	610	23		1.9E+05	1.0E+05	3.8E+03	6.9E+01	1.21	4.11	8.23	12.34	16.46	8.4E+12	3.9E+11	5.1E+10	8.3E+09	2.3E-08	2.6E-07	7.5E-08	0.0E+00	3.6E-06
NNW	25	1.700	3.400	5.100	6.800	0.24	1070	684	45	1	7.4E+04	4.7E+04	3.1E+03		1.21	2.06	4.11	6.17	8.23	4.0E+14	8.4E+12	9.3E+11	3.9E+11	1.8E-10	5.6E-09	3.3E-09	1.8E-10	9.3E-08

Hs = 1.3

Hs = 1.3	Delta F	s1 [MPa]	s2 [MPa]	s3 [MPa]	s4 [MPa]	p %					n1	n2	n3	n4	SCF	s.hot1 [MPa]	s.hot2 [MPa]	s.hot3 [MPa]	s.hot4 [MPa]	N1	N2	N3	N4	n/N1	n/N2	n/N3	n/N4	Dd
North	5	0.340	0.680	1.020	1.360	0.01	1601	198	1		3.8E+03	4.7E+02	2.4E+00	0.0E+00	1.21	0.41	0.82	1.23	1.65	8.4E+17	3.9E+16	5.1E+15	8.3E+14	4.5E-15	1.2E-14	4.7E-16	0.0E+00	1.7E-13
NNE	0	0.000	0.000	0.000	0.000	0.00					0.0E+00	0.0E+00	0.0E+00	0.0E+00	1.21	0.00	0.00	0.00	0.00	0.0E+00	0.0E+00	0.0E+00	0.0E+00	0.0E+00	0.0E+00	0.0E+00	0.0E+00	0.0E+00
NE	0	0.000	0.000	0.000	0.000	0.00					0.0E+00	0.0E+00	0.0E+00	0.0E+00	1.21	0.00	0.00	0.00	0.00	0.0E+00	0.0E+00	0.0E+00	0.0E+00	0.0E+00	0.0E+00	0.0E+00	0.0E+00	0.0E+00
ENE	150	10.200	20.400	30.600	40.800	0.02	509	913	356	22	3.6E+03	6.5E+03	2.5E+03	1.6E+02	1.21	12.34	24.68	37.03	49.37	5.1E+10	9.2E+08	1.1E+08	5.0E+07	7.1E-08	7.1E-06	2.2E-05	3.1E-06	3.3E-04
East	350	23.800	47.600	71.400	95.200	0.01	1071	672	55	2	2.5E+03	1.6E+03	1.3E+02	4.8E+00	1.21	28.80	57.60	86.39	115.19	6.5E+08	1.6E+07	2.9E+06	8.2E+05	3.9E-06	1.0E-04	4.6E-05	5.8E-06	1.6E-03
ESE	0	0.000	0.000	0.000	0.000	0.00					0.0E+00	0.0E+00	0.0E+00	0.0E+00	1.21	0.00	0.00	0.00	0.00	0.0E+00	0.0E+00	0.0E+00	0.0E+00	0.0E+00	0.0E+00	0.0E+00	0.0E+00	0.0E+00
SE	0	0.000	0.000	0.000	0.000	0.00					0.0E+00	0.0E+00	0.0E+00	0.0E+00	1.21	0.00	0.00	0.00	0.00	0.0E+00	0.0E+00	0.0E+00	0.0E+00	0.0E+00	0.0E+00	0.0E+00	0.0E+00	0.0E+00
SSE	0	0.000	0.000	0.000	0.000	0.00					0.0E+00	0.0E+00	0.0E+00	0.0E+00	1.21	0.00	0.00	0.00	0.00	0.0E+00	0.0E+00	0.0E+00	0.0E+00	0.0E+00	0.0E+00	0.0E+00	0.0E+00	0.0E+00
South	0	0.000	0.000	0.000	0.000	0.00					0.0E+00	0.0E+00	0.0E+00	0.0E+00	1.21	0.00	0.00	0.00	0.00	0.0E+00	0.0E+00	0.0E+00	0.0E+00	0.0E+00	0.0E+00	0.0E+00	0.0E+00	0.0E+00
SSW	0	0.000	0.000	0.000	0.000	0.00					0.0E+00	0.0E+00	0.0E+00	0.0E+00	1.21	0.00	0.00	0.00	0.00	0.0E+00	0.0E+00	0.0E+00	0.0E+00	0.0E+00	0.0E+00	0.0E+00	0.0E+00	0.0E+00
SW	0	0.000	0.000	0.000	0.000	0.00					0.0E+00	0.0E+00	0.0E+00	0.0E+00	1.21	0.00	0.00	0.00	0.00	0.0E+00	0.0E+00	0.0E+00	0.0E+00	0.0E+00	0.0E+00	0.0E+00	0.0E+00	0.0E+00
WSW	0	0.000	0.000	0.000	0.000	0.00					0.0E+00	0.0E+00	0.0E+00	0.0E+00	1.21	0.00	0.00	0.00	0.00	0.0E+00	0.0E+00	0.0E+00	0.0E+00	0.0E+00	0.0E+00	0.0E+00	0.0E+00	0.0E+00
West	500	34.000	68.000	102.000	136.000	0.01	567	940	283	10	1.3E+03	2.2E+03	6.7E+02	2.4E+01	1.21	41.14	82.28	123.42	164.56	8.4E+07	3.9E+06	7.5E+05	4.1E+05	1.6E-05	5.7E-04	9.0E-04	5.8E-05	1.5E-02
WNW	150	10.200	20.400	30.600	40.800	0.08	753	898	148	1	1.8E+04	2.1E+04	3.5E+03	2.4E+01	1.21	12.34	24.68	37.03	49.37	5.1E+10	9.2E+08	1.1E+08	5.0E+07	3.5E-07	2.3E-05	3.1E-05	4.8E-07	5.5E-04
NW	50	3.400	6.800	10.200	13.600	0.29	601	928	246	25	5.0E+04	7.7E+04	2.0E+04	2.1E+03	1.21	4.11	8.23	12.34	16.46	8.4E+12	3.9E+11	5.1E+10	8.3E+09	6.0E-09	2.0E-07	4.0E-07	2.5E-07	8.6E-06
NNW	50	3.400	6.800	10.200	13.600	0.11	1508	291	1		4.7E+04	9.0E+03	3.1E+01	0.0E+00	1.21	4.11	8.23	12.34	16.46	8.4E+12	3.9E+11	5.1E+10	8.3E+09	5.6E-09	2.3E-08	6.1E-10	6.1E-10	2.9E-07

Hs = 1.5

Hs = 1.5	Delta F	s1 [MPa]	s2 [MPa]	s3 [MPa]	s4 [MPa]	p %					n1	n2	n3	n4	SCF	s.hot1 [MPa]	s.hot2 [MPa]	s.hot3 [MPa]	s.hot4 [MPa]	N1	N2	N3	N4	n/N1	n/N2	n/N3	n/N4	Dd
North	5	0.340	0.680	1.020	1.360	0.02	1264	524	12		6.0E+03	2.5E+03	5.7E+01	0.0E+00	1.21	0.41	0.82	1.23	1.65	8.4E+17	3.9E+16	5.1E+15	8.3E+14	7.2E-15	6.3E-14	1.1E-14	0.0E+00	8.2E-13
NNE	0	0.000	0.000	0.000	0.000	0.00					0.0E+00	0.0E+00	0.0E+00	0.0E+00	1.21	0.00	0.00	0.00	0.00	0.0E+00	0.0E+00	0.0E+00	0.0E+00	0.0E+00	0.0E+00	0.0E+00	0.0E+00	0.0E+00
NE	0	0.000	0.000	0.000	0.000	0.00					0.0E+00	0.0E+00	0.0E+00	0.0E+00	1.21	0.00	0.00	0.00	0.00	0.0E+00	0.0E+00	0.0E+00	0.0E+00	0.0E+00	0.0E+00	0.0E+00	0.0E+00	0.0E+00
ENE	0	0.000	0.000	0.000	0.000	0.02					0.0E+00	0.0E+00	0.0E+00	0.0E+00	1.21	0.00	0.00	0.00	0.00	0.0E+00	0.0E+00	0.0E+00	0.0E+00	0.0E+00	0.0E+00	0.0E+00	0.0E+00	0.0E+00
East	0	0.000	0.000	0.000	0.000	0.00					0.0E+00	0.0E+00	0.0E+00	0.0E+00	1.21	0.00	0.00	0.00	0.00	0.0E+00	0.0E+00	0.0E+00	0.0E+00	0.0E+00	0.0E+00	0.0E+00	0.0E+00	0.0E+00
ESE	0	0.000	0.000	0.000	0.000	0.00					0.0E+00	0.0E+00	0.0E+00	0.0E+00	1.21	0.00	0.00	0.00	0.00	0.0E+00	0.0E+00	0.0E+00	0.0E+00	0.0E+00	0.0E+00	0.0E+00	0.0E+00	0.0E+00
SE	0	0.000	0.000	0.000	0.000	0.00					0.0E+00	0.0E+00	0.0E+00	0.0E+00	1.21	0.00	0.00	0.00	0.00	0.0E+00	0.0E+00	0.0E+00	0.0E+00	0.0E+00	0.0E+00	0.0E+00	0.0E+00	0.0E+00
SSE	0	0.000	0.000	0.000	0.000	0.00					0.0E+00	0.0E+00	0.0E+00	0.0E+00	1.21	0.00	0.00	0.00	0.00	0.0E+00	0.0E+00	0.0E+00	0.0E+00	0.0E+00	0.0E+00	0.0E+00	0.0E+00	0.0E+00
South	0	0.000	0.000	0.000	0.000	0.00					0.0E+00	0.0E+00	0.0E+00	0.0E+00	1.21	0.00	0.00	0.00	0.00	0.0E+00	0.0E+00	0.0E+00	0.0E+00	0.0E+00	0.0E+00	0.0E+00	0.0E+00	0.0E+00
SSW	0	0.000	0.000	0.000	0.000	0.00					0.0E+00	0.0E+00	0.0E+00	0.0E+00	1.21	0.00	0.00	0.00	0.00	0.0E+00	0.0E+00	0.0E+00	0.0E+00	0.0E+00	0.0E+00	0.0E+00	0.0E+00	0.0E+00
SW	0	0.000	0.000	0.000	0.000	0.00					0.0E+00	0.0E+00	0.0E+00	0.0E+00	1.21	0.00	0.00	0.00	0.00	0.0E+00	0.0E+00	0.0E+00	0.0E+00	0.0E+00	0.0E+00	0.0E+00	0.0E+00	0.0E+00
WSW	0	0.000	0.000	0.000	0.000	0.00					0.0E+00	0.0E+00	0.0E+00	0.0E+00	1.21	0.00	0.00	0.00	0.00	0.0E+00	0.0E+00	0.0E+00	0.0E+00	0.0E+00	0.0E+00	0.0E+00	0.0E+00	0.0E+00
West	500	0.000	0.000	0.000	0.000	0.00					0.0E+00	0.0E+00	0.0E+00	0.0E+00	1.21	0.00	0.00	0.00	0.00	0.0E+00	0.0E+00	0.0E+00	0.0E+00	0.0E+00	0.0E+00	0.0E+00	0.0E+00	0.0E+00
WNW	250	17.000	34.000	51.000	68.000	0.02	728	910	158	4	5.2E+03	6.5E+03	1.1E+03	2.9E+01	1.21	20.57	41.14	61.71	82.28	4.0E+09	8.4E+07	9.3E+06	3.9E+06	1.3E-06	7.7E-05	1.2E-04	7.2E-06	2.1E-03
NW	100	6.800	13.600	20.400	27.200	0.08	1155	618	27		2.7E+04	1.5E+04	6.4E+02	0.0E+00	1.21	8.23	16.46	24.68	32.91	3.9E+11	8.3E+09	9.2E+08	3.8E+08	7.0E-08	1.8E-06	7.0E-07	0.0E+00	2.5E-05
NNW	50	3.400	6.800	10.200	13.600	0.08	1103	671	26		2.6E+04	1.6E+04	6.2E+02	0.0E+00	1.21	4.11	8.23	12.34	16.46	8.4E+12	3.9E+11	5.1E+10	8.3E+09	3.1E-09	4.1E-08	1.2E-08	0.0E+00	5.6E-07

24.5 Fatigue pile-head: front-/ side plates

Hs = 0.5

	Delta F	s1 [MPa]	s2 [MPa]	s3 [MPa]	s4 [MPa]	p %				n1	n2	n3	n4	N1	N2	N3	N4	(n/N)1	(n/N)2	(n/N)3	(n/N)4	Dd
North	5	0.044	0.087	0.131	0.174	0.13	1800	159		6.9E+04	0.0E+00	0.0E+00	0.0E+00	1.1E+30	2.1E+27	5.4E+25	4.1E+24	6.5E-26	0.0E+00	0.0E+00	0.0E+00	6.5E-26
NNE	5	0.044	0.087	0.131	0.174	0.14	1641	529	11	6.6E+04	6.4E+03	0.0E+00	0.0E+00	1.1E+30	2.1E+27	5.4E+25	4.1E+24	6.2E-26	3.1E-24	0.0E+00	0.0E+00	3.2E-24
NE	10	0.087	0.174	0.261	0.348	0.43	1260	822	65	1.6E+05	6.7E+04	1.4E+03	0.0E+00	2.1E+27	4.1E+27	1.1E+23	7.9E+21	7.7E-23	1.6E-20	1.3E-20	0.0E+00	3.0E-20
ENE	10	0.087	0.174	0.261	0.348	2.28	913	625	35	6.1E+05	5.5E+05	4.3E+04	0.0E+00	2.1E+27	4.1E+24	1.1E+23	7.9E+21	2.9E-22	1.4E-19	4.1E-19	0.0E+00	5.5E-19
East	75	0.653	1.305	1.958	2.610	5.63	1140	493	1	1.9E+06	1.0E+06	5.8E+04	0.0E+00	2.8E+19	5.4E+16	1.4E+15	1.1E+14	6.8E-14	1.9E-11	4.1E-11	0.0E+00	6.0E-11
ESE	25	0.218	0.435	0.653	0.870	5.22	1306	706	41	2.0E+06	7.5E+05	1.5E+03	0.0E+00	5.4E+23	1.1E+23	2.8E+19	2.1E+18	3.7E-18	7.1E-16	5.5E-17	0.0E+00	7.7E-16
SE	10	0.087	0.174	0.261	0.348	2.77	1053	70		8.5E+05	5.7E+05	3.3E+04	0.0E+00	2.1E+27	4.1E+24	1.1E+23	7.9E+21	4.1E-22	1.4E-19	3.1E-19	0.0E+00	4.6E-19
SSE	5	0.044	0.087	0.131	0.174	0.38	1730			1.9E+05	7.8E+03	0.0E+00	0.0E+00	1.1E+30	2.1E+27	5.4E+25	4.1E+24	1.8E-25	3.8E-24	0.0E+00	0.0E+00	4.0E-24
South	5	0.044	0.087	0.131	0.174	0.08	1800			4.3E+04	0.0E+00	0.0E+00	0.0E+00	1.1E+30	2.1E+27	5.4E+25	4.1E+24	4.0E-26	0.0E+00	0.0E+00	0.0E+00	4.0E-26
SSW	5	0.044	0.087	0.131	0.174	0.08	1800			4.3E+04	0.0E+00	0.0E+00	0.0E+00	1.1E+30	2.1E+27	5.4E+25	4.1E+24	4.0E-26	0.0E+00	0.0E+00	0.0E+00	4.0E-26
SW	10	0.087	0.174	0.261	0.348	0.37	1333	458	9	1.4E+05	4.9E+04	9.6E+02	0.0E+00	2.1E+27	4.1E+24	1.1E+23	7.9E+21	6.9E-23	1.2E-20	9.1E-21	0.0E+00	2.1E-20
WSW	15	0.131	0.261	0.392	0.522	1.11	776	916	108	2.5E+05	3.0E+05	3.5E+04	0.0E+00	5.4E+25	1.1E+23	2.7E+21	1.1E+20	4.7E-21	2.8E-18	1.3E-17	0.0E+00	1.6E-17
West	75	0.653	1.305	1.958	2.610	2.25	1500	299	1	9.9E+05	2.0E+05	6.6E+02	0.0E+00	2.8E+19	5.4E+16	1.4E+15	1.1E+14	3.6E-14	3.6E-12	4.7E-13	0.0E+00	4.1E-12
WNW	10	0.087	0.174	0.261	0.348	2.57	1066	711	23	8.0E+05	5.3E+05	1.7E+04	0.0E+00	2.1E+27	4.1E+24	1.1E+23	7.9E+21	3.9E-22	1.3E-19	1.6E-19	0.0E+00	3.0E-19
NW	10	0.087	0.174	0.261	0.348	1.51	1637	163		7.2E+05	7.2E+04	0.0E+00	0.0E+00	2.1E+27	4.1E+24	1.1E+23	7.9E+21	3.5E-22	1.8E-20	0.0E+00	0.0E+00	1.8E-20
NNW	5	0.044	0.087	0.131	0.174	0.39	1775	25		2.0E+05	2.9E+03	0.0E+00	0.0E+00	1.1E+30	2.1E+27	5.4E+25	4.1E+24	1.9E-25	1.4E-24	0.0E+00	0.0E+00	1.6E-24

Hs = 0.7

	Delta F	s1 [MPa]	s2 [MPa]	s3 [MPa]	s4 [MPa]	p %					n1	n2	n3	n4	N1	N2	N3	N4	(n/N)1	(n/N)2	(n/N)3	(n/N)4	Dd
North	5	0.044	0.087	0.131	0.174	0.09	1800				4.7E+04	0.0E+00	0.0E+00	0.0E+00	1.1E+30	2.1E+27	5.4E+25	4.1E+24	4.4E-26	0.0E+00	0.0E+00	0.0E+00	4.4E-26
NNE	10	0.087	0.174	0.261	0.348	0.03	1246	538	16		1.2E+04	5.1E+03	1.5E+02	0.0E+00	2.1E+27	4.1E+24	1.1E+23	7.9E+21	5.7E-24	1.3E-21	1.4E-21	0.0E+00	2.7E-21
NE	25	0.218	0.435	0.653	0.870	0.21	1304	482	14		8.1E+04	3.0E+04	8.7E+02	0.0E+00	5.4E+23	1.1E+21	2.8E+19	2.1E+18	1.5E-19	2.8E-17	3.1E-17	0.0E+00	6.0E-17
ENE	25	0.218	0.435	0.653	0.870	1.74	834	888	75	3	4.2E+05	4.5E+05	3.8E+04	1.5E+03	5.4E+23	1.1E+21	2.8E+19	2.1E+18	7.8E-19	4.3E-16	1.4E-15	7.4E-16	2.5E-15
East	100	0.870	1.740	2.610	3.480	3.80	361	868	501	70	4.0E+05	9.6E+05	5.6E+05	7.8E+04	2.1E+18	4.1E+15	1.1E+14	1.1E+12	1.9E-13	2.4E-10	5.3E-09	9.8E-09	1.5E-08
ESE	25	0.218	0.435	0.653	0.870	2.09	391	988	371	50	2.4E+05	6.0E+05	2.3E+05	3.0E+04	5.4E+23	1.1E+21	2.8E+19	2.1E+18	4.4E-19	5.7E-16	8.2E-15	1.5E-14	2.3E-14
SE	25	0.218	0.435	0.653	0.870	0.42	1145	638	17		1.4E+05	7.7E+04	2.1E+03	0.0E+00	5.4E+23	1.1E+21	2.8E+19	2.1E+18	2.6E-19	7.3E-17	7.5E-17	0.0E+00	1.5E-16
SSE	10	0.087	0.174	0.261	0.348	0.03	1668	131	1		1.6E+04	1.2E+03	9.5E+00	0.0E+00	2.1E+27	4.1E+24	1.1E+23	7.9E+21	7.7E-24	3.1E-22	9.0E-23	0.0E+00	4.1E-22
South	0	0.000	0.000	0.000	0.000	0.00					0.0E+00	0.0E+00	0.0E+00	0.0E+00	2.1E+63	4.1E+60	1.1E+59	7.9E+57	0.0E+00	0.0E+00	0.0E+00	0.0E+00	0.0E+00
SSW	0	0.000	0.000	0.000	0.000	0.00					0.0E+00	0.0E+00	0.0E+00	0.0E+00	2.1E+63	4.1E+60	1.1E+59	7.9E+57	0.0E+00	0.0E+00	0.0E+00	0.0E+00	0.0E+00
SW	25	0.218	0.435	0.653	0.870	0.05	1206	580	14		1.7E+04	8.3E+03	2.0E+02	2.0E+02	5.4E+23	1.1E+21	2.8E+19	2.1E+18	3.2E-20	7.8E-18	7.2E-18	2.1E-18	1.5E-17
WSW	25	0.218	0.435	0.653	0.870	0.42	389	1018	357	36	4.8E+04	1.3E+05	4.4E+04	4.5E+03	5.4E+23	1.1E+21	2.8E+19	2.1E+18	8.9E-20	1.2E-16	1.6E-15	2.1E-15	3.9E-15
West	125	1.088	2.175	3.263	4.350	1.21	838	847	113	2	3.0E+05	3.0E+05	4.0E+04	7.0E+02	2.8E+17	5.4E+14	1.4E+13	1.1E+12	1.1E-12	5.5E-10	2.8E-09	6.6E-10	4.0E-09
WNW	25	0.218	0.435	0.653	0.870	1.92	1292	502	6		7.3E+05	2.8E+05	3.4E+03	3.0E+00	5.4E+23	1.1E+21	2.8E+19	2.1E+18	1.3E-18	2.7E-16	1.2E-16	0.0E+00	3.9E-16
NW	15	0.131	0.261	0.392	0.522	1.28	943	797	59		3.5E+05	3.0E+05	2.2E+04	3.7E+02	5.4E+25	1.1E+23	2.7E+21	2.1E+20	6.5E-20	2.8E-18	8.0E-18	1.8E-18	1.3E-17
NNW	10	0.087	0.174	0.261	0.348	0.28	1489	310	1	1	1.2E+05	2.5E+04	8.1E+01	0.0E+00	2.1E+27	4.1E+24	1.1E+23	7.9E+21	5.8E-23	6.2E-21	7.7E-22	0.0E+00	7.0E-21

Hs = 0.9

	Delta F	s1 [MPa]	s2 [MPa]	s3 [MPa]	s4 [MPa]	p %					n1	n2	n3	n4	N1	N2	N3	N4	(n/N)1	(n/N)2	(n/N)3	(n/N)4	Dd
North	5	0.044	0.087	0.131	0.174	0.05	1800				2.6E+04	0.0E+00	0.0E+00	0.0E+00	1.1E+30	2.1E+27	5.4E+25	4.1E+24	2.4E-26	0.0E+00	0.0E+00	0.0E+00	2.4E-26
NNE	25	0.218	0.435	0.653	0.870	0.01	1458	340	2		3.5E+03	8.1E+02	4.8E+00	0.0E+00	5.4E+23	1.1E+21	2.8E+19	2.1E+18	6.4E-21	7.6E-19	1.7E-19	0.0E+00	9.4E-19
NE	50	0.435	0.870	1.305	1.740	0.05	1397	395	8		2.0E+04	5.6E+03	1.1E+02	0.0E+00	1.1E+21	2.1E+18	5.4E+16	4.1E+15	1.9E-17	2.7E-15	2.1E-15	0.0E+00	4.9E-15
ENE	75	0.653	1.305	1.958	2.610	0.56	1103	676	21		1.8E+05	1.1E+05	3.4E+03	0.0E+00	2.8E+19	5.4E+16	1.4E+15	1.1E+14	6.6E-15	2.1E-12	2.5E-12	0.0E+00	4.5E-12
East	150	1.305	2.610	3.915	5.220	0.83	239	1066	484	11	5.8E+04	2.6E+05	1.2E+05	2.7E+03	5.4E+16	1.1E+14	2.7E+12	2.1E+11	1.1E-12	2.5E-09	4.3E-08	1.3E-08	5.8E-08
ESE	50	0.435	0.870	1.305	1.740	0.14	616	1005	174	5	2.5E+04	4.1E+04	7.0E+03	2.0E+02	1.1E+21	2.1E+18	5.4E+16	4.1E+15	2.3E-17	2.0E-14	1.3E-13	5.0E-14	2.0E-13
SE	50	0.435	0.870	1.305	1.740	0.02	1320	474	6		9.4E+03	3.4E+03	4.3E+01	0.0E+00	1.1E+21	2.1E+18	5.4E+16	4.1E+15	8.9E-18	1.6E-15	7.9E-16	0.0E+00	2.4E-15
SSE	0	0.000	0.000	0.000	0.000	0.00					0.0E+00	0.0E+00	0.0E+00	0.0E+00	2.1E+63	4.1E+60	1.1E+59	7.9E+57	0.0E+00	0.0E+00	0.0E+00	0.0E+00	0.0E+00
South	0	0.000	0.000	0.000	0.000	0.00					0.0E+00	0.0E+00	0.0E+00	0.0E+00	2.1E+63	4.1E+60	1.1E+59	7.9E+57	0.0E+00	0.0E+00	0.0E+00	0.0E+00	0.0E+00
SSW	0	0.000	0.000	0.000	0.000	0.00					0.0E+00	0.0E+00	0.0E+00	0.0E+00	2.1E+63	4.1E+60	1.1E+59	7.9E+57	0.0E+00	0.0E+00	0.0E+00	0.0E+00	0.0E+00
SW	0	0.000	0.000	0.000	0.000	0.00					0.0E+00	0.0E+00	0.0E+00	0.0E+00	2.1E+63	4.1E+60	1.1E+59	7.9E+57	0.0E+00	0.0E+00	0.0E+00	0.0E+00	0.0E+00
WSW	75	0.653	1.305	1.958	2.610	0.10	1259	536	5		3.6E+04	1.5E+04	1.4E+02	0.0E+00	2.8E+19	5.4E+16	1.4E+15	1.1E+14	1.3E-15	2.8E-13	1.0E-13	0.0E+00	3.9E-13
West	200	1.740	3.480	5.220	6.960	0.34	600	921	253	26	6.0E+04	9.2E+04	2.5E+04	2.6E+03	4.1E+15	7.9E+12	2.1E+11	1.5E+10	1.5E-11	1.2E-08	1.2E-07	1.7E-07	3.0E-07
WNW	50	0.435	0.870	1.305	1.740	0.89	1207	581	12	7	3.1E+05	1.5E+05	3.1E+03	0.0E+00	1.1E+21	2.1E+18	5.4E+16	4.1E+15	2.9E-16	7.3E-14	5.8E-14	0.0E+00	1.3E-13
NW	25	0.218	0.435	0.653	0.870	0.74	784	886	123	1	1.7E+05	1.9E+05	2.7E+04	1.5E+03	5.4E+23	1.1E+21	2.8E+19	2.1E+18	3.1E-19	1.8E-16	9.6E-16	7.3E-16	1.9E-15
NNW	15	0.131	0.261	0.392	0.522	0.24	1073	678	48		7.4E+04	4.7E+04	3.3E+03	6.9E+01	5.4E+25	1.1E+23	2.7E+21	2.1E+20	1.4E-21	4.4E-19	1.2E-18	3.4E-19	2.0E-18

Hs = 1.1	Delta F	s1 [MPa]	s2 [MPa]	s3 [MPa]	s4 [MPa]	p %					n1	n2	n3	n4	N1	N2	N3	N4	(n/N)1	(n/N)2	(n/N)3	(n/N)4	Dd
North	5	0.044	0.087	0.131	0.174	0.02	1789	11			8.5E+03	5.2E+01	0.0E+00	0.0E+00	1.1E+30	2.1E+27	5.4E+25	4.1E+24	8.0E-27	2.5E-26	0.0E+00	0.0E+00	3.3E-26
NNE	0	0.000	0.000	0.000	0.000	0.00					0.0E+00	0.0E+00	0.0E+00	0.0E+00	2.1E+63	4.1E+60	1.1E+59	7.9E+57	0.0E+00	0.0E+00	0.0E+00	0.0E+00	0.0E+00
NE	50	0.435	0.870	1.305	1.740	0.01	877	835	82	6	2.1E+03	2.0E+03	2.0E+02	1.4E+01	1.1E+21	2.1E+18	5.4E+16	4.1E+15	2.0E-18	9.6E-16	3.6E-15	3.5E-15	8.1E-15
ENE	100	0.870	1.740	2.610	3.480	0.10	521	843	410	26	1.5E+04	2.4E+04	1.2E+04	7.4E+02	2.1E+18	4.1E+15	1.1E+14	7.9E+12	7.2E-15	5.9E-12	1.1E-10	9.4E-11	2.1E-10
East	250	2.175	4.350	6.525	8.700	0.08	729	980	89	2	1.7E+04	2.3E+04	2.1E+03	4.8E+01	5.4E+14	1.1E+12	2.8E+10	2.1E+09	3.2E-11	2.2E-08	7.7E-08	2.3E-08	1.2E-07
ESE	0	0.000	0.000	0.000	0.000	0.00					0.0E+00	0.0E+00	0.0E+00	0.0E+00	2.1E+63	4.1E+60	1.1E+59	7.9E+57	0.0E+00	0.0E+00	0.0E+00	0.0E+00	0.0E+00
SE	0	0.000	0.000	0.000	0.000	0.00					0.0E+00	0.0E+00	0.0E+00	0.0E+00	2.1E+63	4.1E+60	1.1E+59	7.9E+57	0.0E+00	0.0E+00	0.0E+00	0.0E+00	0.0E+00
SSE	0	0.000	0.000	0.000	0.000	0.00					0.0E+00	0.0E+00	0.0E+00	0.0E+00	2.1E+63	4.1E+60	1.1E+59	7.9E+57	0.0E+00	0.0E+00	0.0E+00	0.0E+00	0.0E+00
South	0	0.000	0.000	0.000	0.000	0.00					0.0E+00	0.0E+00	0.0E+00	0.0E+00	2.1E+63	4.1E+60	1.1E+59	7.9E+57	0.0E+00	0.0E+00	0.0E+00	0.0E+00	0.0E+00
SSW	0	0.000	0.000	0.000	0.000	0.00					0.0E+00	0.0E+00	0.0E+00	0.0E+00	2.1E+63	4.1E+60	1.1E+59	7.9E+57	0.0E+00	0.0E+00	0.0E+00	0.0E+00	0.0E+00
SW	0	0.000	0.000	0.000	0.000	0.00					0.0E+00	0.0E+00	0.0E+00	0.0E+00	2.1E+63	4.1E+60	1.1E+59	7.9E+57	0.0E+00	0.0E+00	0.0E+00	0.0E+00	0.0E+00
WSW	75	0.653	1.305	1.958	2.610	0.01	533	968	274	25	1.3E+03	2.3E+03	6.5E+02	5.9E+01	2.8E+19	5.4E+16	1.4E+15	1.1E+14	4.6E-17	4.3E-14	4.6E-13	5.6E-13	1.1E-12
West	300	2.610	5.220	7.830	10.440	0.07	564	904	312	20	1.1E+04	1.7E+04	5.9E+03	3.8E+02	1.1E+14	2.1E+11	5.4E+09	4.0E+08	1.0E-10	8.4E-08	1.1E-06	9.5E-07	2.1E-06
WNW	100	0.870	1.740	2.610	3.480	0.30	1115	670	15		9.8E+04	5.9E+04	1.3E+03	0.0E+00	2.1E+18	4.1E+15	1.1E+14	7.9E+12	4.7E-14	1.5E-11	1.3E-11	0.0E+00	2.7E-11
NW	50	0.435	0.870	1.305	1.740	0.57	1167	610	23		1.9E+05	1.0E+05	3.8E+03	0.0E+00	1.1E+21	2.1E+18	5.4E+16	4.1E+15	1.8E-16	4.9E-14	7.1E-14	0.0E+00	1.2E-13
NNW	25	0.218	0.435	0.653	0.870	0.24	1070	684	45	1	7.4E+04	4.7E+04	3.1E+03	6.9E+01	5.4E+23	1.1E+21	2.8E+19	2.1E+18	1.4E-19	4.4E-17	1.1E-16	3.3E-17	1.9E-16

Hs = 1.3	Delta F	s1 [MPa]	s2 [MPa]	s3 [MPa]	s4 [MPa]	p %					n1	n2	n3	n4	N1	N2	N3	N4	(n/N)1	(n/N)2	(n/N)3	(n/N)4	Dd
North	5	0.044	0.087	0.131	0.174	0.01	1601	198	1		3.8E+03	4.7E+02	2.4E+00	0.0E+00	1.1E+30	2.1E+27	5.4E+25	4.1E+24	3.6E-27	2.3E-25	4.4E-26	0.0E+00	2.7E-25
NNE	0	0.000	0.000	0.000	0.000	0.00					0.0E+00	0.0E+00	0.0E+00	0.0E+00	2.1E+63	4.1E+60	1.1E+59	7.9E+57	0.0E+00	0.0E+00	0.0E+00	0.0E+00	0.0E+00
NE	0	0.000	0.000	0.000	0.000	0.00					0.0E+00	0.0E+00	0.0E+00	0.0E+00	2.1E+63	4.1E+60	1.1E+59	7.9E+57	0.0E+00	0.0E+00	0.0E+00	0.0E+00	0.0E+00
ENE	150	1.305	2.610	3.915	5.220	0.02	509	913	356	22	3.6E+03	6.5E+03	2.5E+03	1.6E+02	5.4E+16	1.1E+14	2.7E+12	2.1E+11	6.7E-14	6.2E-11	9.3E-10	7.6E-10	1.8E-09
East	350	3.045	6.090	9.135	12.180	0.01	1071	672	55	2	2.5E+03	1.6E+03	1.3E+02	4.8E+00	2.6E+13	5.1E+10	1.3E+09	1.0E+08	9.7E-11	3.1E-08	9.8E-08	4.7E-08	1.8E-07
ESE	0	0.000	0.000	0.000	0.000	0.00					0.0E+00	0.0E+00	0.0E+00	0.0E+00	2.1E+63	4.1E+60	1.1E+59	7.9E+57	0.0E+00	0.0E+00	0.0E+00	0.0E+00	0.0E+00
SE	0	0.000	0.000	0.000	0.000	0.00					0.0E+00	0.0E+00	0.0E+00	0.0E+00	2.1E+63	4.1E+60	1.1E+59	7.9E+57	0.0E+00	0.0E+00	0.0E+00	0.0E+00	0.0E+00
SSE	0	0.000	0.000	0.000	0.000	0.00					0.0E+00	0.0E+00	0.0E+00	0.0E+00	2.1E+63	4.1E+60	1.1E+59	7.9E+57	0.0E+00	0.0E+00	0.0E+00	0.0E+00	0.0E+00
South	0	0.000	0.000	0.000	0.000	0.00					0.0E+00	0.0E+00	0.0E+00	0.0E+00	2.1E+63	4.1E+60	1.1E+59	7.9E+57	0.0E+00	0.0E+00	0.0E+00	0.0E+00	0.0E+00
SSW	0	0.000	0.000	0.000	0.000	0.00					0.0E+00	0.0E+00	0.0E+00	0.0E+00	2.1E+63	4.1E+60	1.1E+59	7.9E+57	0.0E+00	0.0E+00	0.0E+00	0.0E+00	0.0E+00
SW	0	0.000	0.000	0.000	0.000	0.00					0.0E+00	0.0E+00	0.0E+00	0.0E+00	2.1E+63	4.1E+60	1.1E+59	7.9E+57	0.0E+00	0.0E+00	0.0E+00	0.0E+00	0.0E+00
WSW	0	0.000	0.000	0.000	0.000	0.00					0.0E+00	0.0E+00	0.0E+00	0.0E+00	2.1E+63	4.1E+60	1.1E+59	7.9E+57	0.0E+00	0.0E+00	0.0E+00	0.0E+00	0.0E+00
West	500	4.350	8.700	13.050	17.400	0.01	567	940	283	10	1.3E+03	2.2E+03	6.7E+02	2.4E+01	1.1E+12	2.1E+09	5.4E+07	4.1E+06	1.3E-09	1.1E-06	1.2E-05	5.9E-06	1.9E-05
WNW	150	1.305	2.610	3.915	5.220	0.08	753	898	148	1	1.8E+04	2.1E+04	3.5E+03	2.4E+01	5.4E+16	1.1E+14	2.7E+12	2.1E+11	3.3E-13	2.0E-10	1.3E-09	1.2E-10	1.6E-09
NW	50	0.435	0.870	1.305	1.740	0.29	601	928	246	25	5.0E+04	7.7E+04	2.0E+04	2.1E+03	1.1E+21	2.1E+18	5.4E+16	4.1E+15	4.7E-17	3.7E-14	3.8E-13	5.1E-13	9.3E-13
NNW	50	0.435	0.870	1.305	1.740	0.11	1508	291	1		4.7E+04	9.0E+03	3.1E+01	0.0E+00	1.1E+21	2.1E+18	5.4E+16	4.1E+15	4.4E-17	4.3E-15	5.7E-16	0.0E+00	5.0E-15

Hs = 1.5	Delta F	s1 [MPa]	s2 [MPa]	s3 [MPa]	s4 [MPa]	p %					n1	n2	n3	n4	N1	N2	N3	N4	(n/N)1	(n/N)2	(n/N)3	(n/N)4	Dd
North	5	0.044	0.087	0.131	0.174	0.02	1264	524	12		6.0E+03	2.5E+03	5.7E+01	0.0E+00	1.1E+30	2.1E+27	5.4E+25	4.1E+24	5.7E-27	1.2E-24	1.1E-24	0.0E+00	2.3E-24
NNE	0	0.000	0.000	0.000	0.000	0.00					0.0E+00	0.0E+00	0.0E+00	0.0E+00	2.1E+63	4.1E+60	1.1E+59	7.9E+57	0.0E+00	0.0E+00	0.0E+00	0.0E+00	0.0E+00
NE	0	0.000	0.000	0.000	0.000	0.00					0.0E+00	0.0E+00	0.0E+00	0.0E+00	2.1E+63	4.1E+60	1.1E+59	7.9E+57	0.0E+00	0.0E+00	0.0E+00	0.0E+00	0.0E+00
ENE	0	0.000	0.000	0.000	0.000	0.02					0.0E+00	0.0E+00	0.0E+00	0.0E+00	2.1E+63	4.1E+60	1.1E+59	7.9E+57	0.0E+00	0.0E+00	0.0E+00	0.0E+00	0.0E+00
East	0	0.000	0.000	0.000	0.000	0.00					0.0E+00	0.0E+00	0.0E+00	0.0E+00	2.1E+63	4.1E+60	1.1E+59	7.9E+57	0.0E+00	0.0E+00	0.0E+00	0.0E+00	0.0E+00
ESE	0	0.000	0.000	0.000	0.000	0.00					0.0E+00	0.0E+00	0.0E+00	0.0E+00	2.1E+63	4.1E+60	1.1E+59	7.9E+57	0.0E+00	0.0E+00	0.0E+00	0.0E+00	0.0E+00
SE	0	0.000	0.000	0.000	0.000	0.00					0.0E+00	0.0E+00	0.0E+00	0.0E+00	2.1E+63	4.1E+60	1.1E+59	7.9E+57	0.0E+00	0.0E+00	0.0E+00	0.0E+00	0.0E+00
SSE	0	0.000	0.000	0.000	0.000	0.00					0.0E+00	0.0E+00	0.0E+00	0.0E+00	2.1E+63	4.1E+60	1.1E+59	7.9E+57	0.0E+00	0.0E+00	0.0E+00	0.0E+00	0.0E+00
South	0	0.000	0.000	0.000	0.000	0.00					0.0E+00	0.0E+00	0.0E+00	0.0E+00	2.1E+63	4.1E+60	1.1E+59	7.9E+57	0.0E+00	0.0E+00	0.0E+00	0.0E+00	0.0E+00
SSW	0	0.000	0.000	0.000	0.000	0.00					0.0E+00	0.0E+00	0.0E+00	0.0E+00	2.1E+63	4.1E+60	1.1E+59	7.9E+57	0.0E+00	0.0E+00	0.0E+00	0.0E+00	0.0E+00
SW	0	0.000	0.000	0.000	0.000	0.00					0.0E+00	0.0E+00	0.0E+00	0.0E+00	2.1E+63	4.1E+60	1.1E+59	7.9E+57	0.0E+00	0.0E+00	0.0E+00	0.0E+00	0.0E+00
WSW	0	0.000	0.000	0.000	0.000	0.00					0.0E+00	0.0E+00	0.0E+00	0.0E+00	2.1E+63	4.1E+60	1.1E+59	7.9E+57	0.0E+00	0.0E+00	0.0E+00	0.0E+00	0.0E+00
West	0	0.000	0.000	0.000	0.000	0.00					0.0E+00	0.0E+00	0.0E+00	0.0E+00	2.1E+63	4.1E+60	1.1E+59	7.9E+57	0.0E+00	0.0E+00	0.0E+00	0.0E+00	0.0E+00
WNW	250	2.175	4.350	6.525	8.700	0.02	728	910	158	4	5.2E+03	6.5E+03	1.1E+03	2.9E+01	5.4E+14	1.1E+12	2.8E+10	2.1E+09	9.6E-12	6.1E-09	4.1E-08	1.4E-08	6.1E-08
NW	100	0.870	1.740	2.610	3.480	0.08	1155	618	27		2.7E+04	1.5E+04	6.4E+02	0.0E+00	2.1E+18	4.1E+15	1.1E+14	7.9E+12	1.3E-14	3.6E-12	6.1E-12	0.0E+00	9.7E-12
NNW	50	0.435	0.870	1.305	1.740	0.08	1103	671	26		2.6E+04	1.6E+04	6.2E+02	0.0E+00	1.1E+21	2.1E+18	5.4E+16	4.1E+15	2.5E-17	7.7E-15	1.1E-14	0.0E+00	1.9E-14